JOURNAL OF APPLIED PHYSICS

JOURNAL OF APPLIED

PHYSICS

(Formerly PHYSICS)

SEPTEMBER, 1938 Vol. 9, No. 9

In This Issue

Page

Atom Tracks Exhibition at the Science Museum, London 551

Biological Effects of Low Velocity Cathode Rays
CARYL P. HASKINS 553

Research Foundation of Armour Institute of Technology
HAROLD VAGTBORG 562

Resumés of Recent Research 564

Further Notes on the Physics of Subsidence and Ground Movement in Mines H. P. GREENWALD 567

Physics in Pharmacy RONALD L. MCFARLAN 573

Contributed Original Research

Electromagnetic Waves in Elliptic Hollow Pipes of Metal
LAN JEN CHU 583

Method of Measuring Luminescent Screen Potential
HERBERT NELSON 592

Characteristics of the Glow to Arc Transition in Mercury Vapor
FREDERICK A. MAXFIELD AND GORDON L. FREDENDALL 600

In Every Issue

Here and There 578

Contributors to this Issue 580

Some of the New Books 581

Innovations in Instruments ii

Current Literature of Physics x

Advertising Index xx

BOARD OF EDITORS

ELMER HUTCHISSON, *Editor*

Associate Editors

R. M. BOZORTH
D. W. BRONK
W. P. DAVEY
O. S. DUFFENDACK
SAUL DUSHMAN
A. STUART HUNTER
C. H. KUNSMAN
J. T. LITTLETON
L. L. NETTLETON
W. B. NOTTINGHAM
A. R. OLPIN
JOHN T. TATE

Publication of the American Institute of Physics

ADMINISTRATIVE STAFF

HENRY A. BARTON, *Director*

MADELINE M. MITCHELL, *Publications Manager*

WILLIAM C. COPP, *Advertising Manager*

GOVERNING BOARD

JOHN T. TATE, *Chairman*
KARL T. COMPTON
E. C. CRITTENDEN
WHEELER P. DAVEY
HOMER L. DODGE
HARVEY FLETCHER
ARTHUR C. HARDY
VERN O. KNUDSEN
MELVIN MOONEY
FREDERIC PALMER, JR.
R. L. PEEK, JR.
GEORGE B. PEGRAM
W. B. RAYTON
F. K. RICHTMYER
WALLACE WATERFALL

THE JOURNAL OF APPLIED PHYSICS, published monthly at Prince and Lemon Sts., Lancaster, Pa., is devoted to physics in its role as the science basic to other natural sciences and to the arts and industries. Previous to 1937 this publication was known as PHYSICS. It aims to be of service not only in physical laboratories, but also in the laboratories of industrial, chemical, geological, geophysical, meteorological, radio, and similar concerns. THE JOURNAL OF APPLIED PHYSICS publishes editorials, news of physicists and reviews, as well as technical papers of applied physics.

SUBSCRIPTION PRICE

	U. S., POSS. AND CANADA	FOREIGN
To members of scientific societies	$5.00	$5.70
To all others	7.00	7.70

Manuscripts should be submitted to Elmer Hutchisson, Editor, University of Pittsburgh, Pittsburgh, Pennsylvania.

Changes of address, proofs, and complaints of failure to receive the JOURNAL OF APPLIED PHYSICS should be addressed to the Publications Manager. New copies can be sent free only if notice of nondelivery is received within three months of date of issue.

Subscriptions and orders for back numbers should be addressed to Prince and Lemon Streets, Lancaster, Pa. or to the American Institute of Physics, 175 Fifth Avenue, New York, N. Y.

Advertising rates supplied on request. Orders, advertising copy and cuts should be sent to the American Institute of Physics.

Entered as second class matter at the Post Office at Lancaster, Pennsylvania, under the Act of March 3, 1897. Accepted for mailing at the special rate of postage provided for in the Act of February 28, 1925, authorized May 2, 1932.

Copyright 1938, by the American Institute of Physics.

Journal of Applied Physics

Volume 9 September, 1938 Number 9

Atom Tracks Exhibition at the Science Museum, London

AN exhibition of atom tracks apparatus at the Science Museum, South Kensington, London was opened to the public on November 19, 1937 and remained on view until the end of February, 1938. It was intended to illustrate the results of twenty-five years of research work in atomic physics carried out by the condensation method invented by Professor C. T. R. Wilson in 1911–12, by means of which the tracks of individual atoms and electrons are rendered visible and photographed.

The center piece of the exhibition was Wilson's original apparatus, which was kindly lent by the Cavendish Laboratory, Cambridge, where his pioneer work was carried out. The remainder of the exhibition consisted of a collection of over eighty photographs taken by research workers all over the world using Wilson's condensation method.

An introductory group of twelve photographs was arranged to illustrate in as simple a way as possible some of the main properties of alpha-rays, beta-rays, x-rays, and gamma-rays, for the benefit of those not familiar with them. The main collection of photographs consisted of a series of groups showing typical effects produced by alpha-, beta-, and gamma-rays, x-rays, protons, deuterons, neutrons, and cosmic rays, while a small group illustrated the phenomenon of induced or artificial radioactivity discovered by Curie and Joliot in 1934. Included in the section dealing with cosmic rays was a copy of the photograph taken by Anderson in 1932 which first revealed the existence of the positive electron.

In addition to these photographs a dozen stereoscopic pairs of photographs were mounted for viewing in turn in a stereoscope; these included copies of the first stereoscopic photographs taken by Wilson in 1913, photographs by Skobelzyn showing recoil electrons due to gamma-rays, and several by Anderson showing examples of cosmic-ray "showers."

A small handbook was prepared by Dr. F. A. B. Ward, the museum officer who arranged the exhibition. The exhibition aroused considerable interest among the gen-

For October

Filtration of Sound, by R. B. LINDSAY

Study of Surfaces by Electron Diffraction, by H. R. NELSON

Penetration of Oil Sprays, by P. H. SCHWEITZER

Original research papers on the Time Lag in Gas-Filled Photoelectric Cells, Currents to Conductors Induced by a Moving Point Charge, Drift of Magnetic Permeability at Low Inductions after Demagnetization, Electrical Conduction in Quartz, Periclase, and Corundum at Low Field Strength, On the Starting of HG Vapor Discharge Tubes, Clean Up and Pressure Effects in Low Pressure Mercury Vapor Discharges: A Reversible Electrical Clean Up of Mercury.

FIG. 1. View showing a corner of the Atom Tracks Exhibition. Courtesy of the Science Museum.

eral public as well as among professional physicists and was favorably commented upon by both the scientific and popular press.

No systematic count of the number of visitors attending was made, but from several sample counts it was found that the attendance was approximately one-tenth of the total museum attendance. It was therefore estimated that during its 3½ months' run the exhibition was visited by over 25,000 persons, while over 2000 copies of the exhibition handbook were sold.

At the close of the exhibition the photographs were carefully filed for future reference; they should form a valuable permanent record illustrating the progress of atomic physics. Though space does not at present permit them to be permanently exhibited, a selection of about one dozen of the more important ones have been placed on exhibition together with Wilson's original apparatus.

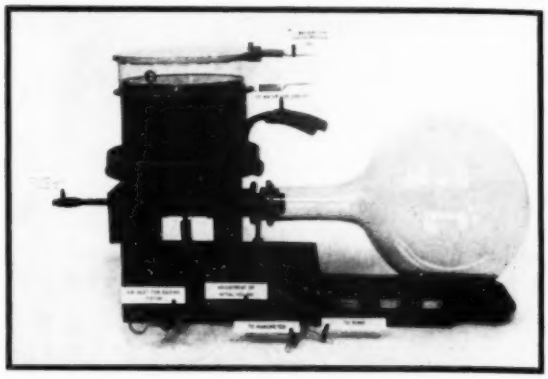

FIG. 2. C. T. R. Wilson's original cloud track apparatus of 1911–1912. Courtesy of the Science Museum.

An organization, steeped in the research idea, its executives and workers all thinking of problems and studying carefully their solutions with something of the zest the scientist brings to his work, is something more than an organization. It is an organism with opportunities for growth stretching out both for the individual and for the company.

HENRY P. KENDALL

The Biological Effects of Low Velocity Cathode Rays

BY CARYL P. HASKINS

Department of Physics, Massachusetts Institute of Technology, and Union College

INTRODUCTION

THE importance of investigations in the field of the biological effects of cathode rays, especially as such investigations might relate to x-ray therapeutic action, was recognized very early in the present century. The work of Dessauer and other early researchers on the "point-heat" hypothesis and other pictures of the mechanics of the x-ray coagulation of proteins or killing of living cells early focused attention upon the possibility that the results observed might be the effect rather of photo and recoil electrons released by the absorption of x-ray energy than that directly of the radiation.

Further progress in the field, however, faced two rather considerable barriers at this point. The first was the lack of a suitable source of cathode rays for experimental work in air, the second, the development of good technique in the selection, preparation, and assay of simple biological media. The Lenard cathode-ray tubes were quite unsuited to work of this character, by reason of the relatively low voltages at which they operated and the difficulty of good quantitative estimates of the density or uniformity of the beam.

The development of high voltage cathode-ray tubes permitted the use of relatively dense and quite uniform essentially parallel beams of electrons in air, provided the region very close to the window was used, and largely removed this obstacle to work. The rapid strides which in the meantime had been made in the science of genetics and in the methods of the study of populations in the opening decades of the twentieth century enabled biologists to provide reasonably reliable comparative biological standards for x-ray and high voltage cathode-ray work by the time that suitable sources were available. Work done on the killing effects of high voltage cathode rays, on genetic effects in maize and other plants, and on vitamin activation has been sufficient to show that, in all biological reactions with which we are familiar, the difference in effects of x-rays and high voltage cathode rays is not a qualitative one, and much evidence has been amassed to confirm the original conjecture that the effects observed with x-rays were primarily due to electrons released within the tissue.

It is probable that high voltage cathode rays are capable of furnishing little more information than this concerning the mechanism of the biological action of x-rays. The energies which are absorbed in tissue in producing characteristic biological reactions with high voltage cathode rays are usually larger by many orders of magnitude than the minimum required to achieve the same effect with x-rays. The electron density of the cathode-ray beam impinging on cellular material is, in general, similarly far higher than the calculated density of released electrons within

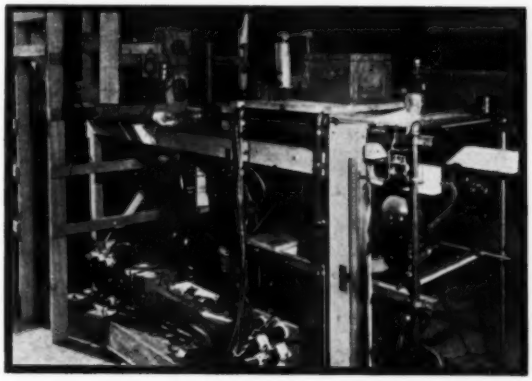

FIG. 1. General view of electron tube.

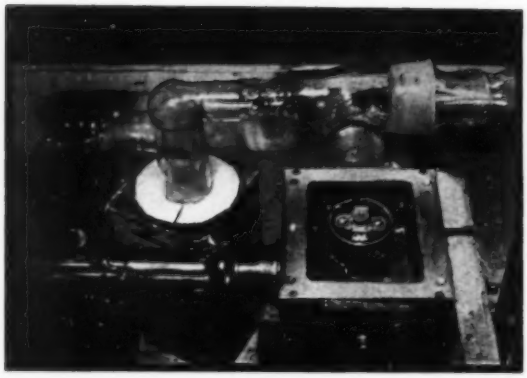

FIG. 2. Electron gun and raying box, with cover removed.

the entire volume of tissue treated with x-rays. Thus the electron densities and velocities required to bring about various specific effects are in most cases hopelessly "over-shot" with high voltage cathode rays, and any work other than of a purely qualitative character becomes impossible.

It seemed clear that, to achieve any further knowledge of the quantitative biological action of x-rays, work would be necessary with cathode rays of low voltage and extremely low electron density, operated in vacuum with biological material which would successfully withstand external gas pressures as low as 10^{-5} mm of mercury.

The design of a very low voltage, low current, cathode-ray tube for biological investigations was undertaken by Dr. D. A. Wells at the University of Cincinnati in 1929, and has been reported by him in two papers.[1] The work, however, was unfortunately discontinued not very long after its inception.

It seemed very desirable that so promising a field should not be abandoned permanently, for a number of reasons. A careful investigation of the relative rate of death of unicellular organisms —and especially of carcinomatic tissue cells— under equivalent total energies of cathode-ray irradiation as a function of voltage over a rather wide range of velocities might be expected to provide extremely interesting information as to the relative efficiency in killing of x-rays over the wave-length region wherein the mean integral range of released secondaries in the treated tissue was equivalent to that of the homogeneous cathode-ray beam employed. Such a study of the differential killing between cancerous and non-cancerous tissue would be especially interesting. Again, studies of the rate of death of single cells under bombardment of cathode rays of widely variant densities over correspondingly varied periods of exposure time might be expected to yield very useful data in confirming or disproving the validity of the Bunsen-Roscoe reciprocity relationship for x-ray dosage, since a cathode-ray tube can be much more flexibly designed for this purpose than can semi-standard x-ray equipment. Third, it is possible so to design a cathode-ray tube that the electron beam shall penetrate irradiated cells to any desired depth, and can thus act as a sort of blunt-ended probe (blunt-ended because of the high release of energy at the end of the electron track) wherewith to determine the relative sensitivity to electron bombardment of various parts of the living single cell. Finally, studies of the phenomenon of mutation under irradiation, already observed very many times with x-rays and with high velocity cathode rays, can be investigated much more quantitatively by the use of low velocity, low current beams. Information of this type

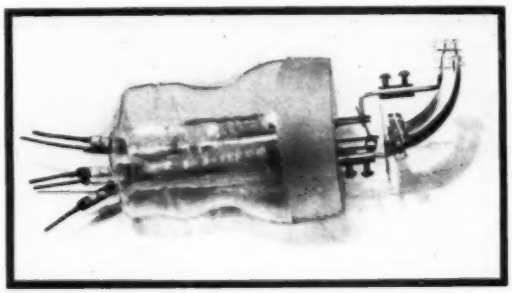

FIG. 3. Electron gun.

should be directly applicable to problems of x-ray cancer therapy. Some of it, however, cannot be obtained at all with x-ray methods, while all of it would seem to be more accurately, readily, and cheaply obtained through experiments with cathode radiation. These reasons have prompted the initiation of a research program which envisages a careful study of the biological effects of cathode-ray irradiation by beams of electrons at voltages ranging from 20

to 150,000 electron volts, and current densities from 10^{-9} to 10^{-6} ampere, upon single cells, upon cancer tissue, and upon any other biological materials which appear of particular interest. It

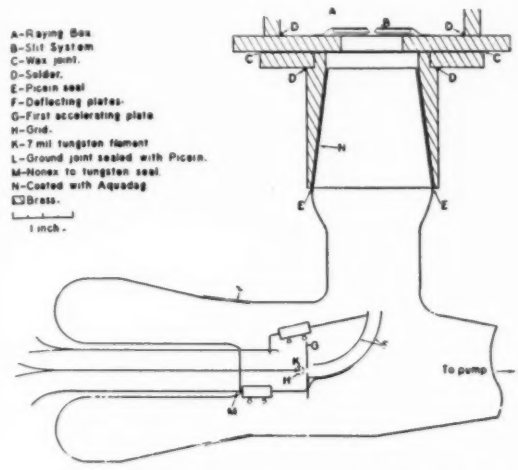

FIG. 4. Diagrammatic sketch of the electron gun.

has been necessary to design and construct three cathode-ray tubes for this purpose. One of these, capable of producing electron beams of high homogeneity, both in velocity and in density distribution, at energies from 1 to 15 electron kilovolts, and currents of the order of 10^{-9} to 10^{-7} ampere, is described herewith, and some results from experiments with it are presented.

The Tube

The general design of cathode-ray tube employed was somewhat similar to that of Wells, but a very considerable number of modifications and refinements have been introduced. As with the tube of Wells, a low voltage electron beam of high homogeneity has been deflected at right angles and made to impinge on a suitable rotatable target, after being suitably mechanically collimated, and a Faraday cage is provided for current measurement.

The problem requires that large numbers of similar unicellular organisms receive the same dosage of electrons of accurately controlled energy, in a voltage range which necessitates that irradiation be done entirely in high vacuum. It was therefore very desirable that the apparatus should provide for the successive bombardment of a number of samples without the necessity of breaking the vacuum seal, but at the same time without exposing the organisms to high vacuum for unduly lengthy periods of time. The requirement of uniform bombardment of sufficient area to accommodate a large number of organisms without mutual shielding has been met by moving the area upon which the material was placed at a uniform rate behind a slit placed in the electron beam. Homogeneity of the beam along the length of the slit has been obtained by the use of a straight-wire bare tungsten filament parallel to the slit as cathode.

Electron gun and raying box have been built as two separate units, the electron beam being electrostatically deflected at an angle of ninety degrees through a slit system into the raying chamber. Heat and possible x-rays attendant upon the electron beam are thus prevented from reaching the biological material. A general view of the equipment is shown in Fig. 1, and of the electron gun and raying box assembly, with raying box cover removed, in Fig. 2.

The Electron Gun

The electron gun is housed in glass, the entire assembly being mounted on one-half of a two-

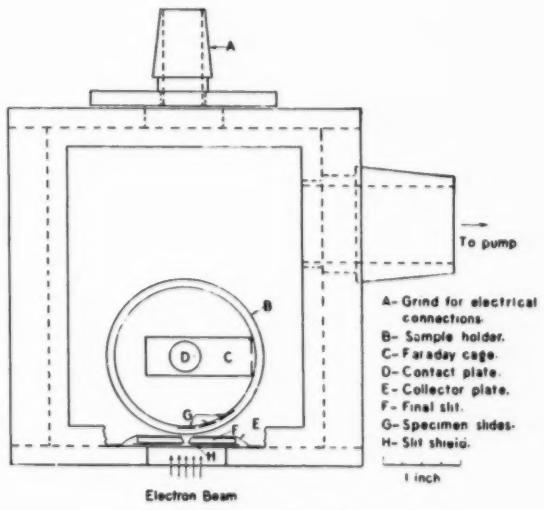

FIG. 5. The raying box and slit system.

inch glass grind (Figs. 3, 4). The glass housing is connected to the brass raying box through the metal-to-glass grind, made tight with Picein wax. The cathode assembly consists of a straight-wire

filament, a grid, an accelerating plate, and static deflecting plates, as shown, the electron beam being bent through a ninety degree arc on a 2.54 centimeter radius. The major acceleration given the electrons takes place after their deflection.

The Raying Box

The raying box (Fig. 5) houses the final slit system for defining the electron beam, the rotatable sample holder, and a Faraday cage for current measurement. It consists of a rectangular brass box, 7.6 cm by 9.35 cm by 6.0 cm deep, with a removable top plate to permit access to the sample holder, made vacuum-tight with a beeswax Venice turpentine mixture. Several metal-to-glass seals are provided for vacuum and electrical connections.

The raying box and electron gun are separated by the final slit system for the electron beam, leaving an opening 0.351 mm by 6.31 mm parallel to both the filament and the axis of rotation of the sample holder. Suitable shielding has been introduced, and a collector is provided for the measurement of current due to secondary electrons. The rotatable sample holder (Fig. 6) consists of a short brass cylinder, provided with spring clips along its bottom margin, by which twenty-eight small highly polished chromium-plated brass slides can be mounted on it.

It is mounted upon a turntable connected to a shaft which passes into the air through a grease-packed gland in the bottom of the raying box, and is geared to a Telechron motor mounted far enough below the raying box to eliminate danger of distortion of the electron beam by stray fields from the motor. Connection to the motor is made through a variable gear train, so that it is possible to rotate the sample holder at several accurately known speeds. It is thus possible to vary the total number of electrons reaching any given slide by a considerable factor without varying the density of the electron beam. A Faraday cage, completely shielded and insulated with amber, is mounted inside the sample holder and projects through a window in the side of the cylinder. When in position, it collects the entire beam entering the raying box, the current being carried through a contact arm riding on a circular disk at the top of the sample holder through amber-insulated coaxial cable to a copper-covered box housing the grid resistors of the electrometer (Fig. 7). The electrometer has a maximum current sensitivity of 5×10^{-13} ampere/mm.

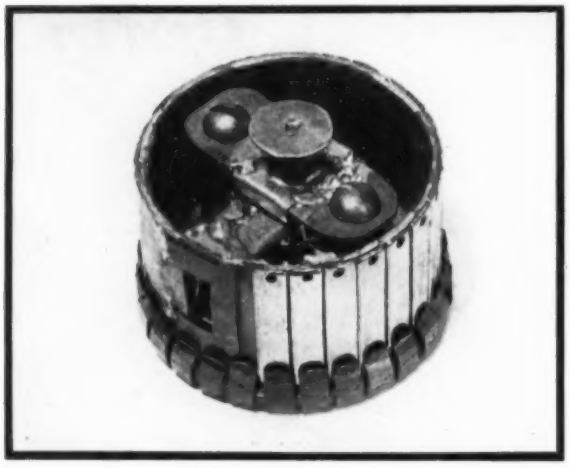

FIG. 6. Rotatable sample holder.

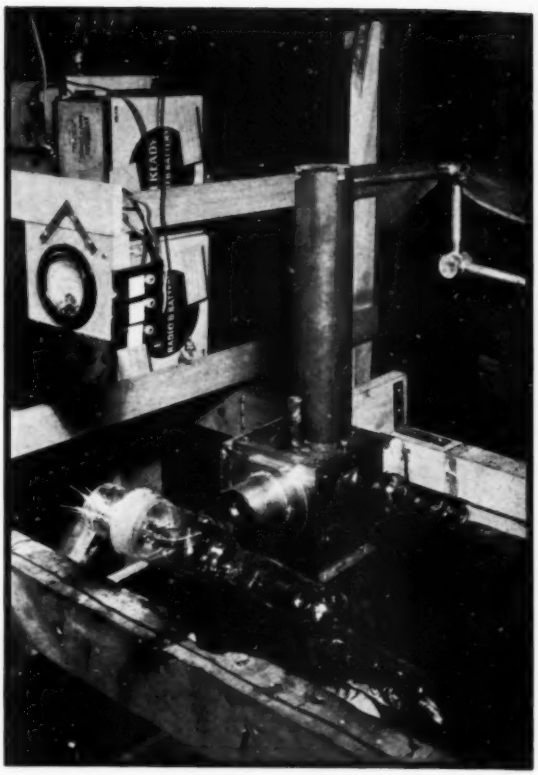

FIG. 7. Coaxial cable shielding of electrometer lead.

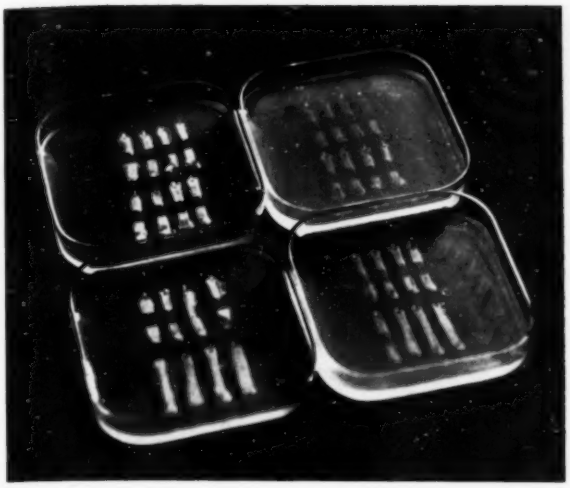

FIG. 8. Appearance of agar plates printed with germinating spores. The blank line traversing each rectangle is the irradiated area.

Power Supply

The tube is designed for operation between 1 kv and 15 kv. Tubes have been designed and are under construction to extend this voltage range to 50 volts on the low and 150 kv on the high sides. The voltage supply consists of a General Electric d.c. Kenotron testing set rated at 15,000 volts, 100 ma, provided with an induction regulator and peak voltmeter. The ripple voltage is smoothed to less than 1 percent by a 0.5 mf. capacitor. For voltages below 4 kv a voltage doubling circuit is used, powered by a sign lighting transformer. Batteries floated at the high potential supply filament current and grid and plate potentials.

The entire system is held at a pressure of less than 10^{-5} mm of mercury during operation. The vacuum system consists of two Langmuir pumps, one of metal and the other of glass, provided with liquid-air traps of conventional design inserted between each of them and the tube, each backed by a Hyvac. They are so arranged that the electron gun and the raying box are pumped independently, so that the slit system constitutes no barrier to pumping speed.

A more detailed description of the tube has been published elsewhere.[2]

Materials and Methods

It has already been stated that the primary purpose of this work is a survey of the relative killing efficiencies of cathode-ray beams over a wide range of velocities, with the particular object of investigating the relative susceptibility of cancerous and noncancerous tissue cells at these velocities. Cancer tissue, however, will not tolerate vacuum conditions. Hence it was necessary at these voltages to use as test objects organisms which would exhibit negative vacuum injury. Above 10 kv it will be possible to use thin Cellophane windows to conduct the beam for a very short distance in air, and to experiment directly with the material desired. The purpose of these experiments, therefore, is to establish a curve into the extremely low voltage region, where carcinomatic tissue cannot be used, and to extend it into the higher ranges where direct comparison with cancer tissue is possible. It may then be feasible to make at least a suggestive extrapolation to lower voltages for the cancer tissue.

The most suitable biological materials so far

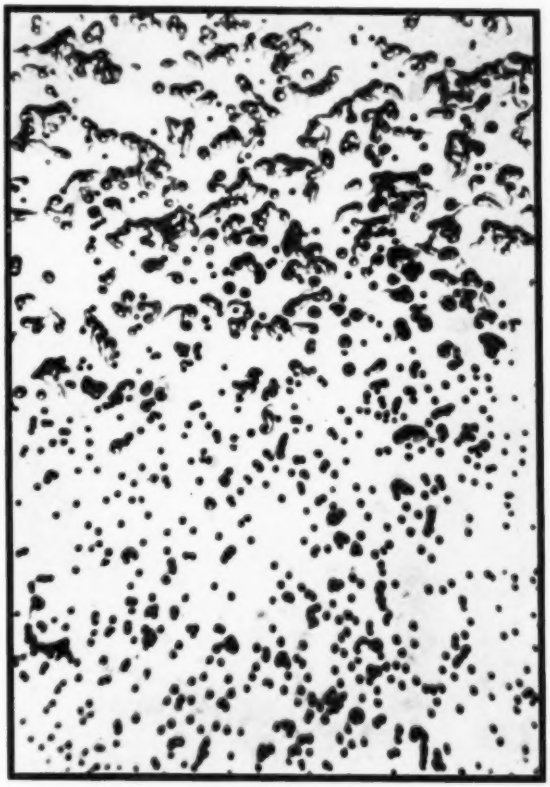

FIG. 9. Photomicrograph of area half-irradiated, half-shielded, at edge of rayed band.

found for this work have been the spores of the ascomycete fungi, *aspergillus niger* and *penicillium* sp. These spores are spherical, with single, centrally placed nuclei, and are from 3–5 microns in diameter. They exhibit good uniformity of structure, are readily handled on the slides and germinated, and show essentially no vacuum killing. They can be grown from extremely uniform cultures on carefully standardized growth media, and can be closely selected for age. They can probably be made to constitute as nearly a completely homogeneous population as could be found among organisms which will exhibit good vacuum resistance.

Spores of *aspergillus* or *penicillium*, uniform in age, culture condition, and nearly so in size, are dusted with a camels' hair brush upon the polished chromium slides already described. Care is taken to see that each spore is free of neighbors, and that no spore is shielded by any irregularity of the slide. Twenty-four slides so prepared are mounted on the rotatable sample holder, which is placed upon its turntable. An additional slide

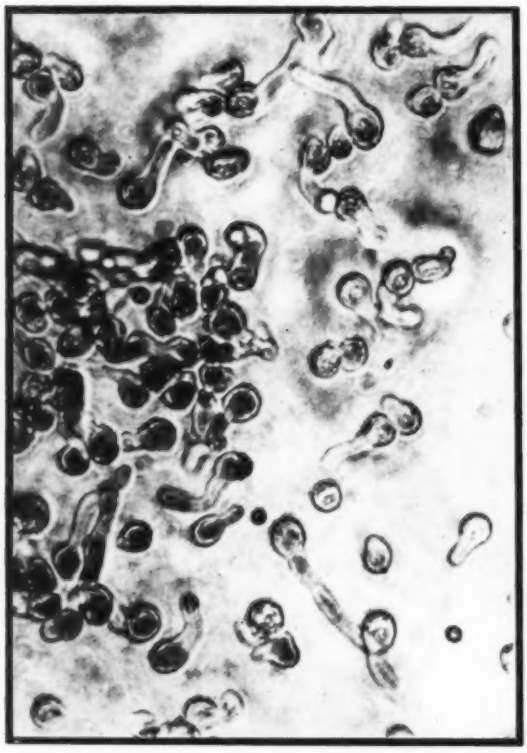

FIG. 10. Photograph of control germinating spores at high magnification.

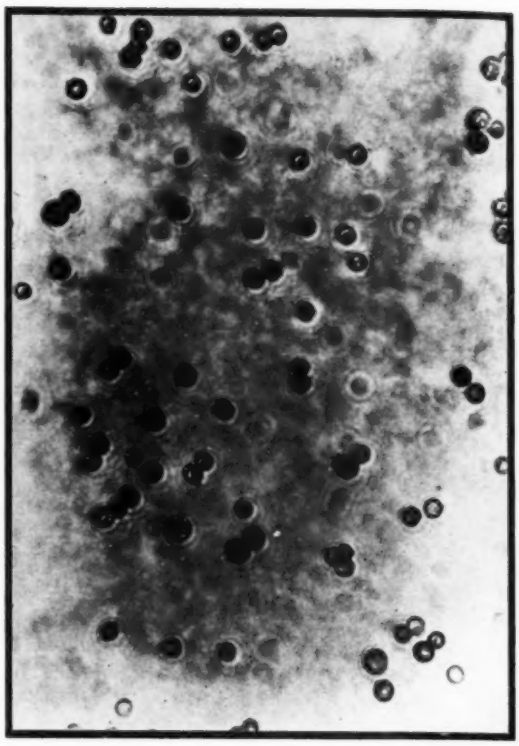

FIG. 11. Photomicrograph of heavily irradiated spores at high magnification showing killing.

is placed within the cylinder, where it will be completely shielded from the electron beam, as control. The cover of the raying box is sealed in place with wax, and the system evacuated. The Faraday cage is then rotated into position opposite the slit system, the filament lighted, high voltage applied to the tube, and the proper field applied across the plates to center the beam on the slit. After the current has been set to a predetermined value, a large negative voltage is applied to the grid of the electron gun, cutting off the beam to the raying box. The turntable is revolved until the edge of the slide to be treated is opposite the slit system. The gear train to the Telechron motor is then engaged and the motor started. At the same instant, the negative grid bias is removed, permitting the electron beam to fall on the slit. The entire width of the slide is thus scanned by the slit at known speed, and as the far edge of the slide passes from the beam, the negative field is again applied to the grid and the Telechron motor stopped. The gear train is disengaged, the Faraday cage brought into

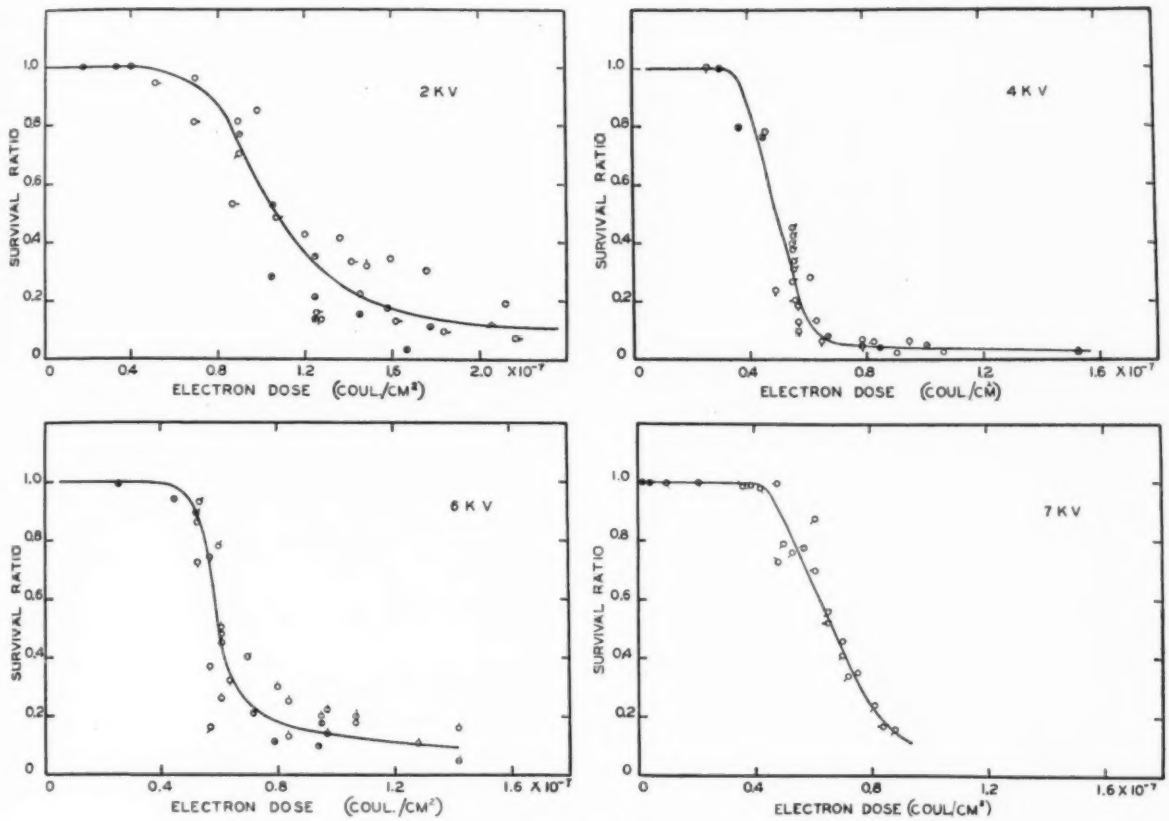

FIG. 12. Samples of survival ratio-dosage curves at four voltages.

position, and the current measurement repeated. A five percent deviation between current readings before and after the treatment of each slide is the maximum allowed. The total electron dosage applied to the slide is calculated from the current to the Faraday cage, the dimensions of the slit, and the speed at which the slide travels. The procedure is repeated for each slide on the holder, voltage, current, and speed of travel of the slide being varied as desired. At the end of the run air is admitted to the tube and the samples are removed.

The spores are printed from the slides onto plates of moist agar and cultured under standard conditions for several hours. At the end of this time it is found that a certain percentage has shown swelling and the production of mycelia, the rest remaining unchanged in size. The agar plates present the appearance shown in Figs. 8, 9, 10, and 11. A control print is made from the slide placed within the sample holder, and all killing results are expressed in terms of the "survival ratio," defined as the ratio of the percentage of unaffected organisms on the rayed slide to that on the control slide. It follows that the survival ratio will always be less than one unless stimulation of growth follows the treatment.

Results

Killing. The most important criterion of biological effectiveness of low voltage cathode rays for the present material is an analysis of the killing curves of the spores exposed to it. Samples of the form of such curves are shown in Fig. 12. It will be seen that all of those for the higher voltages are of "multiple hit" form, indicating that the absorption of more than one electron was necessary for cell death. The length of the plateau, however, changes with voltage in an interesting manner. This is best indicated by the curve of Fig. 13, in which the electron dosage required to produce a survival ratio of 50 percent in the cultures is plotted against voltage. Such a plot represents the relative efficiency of killing

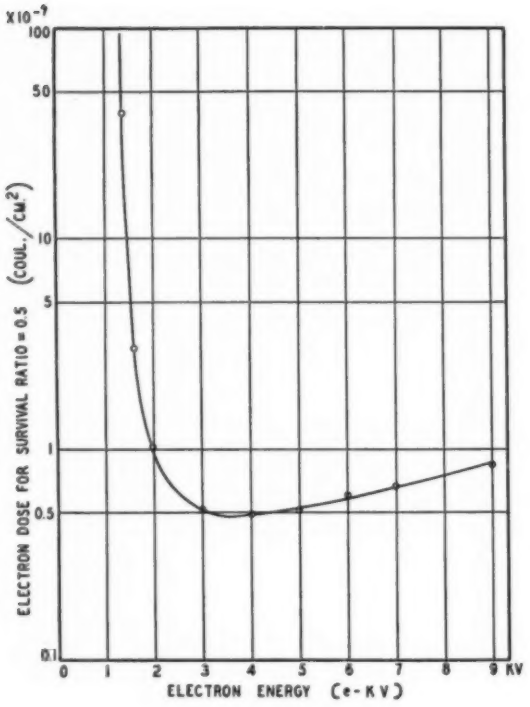

FIG. 13. Killing curve in which the electron dosage required to produce survival ratio of 50 percent is plotted against voltage.

for electrons as a function of voltage. It will be noticed that it is discontinuous. It is too soon to attempt an explanation of this discontinuity. When the survey of voltage ranges is complete, however, it is planned to submit the same biological material to ionizing radiations of such quantum energies that the mean integral ranges of secondaries produced shall fall within such a region or regions of discontinuity.

Killing effect was negligible for these spores below 2 kv. This can be shown to be due to insufficient electron penetration. Work is planned with much smaller organisms, when the curves should be shifted toward the origin along the abscissa.

Mutation. Two mutations have been detected among the progeny of treated *aspergillus* spores. They are shown in Fig. 14. They differ in color and odor from the normal, and are hereditarily transmissable. They have been more fully described elsewhere.[3] It is probable that many more mutants have been produced and have gone undetected, since it has been impossible to culture more than a very small proportion of the spores used in counts. This problem has been considered incidental to the main one, but it is hoped to give more attention to it in future.

Stimulation by low dosage. There are a number of references to be found in the literature[4] to stimulation of the growth of organisms by low dosages of x-rays and other ionizing radiations. Such stimulation has been found very definitely for low voltage cathode rays with *aspergillus.* Survival ratios as high as 1.25 have been found with spores of *aspergillus niger* at 1 and 2 kv. The cause of this stimulation is unknown at present, but may well be connected with a change in permeability of the outer spore coat to water. This is suggested by the fact that spores so treated are sometimes found to have exploded suddenly when placed on moist agar after removal from the tube—a condition possibly brought about by an unduly rapid absorption of water.

Plan of Future Work

The present program of research was undertaken primarily from the standpoint of its use in studies of the mechanism of the killing of organisms by ionizing radiations, and particularly of carcinomatic tissue by x-rays. Chief emphasis, therefore, will be devoted to that field, with such time as may be available devoted to the host of incidental physical and biological

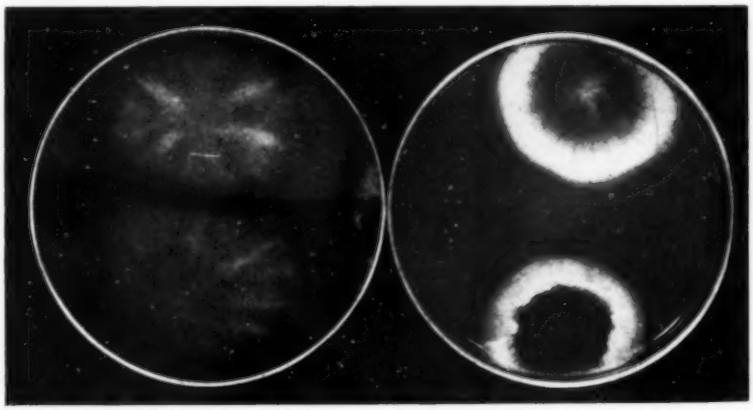

FIG. 14. Mutant strains of *aspergillus niger* produced under low voltage cathode-ray bombardment.

problems which invite investigation. It is planned first to extend the voltage range over which the survey is made to include most of the region between one-half and 150 electron kv. The lower voltage work will be done entirely in vacuum with such vacuum resistant organisms as have already been used and such others as may prove desirable. The range from 10 kv upward will then be investigated on carcinomatic single cell tissue culture directly in air, thin windows being provided for the tube, and work will be done under the same conditions with the vacuum resistant organisms used within the tube in the lower ranges. Some sort of extrapolation into the vacuum region may thus be possible for carcinomatic tissue, which cannot be subjected to low pressures.

This investigation will be paralleled by a similar one using ionizing radiation producing secondaries of comparable mean integral ranges to the electron beams used, with especial emphasis upon any voltage where, for electrons, the killing dosage seems to be discontinuously high. It is thus hoped to correlate results with the two energy forms and to use the cathode-ray beam essentially as a survey tool.

Following this work it is hoped to extend the same general methods to a study of the killing effects of protons over a considerable voltage range, and to similarly correlate it with neutron studies. Work has been initiated in the construction of a special design of proton source adapted for this task.

Bibliography

1. D. A. Wells, Nature **124**, **983** (1929).
2. F. S. Cooper, C. E. Buchwald, C. P. Haskins, and R. D. Evans, Rev. Sci. Inst., to be published.
3. R. M. Whelden, *Mycologia*, in press.
4. O. David, and A. Hirsch, Klin. Wochschr. **2**, 790 (1923). J. C. Fardon, M. J. Carroll, and M. V. Ruddy, Studies Inst. Divi Thomae I, 17–34 (1937). W. V. Mayneord and L. D. Parsons, J. Path. Bact. **45**, 35–38 (1937). A. O. Nathanson and G. A. Cherkes, Strahlentherapie **55**, 96–103 (1936). W. F. Petersen and C. C. Saelhof, Am. J. Med. Sci. **163**, 101–120 (1922). B. N. Singh and R. S. Choudri, Proc. Ind. Acad. Sci. **1B**, 435–51 (1935). F. Weber, Biochem. Zeits. **128**, 495–507 (1922). R. C. Woods, Radiology **27**, 498–499 (1936).

The Research Foundation of Armour Institute of Technology

BY HAROLD VAGTBORG

Managing Director of the Research Foundation

THE Research Foundation of Armour Institute of Technology was organized in September, 1936, as a nonprofit making organization for the purpose of carrying on organized research programs in the fields of pure and applied science.

After a little over a year's operation, the Board of Directors of the Foundation announced that the Foundation will emphasize research in applied physics and experimental engineering. Its highly developed facilities and trained personnel enable through subsidy and special funds the pursuit of investigations in pure science, and provide an industry or group of industries with assistance needed in the execution of research projects. This decision came about through a natural course of events.

The founders believed that the major scientific advancements which were inevitable in the coming years would be in the field of applied physics and it was this field upon which industry would rely largely for its development. The Foundation's original staff, therefore, consisted mainly of physicists, each of whom had specialized in a particular branch of the many offshoots of this science.

FIG. 1. Apparatus used for visual and photographic observations of metallurgical specimens after being ground, polished and etched.

FIG. 2. Copper target x-ray diffraction tube with x-ray spectrograph arranged for photographing thin oil films. The x-ray tube has the special feature that it may be used to produce a strong monochromatic beam of x-rays by reflection from a crystal placed within the tube. The x-ray spectrograph is designed to accommodate a wide variety of specimen holders and cameras for the various types of x-ray diffraction analysis. Both pieces of equipment were constructed in the Research Foundation shop.

As the problems of industry were brought to it, the Foundation made additions to its personnel so that its staff is now well rounded out and its equipment is adequate to undertake long and short term projects in many of the fields of pure and applied science; nevertheless, emphasizing applied physics and experimental engineering, in which divisions the Foundation is able to offer a highly specialized service.

The background of the Foundation is rather interesting. Since 1900 the staff of Armour In-

stitute of Technology has served the industries of the country by carrying out research and testing activities. With the rapid growth in the emphasis placed upon research, both pure and industrial, it became evident that the greatest service to the cause of both industry and scientific knowledge could be rendered by an organization existing as a separate entity, and engaging in research work as its fundamental activity. It was this realization that brought about the formation of the Research Foundation.

For the industry which has no research facilities of its own, the Research Foundation is equipped to serve as a research department. For the industry which already maintains a research department, the Research Foundation is particularly adapted to the carrying out of long-term programs of the type which are frequently interrupted by emergency demands. Where such long term programs are carried on in an isolated laboratory, no emergency interruptions occur. The necessary facilities are definitely allocated to the project until the work has been completed. Meanwhile the regular research facilities of the manufacturer can readily be diverted for use in work of a rush character.

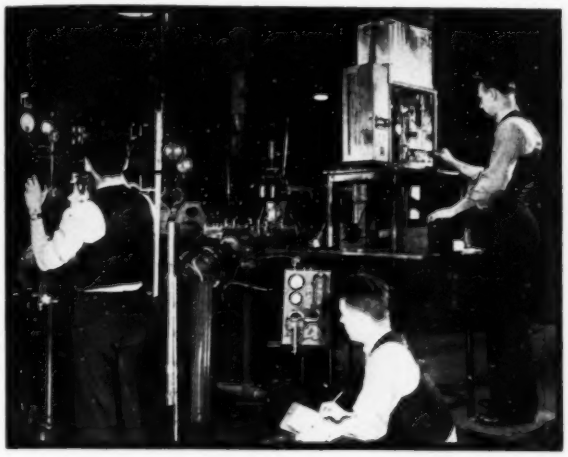

FIG. 3. This picture illustrates a set-up for an industrial research program in the automotive laboratory and is indicative of the manner in which these programs are handled in the various research and engineering laboratories.

A few of the activities of the Foundation will be enumerated to indicate the character of the investigations which are underway. Dr. Thomas C. Poulter, Director of Research, who was chief scientist and second in command of the Byrd expedition of 1933–35 and the recipient of the National Geographic Medal and more recently the Congressional Medal "for scientific accomplishment unequalled in polar research," and his assistant, Dr. A. O. Walker, are investigating as a pure research program the characteristics of fluids under extreme pressures in equipment which recently developed hydrostatic pressures of 1,500,000 pounds per square inch.

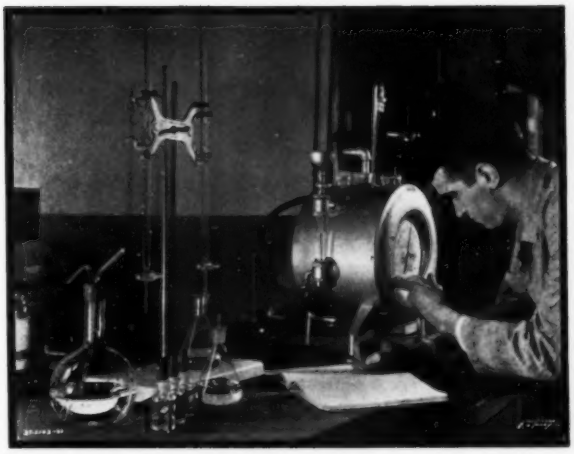

FIG. 4. The wet test gas meter in one of the chemical laboratories of the Research Foundation is used for accurate measurements of gaseous fuels and products of combustion, and, in conjunction with analytical equipment, for investigation of air pollution.

Another pure science research program is a

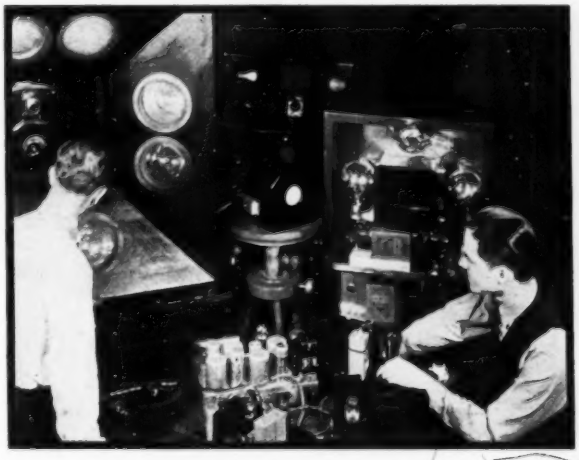

FIG. 5. General equipment used for research work in television.

study of monomolecular films being conducted by Dr. G. E. Ziegler, the findings of which will be published when the investigation is completed.

Dr. F. W. Godwin has made progress in developing a method of removing ash-forming materials from very finely divided coal and is engaging in other problems of basic research leading toward the solution of the problem of profitable disposal of unmarketable coal fines.

Dr. Paul L. Copeland is continuing an investigation of secondary emission of electrons. The preliminary results of this study have already been published and he is now directing his attention toward the finding of information concerning the depths which are controlling factors in secondary emission.

Dr. Max Jakob, Director of the Heat Transfer Laboratory, is setting up equipment to enable an investigation of the true temperature of catalysts. At the present time there is being constructed for his laboratory a 750 pound per square inch, 2000 pound per hour steam producer with unusually designed superheating equipment for investigations in flow. There will shortly be undertaken the construction of an approximately 3300 pound per square inch element boiler which will be electrically heated and used in his investigation of heat transfer under high pressures.

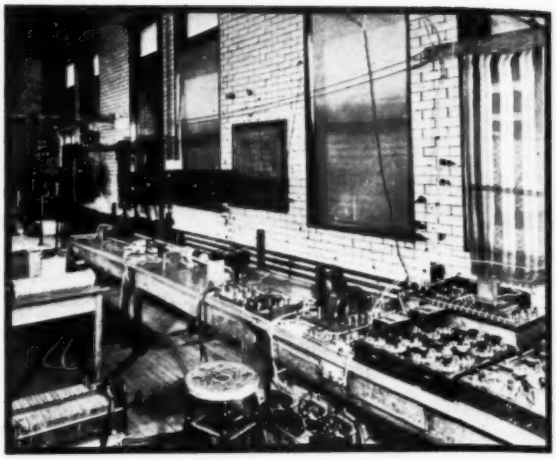

FIG. 6. A view of the electrical laboratory.

Many long and short term industrial research programs are under way in other laboratories and although some of these programs are in chemistry and chemical engineering, by far the largest number relate to applied physics and experimental engineering.

Resumés of Recent Research

Recent advances in experimental and theoretical physics are described in nontechnical language in these columns. It is intended that sufficient background be given to introduce the reader to the subject.

Magnetic Properties of Alloys The magnetic properties of pure ferromagnetic metals, such as iron, are structure sensitive, but not nearly as much so as those of certain alloys. This is because the thermal and mechanical treatment of alloys influences not only grain size, grain orientation, and internal strains but also the arrangements of the different types of atoms within a grain. The present theories of ferromagnetism assume that magnetic properties are determined by the interaction of atoms which are nearest neighbors, and it is therefore to be expected that any treatment that will alter the relative positions of the various types of atoms will also alter the magnetic properties. In a recent article in the July 1,

1938, *Physical Review*, Dr. F. Bitter has made an attempt to combine the theory of orderly arrangements of atoms in alloys with the theory of ferromagnetism. The results of his discussion are put into the form of certain equations of state which define the magnetic properties of alloys in terms of relatively few arbitrary constants. The equations look promising because they can describe some actually observed phenomena, such as the dependence of the Curie temperature on heat treatment, or the appearance of ferromagnetism in alloys of nonmagnetic metals, but more extensive comparisons with experiments are needed to establish the validity of the assumptions made. Experimental data at low temperatures on alloys having various heat treatments are especially to be desired to check the theory.

The Rate of an Atomic Clock in Motion

According to the theory of the relation between matter and the stagnant luminiferous ether, as developed by Larmor and Lorentz, a moving clock should assume a slower rate, proportional to the square of the ratio of its velocity to the velocity of light.

It was pointed out by Einstein in 1907 that the newly discovered Doppler effect in canal rays offered a means for making a test of this prediction. This experimental test, the crucial nature of which has been emphasized repeatedly in the last thirty years (under the designation of the "Transverse Doppler Effect") has not heretofore been performed. It has been commonly considered as beyond experimental practicability, chiefly on the ground that the moving canal rays are not homogeneous in velocity, the "displaced" line is too diffuse for sufficiently exact measurement.

This objection has recently been removed, due to the development, by Dempster, of a design of canal-ray tube which gives displaced lines of a sharpness comparable with the undisplaced. In this form of tube the positive ions produced behind the electrode are accelerated between two slightly separated pierced plates between which a high potential difference exists.

In a recent investigation by Dr. Herbert E. Ives* an experimental test of the Larmor-Lorentz prediction, using canal-ray tubes of the Dempster type has been made. The hydrogen line 4861A was used, observations being made by means of a plane grating of metal on glass of 15,000 lines to the inch, made by Professor R. W. Wood, which, in conjunction with two 5-inch diameter, 5-foot focus telescope objectives formed a sufficiently powerful spectrograph for the purpose. By means of a small concave mirror mounted on the pierced electrodes, end-on observation gave, on one plate, the displaced lines due to motion toward and away from the spectrograph slit. The apparatus was arranged to turn in any desired direction in the horizontal plane.

Observations were made over a range of voltages from 7,000 to 19,000, using the displaced H_2 and H_3 lines. At the higher voltage, for H_2 the directly viewed and reflected displaced lines should, according to the theory, have their com-

* Herbert E. Ives, J. Opt. Soc. Am., in press.

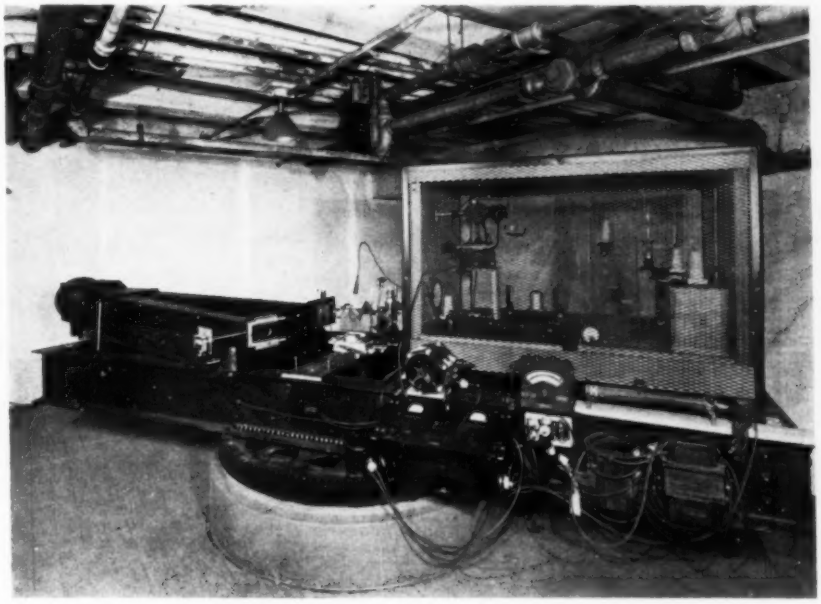

Arrangement as used by Dr. Ives of canal-ray tube in front of spectrographic slit.

mon center of gravity shifted, with respect to the undisplaced line, by approximately 0.05A. The experiment shows the predicted shifts, which are independent of the orientation of the apparatus, and agree, within the errors of measurement with the values indicated by the theory.

On the assumption of a stagnant ether, this experiment, taken in conjunction with the Kennedy-Thorndyke experiment, establishes the physical reality of both the Larmor-Lorentz variation of clock rate, and the Fitzgerald contraction. It is distinguished from the Michelson-Morley and other previous optical experiments by the fact that it yields a positive instead of a null effect.

Origin of Cosmic-Ray Showers A characteristic property of the cosmic radiation is that it is able, in its passage through matter, to produce secondary rays, groups of which fall simultaneously on the detecting apparatus. The number of rays occurring in such cosmic-ray showers varies from two to several thousand. Since it was formerly supposed that large and small showers differed in character and in origin, the larger ones were designated, after their discoverer, as Hoffmann Stösse.[1] The properties of the small showers are well explained by the quantum theory of the passage of electrons through matter. By this theory, a shower is built up by successive electron-pair formation by photons produced in the collisions of electrons, primary and secondary, with nuclei. Thus as a high energy electron proceeds through matter it is accompanied by a group of other secondary electrons which at first grow in number, and then decrease as the electrons are slowed down and finally stopped by ionization. This mechanism did not seem applicable to the large showers, since they would have to proceed, on the average, through a large thickness of material before they would attain their large size. The large showers appeared to emerge from small thicknesses too frequently to be consistent with the picture of the gradual growth of a shower. For this reason Heisenberg postulated a process in which a large number of electrons were produced by a kind of multiple induced radioactivity in a single nucleus. This explosive character of the process avoids the necessity for a large thickness of material in which to build up the shower. However, Dr. W. H. Furry has calculated the magnitude of the fluctuations from the average to be expected in the ordinary "cascade" process described above, and has found them to be extremely large. Using his results, Doctors C. G. Montgomery and D. D. Montgomery of the Bartol Research Foundation of the Franklin Institute have recently presented evidence[2] to show that the explosive process need not be invoked to explain the occurrence of even the largest showers from thin pieces of material, but that these large showers represent deviations from the expected behavior of high energy electrons and their secondaries passing through matter.

[1] Stösse referred to the kicks of the electrometer connected to Hoffmann's ionization chamber.

[2] C. G. Montgomery and D. D. Montgomery, Phys. Rev. **53**, 955 (1938).

Further Notes on the Physics of Subsidence and Ground Movement in Mines*

BY H. P. GREENWALD**

Central Experiment Station, Bureau of Mines, Pittsburgh, Pennsylvania

Introduction

IN a previous paper[1] there was given a general description of studies in the physics of movement of ground resulting from coal mining; studies of that character are in progress in a number of different countries. Mention was made of data that had been collected on the mechanical properties of coal and of rocks associated with coal. These substances have a certain degree of elasticity but also have time yield under constant load.

The present paper describes work that has been done on minerals that show negligible elasticity but instead flow plastically under load. This problem arose in connection with the mining of potash-bearing salt, which is found approximately 1000 feet below the surface in the Permian basin east of Carlsbad, New Mexico. Inasmuch as portions of this deposit are on the public domain, the problem was of direct interest to the United States Government, and the Bureau of Mines cooperated in an investigation to determine some of the physical properties of the salt, knowledge of which would be useful in establishing proper mining methods.

Nature of the Deposit

Measuring downward from the surface at the location in question, there are approximately 160 feet of water-bearing strata below which are alternate beds of salt and shales. The salt consists mainly of halite (sodium chloride), but at different horizons there are beds in which potash-bearing minerals form a high proportion of the deposit. Thus the bed being mined is a heterogeneous mixture of halite and sylvite (potassium chloride) which have crystallized together, with inclusion of enough red clay to give the whole mass a reddish tinge. In a number of analyses the proportion of sylvite ranged from 46 to 65 percent. At present this bed is the most important source of potash in the United States and is some 10 feet thick. There is no clear-cut separation between it and the overlying strata, merely a very rapid decrease in the proportion of sylvite, so that in a few feet the deposit changes to common rocksalt.

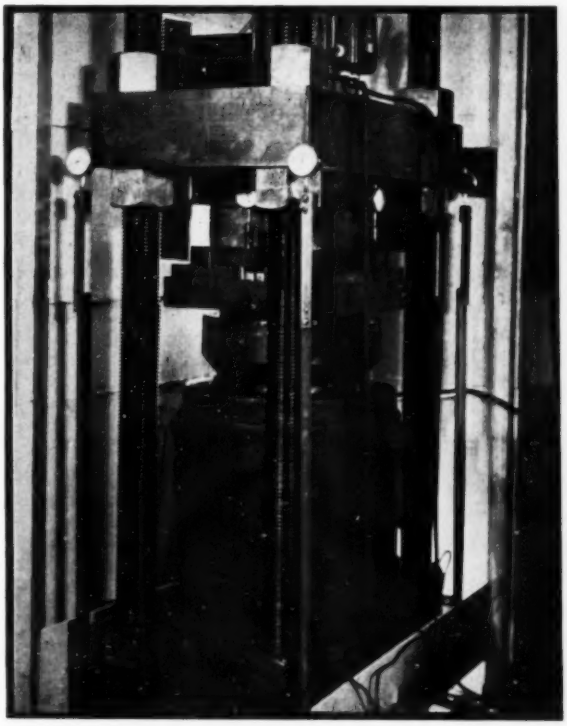

FIG. 1. Final testing assembly, constant temperature cabinet open.

* Published by permission of the Director, Bureau of Mines, United States Department of the Interior. (Not subject to copyright.)

** Supervising engineer, Experimental Coal Mine Section, Central Experiment Station, Bureau of Mines.

Problem of Roof Support

As regards support of mine roof, the problem had two parts. First, under no circumstances could breaks in the roof be allowed that would admit water from overlying strata. Second, the pillars of salt left to support the roof had to be of such size that they could carry the load placed on them without undue compression, which might result either in closing the mine passage-ways or breakage of the roof. Consequently, the mechanical properties of the bed being mined and of the overlying strata were involved.

Blocks of the minerals were cut out in the mine and shipped to the Central Experiment Station of the Bureau of Mines at Pittsburgh, Pennsylvania, where the specimens used in the test work were cut from them. The first tests were to determine the compressibility and bearing strength of the potash salt.[2] Subsequently some additional tests were made to determine the behavior of the roof under cross-bending stress.[3]

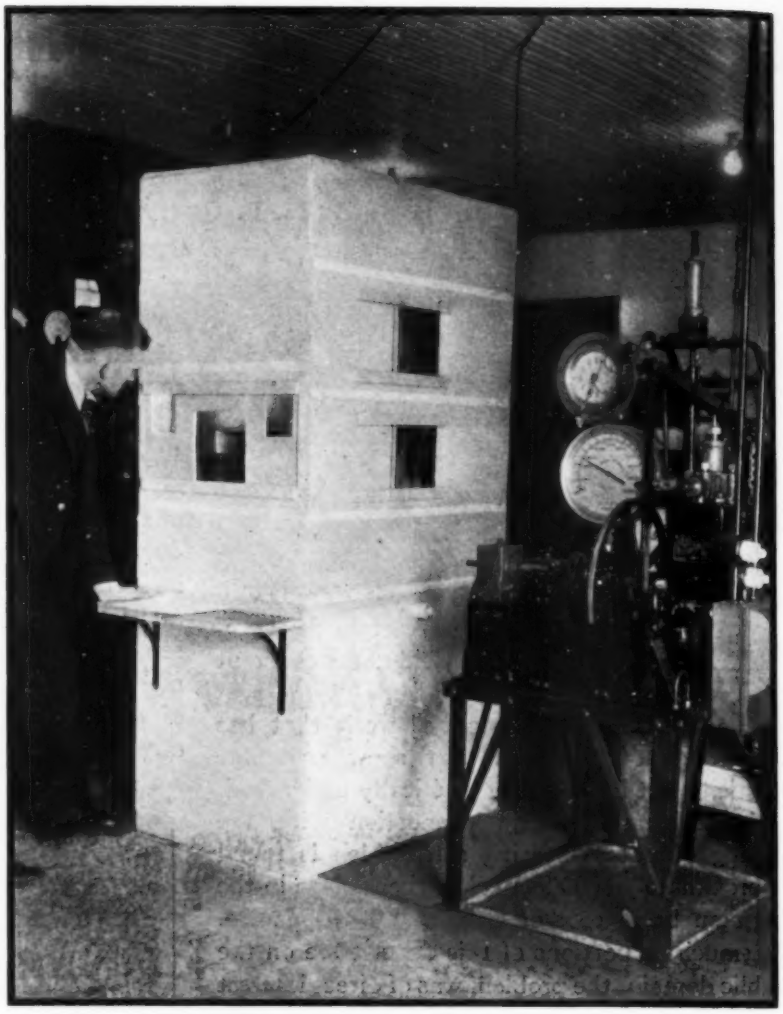

FIG. 2. Complete assembly used in compression tests.

Assembly for Tests of Potash-Bearing Salt

Preliminary compression tests of a 12-inch cube of the potash salt showed that it was a plastic substance, a conclusion that could be predicted from laboratory tests of salt crystals, concerning which there are extensive records in the literature. It was necessary then to include time as a major factor in the test work, and this made desirable use of a hydraulically operated testing machine. Such a machine was not at hand, and one was devised from equipment available. The testing assembly went through several modifications in its development, and only the final arrangements need to be described. Briefly, these comprised a steel frame on the bottom head of which could be placed a 500-ton hydraulic jack, as shown Fig. 1. A spherical bearing was used on top of the ram of the jack. On the square platen of this bearing the specimen under test was placed between steel cover plates. The top cover plate bore directly against the upper head of the frame. Compression of the salt was measured by means of dial gauges attached to the upper cover plate, with their plungers resting against pins fastened to the lower cover plate. The frame was erected in a room in which the temperature fluctuated fairly widely each

day. It was found that these fluctuations caused sufficient thermal expansion and contraction of the salt to affect the records obtained, and it was necessary to enclose the frame in a cabinet as shown in Fig. 2 and to provide electric heat and a thermostat for temperature control.

Figure 2 also shows the automatically controlled pump that maintained pressure in the hydraulic jack. This was merely a single-acting hydraulic pump arranged with gear and cam drive for very slow operation on the downstroke and quick return on the upstroke. Of the two pressure gauges attached to the pump, the larger measured the actual pressure in the line; the second and smaller gauge operated relays that controlled the motor driving the pump. Contacts attached to this gauge could be adjusted to any desired liquid pressure, which was maintained constant within 10 to 15 pounds per square inch. Total liquid pressures were in the range 2000 to 4000 pounds.

Compressibility and Bearing Strength of Potash-Bearing Salt

When an individual specimen was placed under load, it compressed rapidly at first, but the rate of compression decreased and eventually became constant at a considerably lower value. This is illustrated in Fig. 3, which gives the record of specimen 4 for 11 days and of specimen 7 for a little over 4 days. In general, the behavior was that which one would expect from a plastic solid, according to Bingham's analysis.[4] The

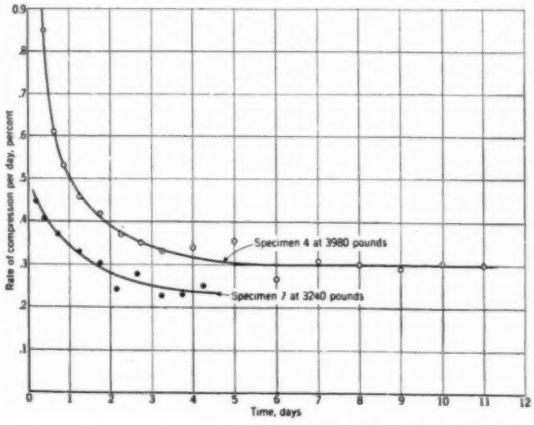

FIG. 3. Rates of compression of potash-bearing salt under constant pressure.

uniform rate of compression established after load had been applied for a few days evidently was the best basis on which to correlate other variables, and it was used throughout the test work. The unit was percentage of the original thickness per day.

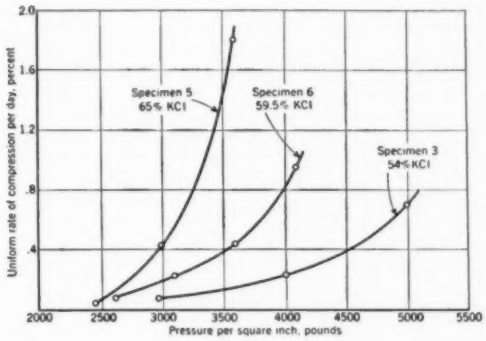

FIG. 4. Effect of pressure and composition on rate of compression of potash-bearing salt at higher loads.

Two of the most important variables were the proportion of sylvite in the mineral and the load applied. The effect of these is shown in Fig. 4. Uniform rate of compression increased rapidly with increasing percentage of sylvite and it was also an exponential function of the load, but there were not sufficient data to justify an attempt at mathematical analysis.

An attempt was made to establish the limiting pressure below which flow would not occur. The data obtained are shown in Fig. 5; in this figure the scale for rate of compression is 10 times that of Fig. 4. It will be observed that in this lower range the curves are no longer properly oriented with regard to percentage of sylvite in the specimen. It was not possible to carry this phase of the work to a satisfactory conclusion, as a limit was reached when the rates of movement became so low that they were of the same order as experimental error.

One other point to be considered was whether the rates of compression would vary with the relative dimensions of the specimen, more especially with the ratio of lateral dimension to height. This was investigated by determining the uniform rate of compression of a given specimen at a number of pressures, after which the specimen was sawed horizontally into two parts, one of which was twice as thick as the other. The rates were then redetermined on the

two portions, and in both instances were found to be the same as with the original specimen. This showed that plastic flow was independent of the ratio of lateral dimension to height so long as the absolute height was sufficient to permit free lateral movement of the salt.

The above data and statements apply up to the start of disintegration of the surface of a specimen—that is, until the compression of the specimen was in the neighborhood of 5 percent. As compression increased beyond this figure, material gradually became detached from the free faces, leaving the balance of the specimen in the shape shown in Fig. 6. This resembles the double-pyramid form of break commonly associated with brittle materials. However, the remaining portion was always entirely solid and without cracks.

As compression continued, the salt flowed laterally, and there was continued spalling of material from the free surfaces. One specimen was compressed 50 percent and after removal from the testing assembly was found to have lost 48 percent of its weight through detachment of material from the free surfaces. The remaining portion was entirely solid and was sawed in two so that the interior could be examined petrographically. Following is a report of the examination:

"Microscopic comparisons of specimens of original and compressed sylvinite, polished and etched with a saturated sodium chloride solution, show that crystals of both potassium chloride and sodium chloride have been plastically deformed by pressure, the deformation being normal to the direction of stress. Sodium chloride has retained quite generally evidence of its original irregularly cubic crystalline structural outline, but potassium chloride has suffered much more severe deformation and in most cases has completely lost its original cubic outline.

"Typical flow structure has been developed, more pronounced with crystals of potassium chloride than with sodium chloride. As mentioned above, the flow has been plastic, therefore there is no evidence of crystal shattering or breakage due to pressure. Some parting along cleavage (slip) planes can be observed in both the compressed and original samples, the number being about equal.

"Adjacent crystals of potassium chloride may coalesce to the extent that grain boundaries are practically eliminated and in some areas coalescence seemed to be complete. Sodium chloride crystals, having suffered less deformation, show far less evidence of coalescence."

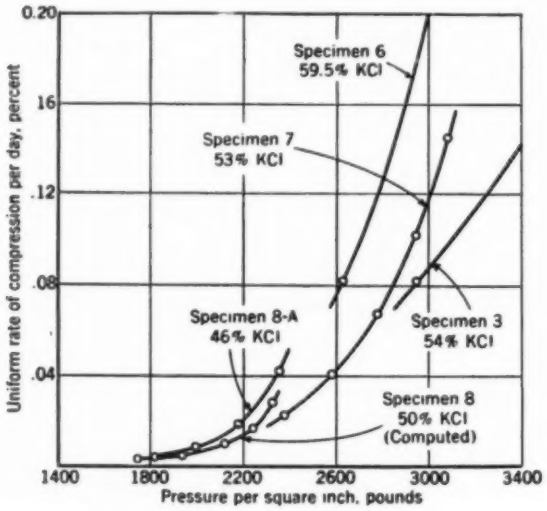

FIG. 5. Effect of pressure and composition on rate of compression of potash-bearing salt at lower loads.

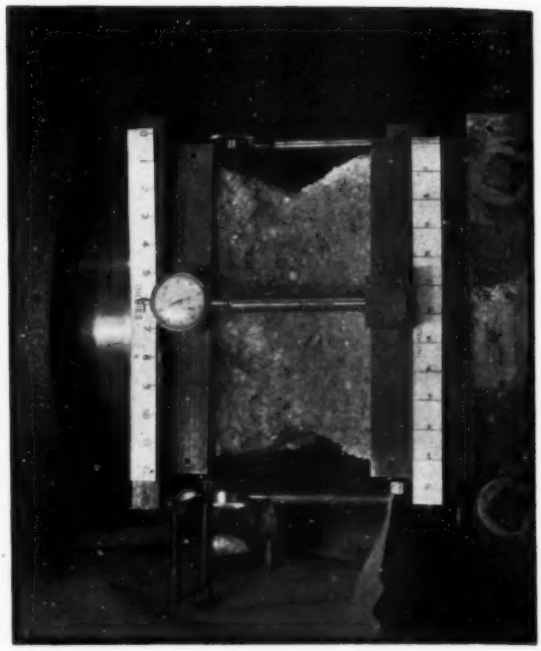

FIG. 6. Disintegration of surface of specimen at high compression.

A second specimen was compressed over 80 percent, with a loss of 93 percent in weight. The part remaining was entirely solid, and plastic flow of the interior had completely obliterated the original crystalline structure insofar as could be told without examination under the microscope.

All the data obtained indicated that failure of a mine pillar would be by plastic flow and that

the time during which a given load will be supported is as important in determining the behavior of a pillar as is the load itself. Such behavior is a great advantage in that sudden failures are not likely and periodic measurements of proper accuracy will indicate whether or not movement is taking place, even though this movement is too small to be observed by eye during ordinary mining operations.

Behavior of Roof Salt Under Cross-Bending Stress

The foregoing tests gave a good idea of what behavior might be expected from pillars of the potash-bearing salt, but gave no indication concerning the behavior of the fairly pure rocksalt that formed the roof. Sodium chloride is known to be much less plastic than potassium chloride, and in consequence it is to be expected that the roof would be far more rigid than the pillars. There would then be more danger of cracks in it as the result of localized concentration of stress. In some quarters it was feared that the roof might shear along the edges of supporting pillars, with resultant opening of cracks to water-bearing strata. Obviously, this phase of the problem was far more complicated than simple determination of the behavior of the potash-bearing salt under compressive stress, and it was realized that such tests as could be made would give only general indications of the behavior that might be expected in the mine.

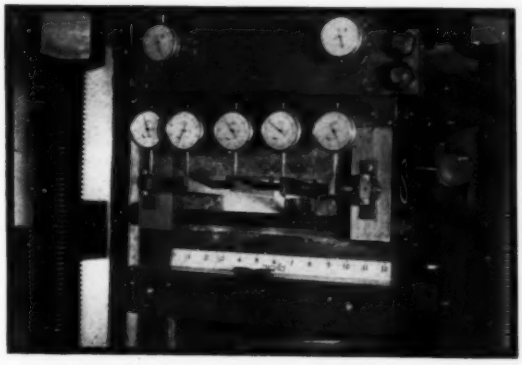

FIG. 8. Complete assembly used in cross-bending tests of roof salt.

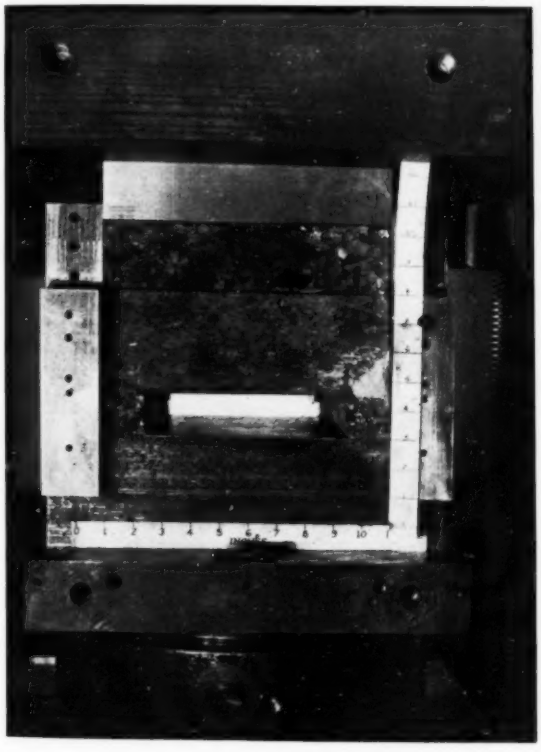

FIG. 7. Part of assembly used in cross-bending tests of roof salt.

So long as the roof strata remain unbroken, any portion thereof delimited by imaginary vertical planes is restrained on all sides by the surrounding material, and this restraint causes important modifications in behavior. It was necessary to have some reproduction of this restraint in the test work and this was obtained by constructing a heavy steel frame in which the assemblies under test were placed. Fig. 7 shows this frame partly disassembled, with an assembly of potash-bearing and roof salt in it. This assembly consists of two blocks of the potash-bearing salt, representing mine pillars, resting on the bottom of the frame. Resting on them is a slab of the roof salt; the free space under this slab represents a mine passageway. It was necessary that the material transmitting the load to the roof salt be able to follow any bending or distortion thereof and a slab of the more plastic potash-bearing salt was inserted under the steel block that acted as a plunger in the frame. Fig. 8 shows the assembly completed; dial gauges were used on both ends to determine movement of different parts of the roof-salt slab and to indicate any distortion of the restraining frame

itself. The restraining frame rests on the square platen of the aforementioned spherical bearing, and the steel block acting as a plunger in the frame bears against the top head of the large frame shown in Fig. 1.

When one of these assemblies was kept under constant load, curves relating movement of different portions of the roof salt slab to time were of the same shape as those shown in Fig. 3. Uniform rates of movement were established, but a longer time was required to establish them than was the case with simple compression. About 60 days were required to carry each test to a satisfactory conclusion.

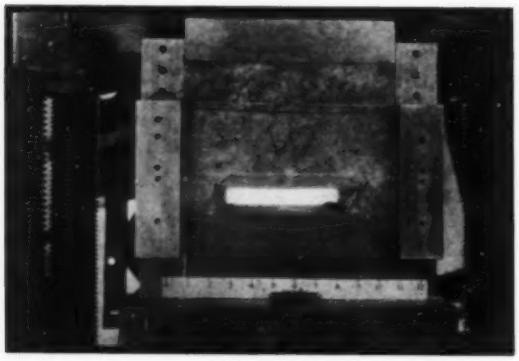

FIG. 9. Assembly of potash-bearing and roof salts after test.

Figure 9 shows the condition of one assembly after test. The roof-salt slab was bowed downward in the middle, as can be seen by comparison of its top and bottom surfaces with straight lines that have been marked above them. In this assembly the pillar at the right was loaded sufficiently to start disintegration.

A tension crack developed near the center of the under surface of the roof-salt slab, but this did not extend any great distance upward into the slab. Of greater importance was the development of an arch-shaped crack over the free span. The lateral restraint offered by the steel frame is responsible for development of this manner of failure.

It can be recognized at once that there are two important gaps in the data so obtained: First, the amount and distribution of lateral restraint was not measured, and, second, the frictional forces between the salt and the steel frame were unknown. However, the information obtained sufficed to make qualitative application to the problem in hand, and it was judged that the value of further test work was insufficient to justify the expensive and complicated apparatus that would be required to measure friction and lateral restraint.

Summary

The compression tests of blocks of potash-bearing salt indicated that load on mine pillars composed thereof should not be much more than 2,000 pounds per square inch when these pillars are expected to stand a considerable number of years. So long as the roof strata remain unbroken, there is little likelihood of shearing along the edges of pillars. Apparently the immediate roof stratum is sufficiently thick to permit development of the arch-shaped crack without having this crack reach the top of the stratum. It is a crack of this nature that should be looked for as a first indication that the roof is overloaded. The observed behavior of these materials, which results in large part from their plastic properties is of great practical importance as it is possible to devise methods of mining by which practically all of the valuable potash-bearing salt can be recovered without breaking the roof. Instead, the roof can be made to subside gradually into the area from which the potash-bearing salt has been removed.

References

1. H. P. Greenwald, "The Physics of Subsidence and Ground Movement in Coal Mines," J. App. Phys. **8**, 462–469 (1937).
2. For a full account of this work see H. P. Greenwald, and H. C. Howarth, "Tests of the Compressibility and Bearing Strength of Potash Salt," Tech. Paper 575, Bureau of Mines, 1937, 32 pp.
3. For a description of this work see H. P. Greenwald, and H. C. Howarth, "Compression Tests of Roof-Salt Slabs Supported by Potash Salt Pillars," Report of Investigations 3386, Bureau of Mines, February 1938, 16 pp.
4. Eugene C. Bingham, *Fluidity and Plasticity*, Chap. VIII (1922), pp. 215–240.

Physics in Pharmacy

BY RONALD L. MCFARLAN

United Drug Company, Boston, Massachusetts

Introduction

ALL of the officially recognized formulas and assay methods of the pharmaceutical industry are contained in two compilations, the *United States Pharmacopoeia* and the *National Formulary*. The formulas and assay methods thus listed have been adopted as the best available on the basis of long and extensive tests. It is consequently of interest to note that many of the assay methods listed involve the use of physical principles. But it is only comparatively recently that the possible pharmaceutical applications inherent in the science of physics have begun to be seriously explored. Many of the most fruitful of these applications have been made in the field of optics, where it has been found possible in many cases to make quantitative analyses and assays more accurately and rapidly than by chemical and biological methods.

Spectroscopy

The use of spectroscopy as a tool for quantitative chemical analysis has long been known. With the development of modern techniques spectroscopic methods have afforded unique advantages for certain types of analyses, although these assay methods are still too new to be officially recognized by the *Pharmacopoeia*. The use of emission spectra for the detection of small metallic impurities is rapidly gaining in popularity. The high sensitivity of emission spectral methods of analysis, the speed of working, the extremely small quantity of substance required, and the ability to simultaneously analyze for many metals all contribute to the efficacy of this type of analytical method. The lowest limit for detecting and measuring many substances is less than one part per million, and—depending on the type of analysis—the time required per analysis may vary from fifteen to sixty man-minutes. Typical examples of this type of analysis are found in the analysis of sodium bromide for concentrations of potassium ranging from 0.05 percent to 2 percent, and the analysis of potassium bromide for concentrations of sodium ranging from 0.01 percent to 2 percent.[1]

The usefulness of absorption spectra as an analytical tool has also become widely recognized. Many substances which otherwise could be assayed only by biological methods or very complex chemical analyses are readily identified and measured by means of their absorption spectrum. A good illustration of such a procedure is found in the determination of the vitamin A potencies of fish liver oils. The existence of a relation between the vitamin A potencies of fish liver oils and their ultraviolet absorption spectrum has been known for some time.[2] Comparisons of physical tests and the biological activity of these oils have led to the establishment of a relationship between the 3280A absorption band and the vitamin A content. The ultraviolet absorption curve of vitamin A is shown in Fig. 1.[3]

On the basis of this relationship various physical instruments have been developed for measuring vitamin A concentrations.[4–7] All these instruments measure quantitatively the absorption of light in the 3280A region by oils containing vitamin A. A schematic diagram of one such instrument—which has been in commercial operation for eighteen months—is shown in Fig. 2.[6] With this instrument it has been found possible to obtain a measurement of the vitamin A potency of a properly diluted oil to one percent accuracy in less than two minutes, exclusive of the time required for diluting the oil. The potency of vitamin A containing materials varies enormously, and it is a tribute to the efficacy of modern spectroscopic technique that a satisfactory degree of accuracy can be obtained not only with concentrates—ranging from 20–100 percent vitamin A—but also for butters containing as little as perhaps 0.0004 percent of

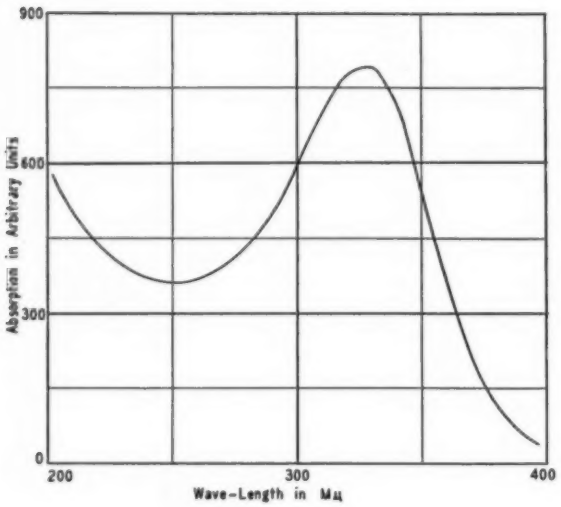

FIG. 1. Ultraviolet absorption curve of vitamin A.

vitamin A. Absorption spectral methods for assaying some of the other vitamins are known, and it is undoubtedly just a matter of time before some of these methods will be officially described in the *Pharmacopoeia*.

Fluorescence

In the routine examination of drugs for control purposes there is often a need for a quick method of detecting the presence of impurities. One excellent tool for this purpose is a properly constructed fluorescent lamp. With such a lamp, for example, it is possible to show very easily the presence of petrolatum in other fats, beeswax in carnauba wax, and mineral oil in other oils.

Not only does the fluorescent lamp provide a a ready means for differentiating between certain drugs, but it also serves as a quick method of qualitative analysis. To illustrate, ergot fluoresces blue, digitallin a weak yellowish-green, and strophanthin a bright blue. Hydrastine sulphate shows no fluorescence when first prepared, but slowly develops a fluorescence on standing in the cold. In many cases spectrophotometric curves of drug fluorescence have been plotted, and can be used for quantitative analysis.

The photoelectric fluorometer has recently been adapted to the measurement of aneurin—vitamin B_1.[8] This method depends on the quantitative oxidation of vitamin B_1 by potassium ferricyanide with the consequent formation of fluorescent thiochrome. Results are obtained which are in fair agreement with those from the animal experimentation method.

Fluorescence also affords a very rapid means of checking on the stability of certain drugs, particularly when these drugs pass through a somewhat complicated manufacturing process. By observing the change in the color of fluorescence of these drugs at various stages of the manufacturing process it is possible to tell whether the drug is present in its original form, or whether it has partially or completely broken down. To illustrate, aspirin—acetyl salicylic acid—shows little or no fluorescence in its pure form, but one of its decomposition products, salicylic acid, fluoresces a strong bluish-white. When aspirin is mixed with effervescent salts as is done in preparing some pharmaceutical products, it shows a definite tendency to decompose if appreciable amounts of moisture are present. A simple, routine check of the finished product under the fluorescent lamp provides an excellent test for the presence of salicylic acid, and consequently for the state of the aspirin incorporated in the product.

Colorimetry

The colorimetric tests that are officially recognized at present by the *Pharmacopoeia* consist of the visual comparison of the colors of pharmacopoeial drugs or pharmacopoeial tests with the colors of standard colorimetric solutions. Examples of such standard solutions are cobaltous chloride solution, ferric chloride solution and cupric sulfate solution, and are prepared in accordance with a definitely specified procedure.

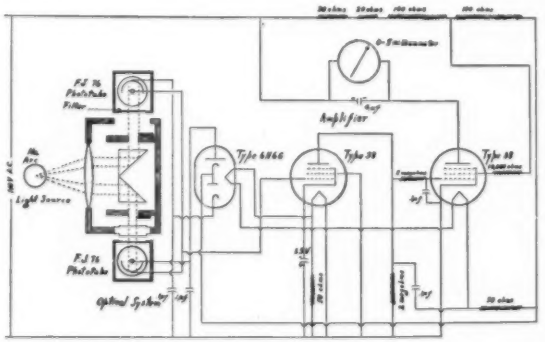

FIG. 2. Diagram of photoelectric vitamin A photometer.

In making comparisons the *Pharmacopoeia* states that the several containers shall be of clear colorless glass which must be alike in cross section, and that the comparison of colors must be made of layers of equal thickness viewing them transversely against a background of white porcelain or glass.

It is possible to assay vitamin A with some accuracy by means of a colorimetric method. When vitamin A-containing oils are treated with the reagent of Carr and Price[9]—a saturated solution of antimony trichloride in pure, alcohol-free chloroform—a blue color is produced. When this color is examined by means of a visual spectroscope it is seen to result largely from a sharp absorption band with its maximum near 6200A. The intensity of the blue color produced is used as a measure of the vitamin A concentration.

A further extension of the antimony trichloride colorimetric method to vitamin D has been worked out by Heggie and Milas.[10] Oils containing both vitamins A and D are treated with antimony trichloride, and the resulting absorption properties are analyzed with a Hardy color analyzer. Two absorption peaks—whose intensity does not remain constant with time—are found, one due to vitamin A and the other due to vitamin D. Since it has heretofore been impracticable to assay vitamin D by means of its absorption spectrum, the antimony trichloride colorimetric absorption offers considerable promise as a future practical assay method.

The rapidly increasing number of commercially available colorimeters and color analyzers is indicative of the rapidly growing importance of this kind of analytical technique.

Polarization

Among the materials recognized in the *Pharmacopoeia* there are a number, particularly certain essential and volatile oils and related bodies, for which the determination of optical activity is of great importance. Since the property of optical activity is inherently related to the chemical structure of the substance possessing this property information regarding the amount and character of its optical activity may serve to determine its concentration or purity in a solution where the other components are optically inactive. In some cases the proof of optical inactivity is also very significant.

Both the polarizing microscope and the polariscope are extensively used in this connection. The polarizing microscope is most frequently used for testing solid substances whereas the polariscope is primarily adapted for liquids. Because of its ability to accurately determine the various indices of refraction associated with crystals the polarizing microscope affords an excellent means of crystal identification. This identification can be carried out even though the crystals are available only in small fragments or in minute quantities. In addition, the polarizing microscope can be used to detect impurities and to study surface phenomena in various suspensions. This latter application is of importance in the study of colloidal suspensions after passing through the homogenizer. For example, various ointments can be examined to make certain that the oil globules have been broken down to the proper size and uniformity. Both the polarizing microscope and the polariscope afford quick and accurate means of processing control.

Index of Refraction

Indices of refraction are readily determined by means of a polarizing microscope or a refractometer. As mentioned above, the polarizing microscope is applicable to the measurement of solids, while the refractometer is generally employed for examining liquids. Several types of refractometers which permit rapid and accurate determination of the indices of refraction are available. For making observations over the entire range of refractive indices of pharmacopoeial materials the Abbe and Zeiss immersion refractometers are the ones generally employed. A knowledge of the index of refraction is important, for example, in judging the purity of flavoring oils and determining the sugar content of syrups.

Photoelectricity

With the increasing application of optical principals to the problems of pharmaceutical analysis it is natural that photoelectric devices should frequently be employed to measure the

light intensities by means of which many pharmaceuticals are analyzed. The application of photoelectric technique to the measurement of the vitamin A content of fish liver oils has been mentioned earlier. It is but a matter of time before photoelectric instruments will be used to assay other vitamins as well. These instruments are not only supplanting and replacing many of the older methods, but are also opening new fields of research.

Color comparators and analyzers which are based on photoelectric methods of light intensity measurement are finding many useful applications. The reason for the growing popularity of photoelectric color-measuring equipment lies in the rapidity of making observations, the absence of eye fatigue, the elimination of the necessity for a trained observer, the full intensity at the end regions of the spectrum, and the high accuracy of the observations. Among the useful pharmaceutical applications are the colorimetric determinations of hydrogen ion concentrations, fluorescence measurements, micro-analyses, and complex organic and biological assays. The ready adaptability of the photoelectric color comparators to opacity and turbidity measurements increases their usefulness to the pharmaceutical chemist.

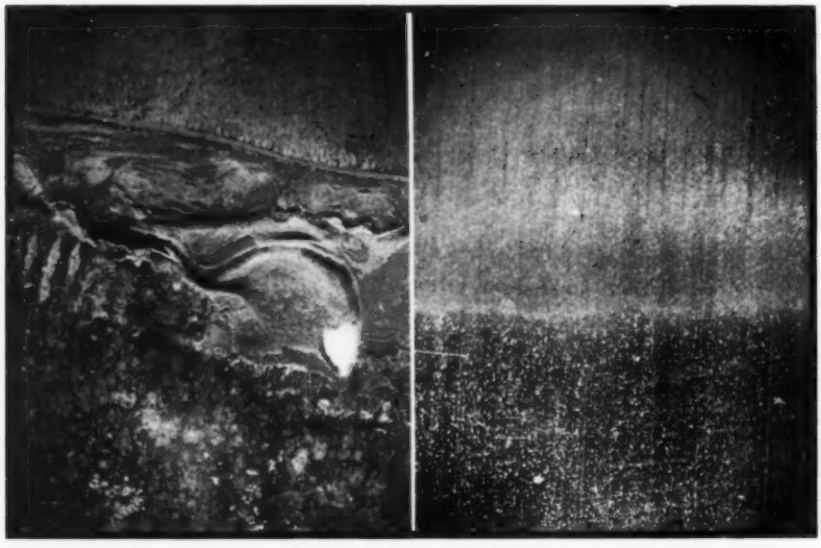

(a) (b)

FIG. 3. (a) Section of collapsible tin tube showing corrosion by untreated milk of magnesia. (b) Section of collapsible tin tube showing absence of corrosion by milk of magnesia containing $\frac{1}{10}$ citric acid.

Miscellaneous Electrical Applications

One of the most useful quantities with which the modern pharmaceutical chemist has to deal is hydrogen ion concentration or *p*H, as its negative logarithm is called. By measuring the *p*H of a solution accurately it is possible to describe quantitatively the acidity or alkalinity of the solution. The latest edition of the *Pharmacopoeia*, known as U.S.P. XI, contains several preparations that require *p*H control. Milk of magnesia furnishes a good illustration of one of these preparations.[11] If left standing in a glass bottle for several months it shows a definite tendency to increase in alkalinity, which increase is accompanied by the development of an unpleasant taste. The addition of a very small amount of citric acid prevents the alkalinity from increasing, and consequently the U.S.P. XI provides for the addition to milk of magnesia of amounts of U.S.P. citric acid up to 0.1 percent.

The *Pharmacopoeia* provides for the determination of the *p*H of solutions by means of indicator solutions, a method which is accurate to about 0.2 *p*H. With properly designed vacuum tube voltmeters *p*H measurements are easily and rapidly carried out to 0.01 *p*H. One method of doing this is based on the fact that when glass electrodes are immersed in liquids of various degrees of acidity and alkalinity different potentials are developed at the surface of the electrodes. These potentials correspond to definite hydrogen ion concentrations, and are rapidly measured with appropriate vacuum tube voltmeters.

By accurately determining the dielectric constant of various materials it is possible to gain useful information for the pharmaceutical chemist. For example, in the manufacture of effervescent tablets it is very important that the

moisture content of the tablet be kept very low. Since the dielectric constant of such a tablet varies sharply with its moisture content the capacity bridge affords an excellent method for the routine measurement of the moisture content of such tablets. The capacity bridge is especially well adapted for such measurements since the tablets are apt to vary slightly in thickness as they come off the punching machine.

In addition, dielectric constant measurements can be used as sensitive means of detecting the presence of small concentrations of certain impurities. The close relation between dipole moment and the structure of organic compounds is being extensively studied, and offers considerable promise as a future method for pharmaceutical control.

It is often necessary to measure the viscosity of many heavy and opaque viscous liquids, such, for example, as milk of magnesia. The vacuum tube amplifier makes possible one very simple method of checking the viscosity of such liquids.[12] A quantity of the liquid to be tested is placed in an inclined glass tube which is inserted between two spaced coils in the grid circuit of a vacuum tube. A heavy steel ball is then rolled through the liquid in the glass tube, and when this ball passes through the two coils it produces impulses in the plate circuit that are readily detected. The time required for the ball to roll the distance in the tube between the two coils at a given angle and temperature is a measure of the viscosity of the liquid.

X-Rays

The use of x-rays as a tool for both qualitative and quantitative chemical analysis offers the pharmaceutical chemist certain advantages. In many cases it is possible to identify and quantitatively measure unknown compounds without destroying the sample in any way. In particular, x-ray powder diffraction patterns supply information desired by the pharmaceutical chemist. It is often important to know whether a mixture is homogeneous or heterogeneous, and what the grain size of the components of the mixture are. For example, x-ray powder diffraction photographs afford a sensitive test for particle size and homogeneity of dispersion of aspirin when mixed in a glucose-sucrose base.

Miscellaneous Applications

In the manufacture of many pharmaceutical products humidity control is of great importance. This is particularly true in the case of some effervescent salt preparations, which are not only hygroscopic but decompose as the result of the catalytic action of any moisture which they may pick up. These preparations must be manufactured under a relative humidity not exceeding 30 percent, and must be so packaged that they will not pick up enough moisture to start decomposition until they are used. This means that the containers must have an air-tight seal, or else the air flow into and out of the containers as a result of barometric pressure changes would pump sufficient water vapor into the containers to start decomposition. But, on the other hand, the seal must be capable of permitting gases under high pressure to escape from the container since, if decomposition commences, large amounts of gas are generated and the container might otherwise burst.

The optical properties of the containers are at times of considerable importance. Many pharmaceuticals lose their potency on continued exposure to daylight, and consequently must be packaged in dark containers. Cod-liver oil, for example, if allowed to stand exposed to daylight for a few hours shows a marked decrease in its vitamin A potency.

Cod-liver oil also furnishes an example of the successful application of modern high vacuum technique to the concentration of vitamin A.[13] By the molecular distillation of cod liver oil under very high vacuum Hickman has succeeded in producing a tasteless cod liver oil and also a high concentrate of vitamin A, both on a commercial scale. An integral part of this development has been the design and construction of very efficient molecular diffusion pumps.

Conclusions

The principal purpose of this article has been to describe briefly some of the applications of physical principles to pharmaceutical problems that are now in actual use. The possibilities for further applications in the future are large, and such applications should be made rapidly. Spectroscopy—from ultraviolet to infra-red—vacuum

tube techniques, possibly some of the methods of nuclear physics—such as marked radioactive atoms—as well as other fields of physics all appear to offer excellent possibilities for future application to the problems of the pharmaceutical chemist. It is probably only a matter of time before many of these methods will be so universally adopted as to be officially recognized by incorporation into the *United States Pharmacopoeia*.

Bibliography

1. J. S. Owens, J. Ind. & Eng. Chem., Anal. Ed. **10**, 64 (1938).
2. Morton and Heibron, Biochem. J. **22**, 987 (1928). Drummond and Morton, Biochem. J. **23**, 785 (1929). Coward, Dyer, Morton and Gaddum, Biochem. J. **25**, 1102 (1931); **26**, 1593 (1932).
3. Morton, *Absorption Spectra of Vitamins and Hormones*, P.
4. Olav Notevarp, Biochem. J. **29**, 1227 (1935).
5. Milas and Farmer, Presented at Am. Chem. Soc. Meeting, Sept., 1936.
6. McFarlan, Reddie, and Merrill, J. Ind. & Eng. Chem. **9**, 324 (1937).
7. Bills and Wallenmeyer, Presented at Meeting of A m Soc. Biol. Chem., April, 1938.
8. Jansen, Rec. trav. chim. **55**, 1046–1052 (1936). Zeits. f. Vitaminforsch **5**, 254 (1936).
9. Carr and Price, Biochem. J. **20**, 497 (1926).
10. Heggie and Milas, Presented at Am. Chem. Soc. Meeting, April, 1937.
11. Bowles and Merrill, J. Am. Pharm. Assoc. **26**, 717 (1937).
12. L. Podolsky, Electronics, July (1933).
13. K. C. D. Hickman, J. Ind. & Eng. Chem. **29**, 968 (1937).

Here and There

New Appointments and Promotions

The following changes have been made in the Department of Physics at the University of Illinois: Professor F. W. Loomis, head of the department, has leave of absence during the first semester of 1938–39. During his absence Associate Professor P. Gerald Kruger will be acting head. Dr. M. Goldhaber, formerly at the Cavendish Laboratory, Cambridge, England, and Dr. J. R. Richardson, formerly national research fellow at the University of Michigan, have been appointed Assistant Professor of Physics. Dr. L. J. Haworth, formerly Lalor fellow in physical chemistry at the Massachusetts Institute of Technology, and Dr. E. M. Lyman, formerly of the University of California, have been appointed associates, and Dr. D. W. Kerst, formerly with the General Electric X-Ray Corporation, has been appointed instructor.

★

Howard V. Smith of Eldorado, Kansas, has been appointed chief chemical engineer of the Barber Asphalt Corporation in charge of the company's technical department, James E. Auten, president, announced. J. Strother Miller, Jr., formerly director of the technical department of the Barber Asphalt Corporation, has been advanced to be technical adviser to the company.

Dr. Melba Phillips, of Connecticut College, Dr. Arthur R. Sayer, of Northwestern University, and Mr. Donald B. Woodbridge, of the College of Charleston, have accepted positions as instructors in the Physics Department at Brooklyn College.

★

Dr. E. C. McCracken has resigned his position in the Physics Department at the Iowa State College. He has accepted a position at Teachers College, Columbia University, where he will have charge of the work in Physics.

★

At Cornell University, Dr. Jacob R. Collins has been promoted from an assistant professorship to a full professorship in physics and Dr. Lyman G. Parratt has been promoted from an instructorship to an assistant professorship in physics.

★

Dr. H. J. Gough, superintendent of the department of engineering of the National Physical Laboratory, has been appointed to the new post of director of scientific research at the British War Office.

Nonresident Lecturers at Cornell

During the academic year 1937–38 reports by nonresident speakers were presented at meetings of the faculty and graduate students in physics at Cornell University as follows:

Nov. 1. **Molecular Beam Methods of Measuring Nuclear Moments,** I. I. RABI, *Columbia University.*
Nov. 22. **The Diffraction of Fast Electrons by Gas Molecules,** LINUS PAULING, *California Institute of Technology.*
Dec. 16 and 17. **The Dielectric Constant of Liquids and Solids; and Ferromagnetic Anisotropy,** J. H. VAN VLECK, *Harvard University.*
Jan. 17. **Stresses and Constitutional Changes in Glass During Cooling,** H. R. LILLIE, *Corning Glass Works.*
Feb. 14. **Some Vacuum Tube Research Problems,** B. J. THOMPSON, *RCA Research Laboratory.*
Mar. 21. **Some Problems of Galactic Dynamics,** K. LUNDMARK, *University of Lund.*
Mar. 24. **Transmutations of Heavy Nuclei,** V. WEISSKOPF, *University of Rochester.*
Apr. 18. **Recent Work in the Cavendish Laboratory,** M. GOLDHABER *University of Cambridge.*
May 9. **Some Physical Phenomena at the Temperature of Liquid Helium,** E. F. BURTON, *University of Toronto.*
May 23. **Crystal Fluorescence,** FREDERICK SEITZ, *General Electric Research Laboratory.*

★

Honorary Degrees Conferred

The University of Western Ontario at London, Canada, conferred on June 1 the doctorate of laws on Dr. Henry Asbury Christian, Hersey professor of the theory and practice of physics at Harvard University, who gave the commencement address.

★

The doctorate of science was conferred by Rutgers University on June 12 on Dr. Gano Dunn, of New York City, for "achievement in electrical engineering," and on Lincoln Ellsworth, polar explorer.

★

Dr. Robert A. Millikan, chairman of the executive council of the California Institute of Technology, received an honorary degree at the seventy-second commencement of Loyola University, Los Angeles.

★

The Doctorate of Science was conferred at its two hundred and eighty-seventh commencement by Harvard University on Dr. Irving Langmuir, associate director of the Laboratories of the General Electric Company at Schenectady, New York.

★

The University of Nebraska at its sixty-seventh annual commencement conferred the Doctorate of Science on Dr. John Torrence Tate, Professor of Physics and Dean of the College of Science, Literature and Arts of the University of Minnesota.

★

The University of Pittsburgh conferred the doctorate of science degree on Dr. F. L. Bishop, Professor of Physics, for "his outstanding work in physics and engineering."

Dr. Floyd K. Richtmyer, Professor of Physics and Dean of the Graduate School of Cornell University, received the honorary degree of Doctor of Science at the commencement exercises of Lehigh University on June 14.

★

Arthur C. Hardy, Professor of Optics and Photography, received an honorary doctor of science degree from St. Lawrence University on June 13. This degree was conferred for Dr. Hardy's "distinct contribution to education as a physicist, author, and inventor."

★

Dr. John H. Dellinger, chief of the radio section of the National Bureau of Standards in Washington, received the gold medal of honor of the Institute of Radio Engineers at the opening convention of the institute in New York City on June 16. The Morris Liebmann memorial prize of $290 was given to George C. Southworth, of the Bell Telephone Laboratories, for his work on ultra-high frequency waves. Arthur L. Samuel, also of the Bell Telephone Laboratories, received an award of $100 for the best paper published in the *Proceedings* of the institute during 1937.

★

Dr. Janet Howell Clark, formerly associate professor and now lecturer at Johns Hopkins University, and since 1935 head of the Bryn Mawr School in Baltimore, has been appointed professor in the Division of Biological Sciences and Dean of the College for Women at the University of Rochester.

★

Willis R. Whitney, non-resident Professor of Chemical Research, received the Marcellus Hartley Public Welfare Medal of the National Academy of Sciences in April.

★

Gilbert N. Lewis, Former Staff, received the Theodore William Richards Medal of the Northeastern Section, American Chemical Society, May 13.

★

Round Table Discussion

A Round Table Discussion on the Nature of Hardness has been organized by the Physics of Metals Committee. This discussion is to take place on the evening of October 19 during the forthcoming A. S. M. meeting at Detroit. A complete program of papers dealing with the following subjects has been arranged: Mechanical and Metallurgical Aspects of Hardness, Work Expended in Indentation Hardness Tests, Physical Quantities Relative to Interatomic Forces, Relation of Compressibility to Hardness, Relation of Plastic Behavior to Hardness, Plastic Deformation of Metallic Single Crystals as Related to Hardness, Quantum Mechanical View of the Interatomic Forces Relative to Hardness.

Further details may be obtained from the meeting chairman, Professor D. E. Ackerman, Purdue University, Lafayette, Indiana.

Contributors to This Issue

Dr. Ronald L. McFarlan received his A.B. degree from the University of Cincinnati in 1926, and his Ph.D. degree from the University of Chicago in 1930. He was a National Research Council fellow in physics at Harvard University from 1930–1932, and an instructor in physics at Harvard University from 1932–1935. Since 1935 he has been research physicist with the United Drug Company.

Dr. Frederick A. Maxfield received his B.S. in Electrical Engineering from the University of Wisconsin in 1929, his M.S. in Physics from the University of Pittsburgh in 1934, and his Ph.D. from the University of Wisconsin in 1938. Between 1929 and 1934 he was engaged in research work on mercury arc rectifiers at the Westinghouse Electric & Manufacturing Co. Since 1934 he has been instructor in Electrical Engineering at the University of Wisconsin.

Mr. Herbert Nelson received his B.S. from Hamline University, Minnesota, in 1927 and his M.A. in physics from the University of Minnesota in 1929. He was connected with the Engineering Department of the Westinghouse Electric & Manufacturing Company, Bloomfield, N. J. from 1929 to 1930. Since 1930 he has been engaged in research on thermionic and secondary electron emission problems in the Research and Engineering Department of the RCA Manufacturing Company, Inc., Harrison, N. J.

Dr. Lan Jen Chu received his B.S. in Electrical Engineering from Chiao Tung University, Shanghai, China, in 1934, and his S.M. and D.Sc. in Electrical Engineering from Massachusetts Institute of Technology in 1935 and 1938. He is a Post Doctorate Research Fellow at Massachusetts Institute of Technology.

Dr. G. L. Fredendall received his Ph.D. degree from the University of Wisconsin in 1936. From 1933 until 1935 he conducted research in mercury arc phenomena under a Regent's Fellowship at the University of Wisconsin. Since 1936 he has been Research Engineer in Television at the RCA Manufacturing Company.

G. L. Fredendall

Frederick A. Maxfield

Herbert Nelson

Harold Vagtborg

Ronald L. McFarlan

Lan Jen Chu

Caryl P. Haskins

Dr. Caryl Parker Haskins, Director of the Haskins Laboratory, received the degrees of Ph.B. and Ph.D. in physiology from Yale and Harvard Universities, respectively. From 1931 until 1935 he was Research Chemist with the General Electric Company. Since 1935 he has been Research Associate at Harvard and Massachusetts Institute of Technology. In 1937 he was appointed Research Professor at Union College. At present he is interested in the general biological effects of irradiation.

Mr. Harold Vagtborg received his B.S. from the University of Illinois in 1926 and his M.S. from Armour Institute of Technology in 1931. He is a member of the American Society of Civil Engineers, the American Public Works Association and the Society for the Promotion of Engineering Education. He has been Professor of Municipal and Sanitary Engineering and is now Managing Director of the Research Foundation of Armour Institute of Technology.

Some of the New Books

Piezoelektricität des Quarzes. ADOLF SCHEIBE. Oberregierungsrat als mitglied bei der Physikalisch-Technischen Reichsanstalt. Pp. 233, Figs. 175, Tables 20. Verlag von Theodor Steinkopff, Dresden, 1938.

This is a comprehensive summary of the various investigations of the piezoelectric effect in quartz and its many applications. The first section of the book deals with the static piezoelectric effect. Following a historical introduction, the experimental methods used in demonstrating this property of quartz are discussed in detail. It is shown how pressures in engines, guns, etc., can be measured by the use of different types of piezoelectric pressure chambers. In this connection an ungenerous remark is made that with one exception only German work will be reviewed since it includes all that is worth knowing. It is fortunate for the value of the book that this attitude does not prevail throughout. Detailed explanations are given of the various methods for determining whether a crystal is piezoelectric or not. It is only in this discussion that the author deviates from the special substance, quartz. The general equations for describing the piezoelectric and elastic properties of crystals are given, and other related topics such as that of temperature coefficients are discussed.

The second part of the book deals with quartz crystal resonators. Here again, the many experimental methods for studying the resonance phenomenon and the applications of quartz crystals in radio circuits are neatly summarized. The methods used in studies of electrical and optical characteristics of oscillating quartz crystals are presented with the results of such studies. The third section deals with crystal control of sending circuits in theory and in practice. Other miscellaneous material on crystal clocks, ultrasonic waves, and x-ray diffraction by oscillating quartz plates is treated at the end of the book.

This is a very valuable monograph which contains a great deal of practical information on the many uses of piezoelectric quartz plates. Though restricted to quartz, the experimental methods and general principles are obviously applicable to the study of other crystals, which are, however, at present of far less practical importance than quartz.

JOSEPH VALASEK
University of Minnesota

Moderne Mehrgitter—Elektronenroehren I (Modern Multiple Electrode Tubes). Dr. M. J. O. STRUTT. Pp. 129, Figs. 128. Julius Springer, Berlin, Germany. Price RM 12.60.

Dr. Strutt is a member of the research staff of the Phillips Incandescent Lamp Works, Ltd., at Eindhoven, Holland. He is known to radioengineers in this country for his analyses of conversion detection and anode bend detection.

The purpose of this book as expressed in the author's foreword is to fill a gap in the present scattered world literature with a compact volume "which will present in an easily assimilable and yet not elementary fashion the ideas which furnished the motivation for the development of the modern multiple grid tubes." In this he has succeeded and the book makes a worthy addition to the library of anyone particularly interested in the subject. There is no equivalent publication in the English language.

The book is divided into three parts: (I) High Frequency Voltage Amplifier Tubes, (II) Mixing Tubes, (III) Low Frequency Power Amplifier Tubes. All of the well-known tube types are represented including simple secondary emission and electron deflection tubes. The treatment is concerned principally with the external behavior of the tubes and the analysis of their behavior from the static characteristics. There is little mention of the dependence of the characteristics upon the internal dimensions and geometries of the tubes. The best sections of the book are those dealing with the analysis of distortion and detection effects. In this analysis extensive and powerful use is made of exponential potential series of the form $i = \Sigma A_n e^{a_n V}$. Apparatus is described for checking the results of this analysis. Some good ultra-high frequency techniques are indicated in this connection.

The book is compactly written and well illustrated with self-explanatory curves and diagrams. In style and form the content looks like a cross section of the pages of the *Archiv fur Elektrotechnik*.

The bibliography of some 230 items is an excellent one. The references have been selected with some care and are for the most part source articles of a fundamental nature which furnish a fine key to the continental literature.

KARL SPANGENBERG
Stanford University

Applied Fluid Mechanics. MORROUGH P. O'BRIEN AND GEORGE H. HICKOX. Pp. 360, Figs. 166 and Table. McGraw-Hill Book Company, New York, 1937. Price $3.50.

This book is a modern presentation of the concepts of fluid mechanics. Only within recent years has it become generally recognized that there is a large body of fundamental theory and experimental fact that are common to a number of engineering fields such as hydraulics, aeronautics, heat transfer, acoustics, lubrication, meteorology, and others. The authors of this text have made a successful attempt to present the principles that are common to and underly all of these topics, no matter how far apart they may seem in application.

Instead of presenting hydraulics or some other similar subject as an empirical science, the new fluid mechanics, as exemplified by this book, develops the fundamental principles from truly rational theory. Because of this, the treatment applies to all fluids, whether ideal or viscous, or whether liquids or gases. And it also follows that it must apply to the motion of fluids under all circumstances, no matter what the nature of the case may be.

The authors have written interesting and valuable chapters on such topics as flow phenomena; viscosity, turbulence, and friction; forces exerted by fluids; unsteady flow in pipe lines; and models of open channel flow. In addition to the foregoing there are the more conventional chapters on hydrostatics; frictionless flow; steady flow in hydraulic pipe lines; and flow in open channels. In appendices there are given information on physical properties of various fluids, such as is essential to the application of the theory to a specific case, and certain useful hydraulic tables.

The book is a valuable contribution to the literature and should aid in leading the way to a more logical treatment of the various types of problems that arise in fluid mechanics.

R. L. DAUGHERTY
California Institute of Technology

Kontinuierliche Spektren. WOLFGANG FINKELNBURG, Dozent für Physik an der technischen Hochschule Darmstadt. Pp. 368+xi, Figs. 103. Julius Springer, Leipzig, 1938. Price, RM 33.00; gebunden RM 34.80.

Although continuous spectra are the rule rather than the exception, in nature, in technology, and in the laboratory, they have long remained "the step-child of spectroscopy." This is explained, of course, by their lack of structure, making significant measurements and interpretation difficult. In the book under review, the author brings together, in a very readable survey, observational results and an outline of pertinent theory on continuous spectra, now scattered in the literature of physics, chemistry, and astrophysics. The important physical ideas and formulas are on the whole clearly presented, although from the viewpoint of the theorist the discussion would be described as rather superficial and occasionally somewhat erroneous. Included is a bibliography of over 1700 titles, covering the field up to the beginning of 1938. In the reviewer's opinion, this book should have a desirable stimulating effect on research in continuous spectra, and should be very useful in helping to put research workers in both pure and applied science into contact with the present state of the subject.

Emphasis is placed on undeveloped fields and unsettled questions, and topics already extensively treated elsewhere (e.g., x-ray continua) are subordinated. The last two chapters are devoted to a non-theoretical survey of observed gas continua arranged according to chemical elements, and of the methods of production of continuous emission spectra, with special regard to the experimenter and the technologist.

The first six chapters include introductory sections, discussion of photoionization (absorption) and of recombination (emission) continua of atoms, x-ray and long wavelength continua produced in the stopping of electrons by solids, and Compton continua, together with some astrophysical and technical examples and applications. Nearly half the book is devoted to the continua of molecules in the vapor state. Diatomic molecules are extensively treated, polyatomic briefly. The systematic discussion of the "typical cases" of molecular continua, and the detailed discussion of the spectra of certain groups of diatomic molecules, are well done. Chapter XII deals with the widths of spectrum lines under various conditions, a subject which is closely related to that of continuous spectra. Continuous spectra of liquids, solutions, and crystals are treated very briefly, temperature radiation of solids more fully.

ROBERT S. MULLIKEN
University of Chicago

The Science of Seeing. M. LUCKIESCH AND F. K. MOSS. Pp. 548+viii, Figs. 143, 14×22 cm. D. Van Nostrand Co., Inc., New York, 1937. Price $6.00.

Seeing is perhaps the most important of man's senses. A book dealing with the "Science of Seeing" is therefore most welcome. The authors have been engaged in studying light and its effects on our senses for a long period of time and are in a good position to review the state of the subject. Their tone is semi-popular. The chapters deal with the human "seeing-machine," visual processes and thresholds, physiological effects, conservation of vision, lighting, reading and the relation of eyesight to seeing. There is a tremendous amount of data collected in this volume. Nearly every page contains a curve or chart summarizing the results of a large amount of experimental work. A scientist will probably wish that some of the experiments were more objective but when he realizes the difficulty of making experiments of the kind described in this book he will have to admit that the science of seeing has progressed considerably in the past few years. A very interesting chart is attached to the back cover of this book which allows anyone to test the variation of visibility as a function of the illumination. The reviewer has found this book a very interesting one and believes that anyone concerned with seeing (and who isn't) will likewise find it of extreme interest.

Contributed Original Research

Electromagnetic Waves in Elliptic Hollow Pipes of Metal

LAN JEN CHU*
Massachusetts Institute of Technology, Cambridge, Massachusetts
(Received April 28, 1938)

A theoretical study of the transmission of electromagnetic waves in hollow conducting pipes of elliptic cross section, including field configurations, critical frequencies, velocities of propagation, and attenuations for the six lowest order waves. The pipe of circular cross section is treated as a special case, and the stability of waves in it for small deformation of the cross section is discussed.

THIS paper presents the theory of the transmission of electromagnetic waves in hollow conducting pipes or tubes of elliptic cross section. Pipes of several other cross sections have been studied,** and the importance of a thorough investigation of elliptic pipes has been pointed out. The change in the rate of attenuation of hollow pipe waves in a pipe of circular cross section and the stability of such waves as the cross section of the pipe is deformed into an ellipse, are important practical problems, because some deformation of this kind is unavoidable. A theoretical answer to these and several other problems is reported here.

SOLUTION OF MAXWELL'S EQUATIONS FOR ELLIPTIC CYLINDER

The elliptic coordinate system (x, ζ, η) of Fig. 1 is defined in terms of a right-hand Cartesian system by the equations

$$x=x; \quad y=q\cosh\zeta\cos\eta; \quad z=q\sinh\zeta\sin\eta. \tag{1}$$

The contour surfaces of constant ζ are confocal elliptic cylinders, and those of constant η are confocal hyperbolic cylinders. The constant q represents half the distance between the foci. One of the confocal elliptic cylinders with $\zeta=\zeta_0$, is assumed to coincide with the inner boundary of the elliptic pipe, and the x axis coincides with its longitudinal axis. The major and minor axes of the boundary ellipse are $q\cosh\zeta_0$ and $q\sinh\zeta_0$, respectively, and its eccentricity, e, is given by $1/\cosh\zeta_0$.

A simple harmonic time variation and a propagation in the positive x direction of the

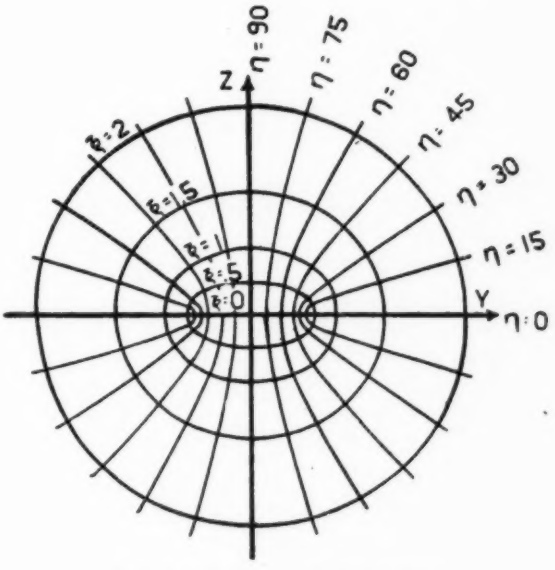

FIG. 1. Elliptic coordinate system.

* This work comprises part of a Doctor's thesis carried out in the Department of Electrical Engineering. It was presented before the joint meeting of the Institute of Radio Engineers and the International Scientific Radio Union in Washington, D.C. April 30, 1938.

** See references 1 to 7 in bibliography at end of paper. Superscript numerals refer to this bibliography.

pipe are assumed. In complex representation, these assumptions result in a multiplication of all wave functions by $e^{i\omega t-hx}$. The propagation constant $h=\alpha+i\beta$, in the x direction is to be determined from the boundary conditions.

The Maxwell's equations† for a wave in a medium characterized by σ, ϵ, and μ may be written:

$$(\sigma+i\omega\epsilon)q_1^2E_x=\frac{\partial(q_1H_\eta)}{\partial\zeta}-\frac{\partial(q_1H_\zeta)}{\partial\eta}, \quad (2a)$$

$$-i\omega\mu q_1^2H_x=\frac{\partial(q_1E_\eta)}{\partial\zeta}-\frac{\partial(q_1E_\zeta)}{\partial\eta}, \quad (2b)$$

$$(k^2+h^2)q_1E_\zeta=-h\frac{\partial E_x}{\partial\zeta}-i\omega\mu\frac{\partial H_x}{\partial\eta}, \quad (2c)$$

$$(k^2+h^2)q_1E_\eta=-h\frac{\partial E_x}{\partial\eta}+i\omega\mu\frac{\partial H_x}{\partial\zeta}, \quad (2d)$$

$$(k^2+h^2)q_1H_\zeta=(\sigma+i\omega\epsilon)\frac{\partial E_x}{\partial\eta}-h\frac{\partial H_x}{\partial\zeta}, \quad (2e)$$

$$-(k^2+h^2)q_1H_\eta=(\sigma+i\omega\epsilon)\frac{\partial E_x}{\partial\zeta}+h\frac{\partial H_x}{\partial\eta}, \quad (2f)$$

where $q_1=q(\sinh^2\zeta+\sin^2\eta)^{\frac{1}{2}}$, and $k^2=\omega^2\epsilon\mu-i\omega\mu\sigma$. The wave equation for E_x and H_x can be derived from (2); it is:

$$\left[\frac{\partial^2}{\partial\zeta^2}+\frac{\partial^2}{\partial\eta^2}+(k^2+h^2)q^2(\sinh^2\zeta+\sin^2\eta)\right]\left\{\begin{matrix}E_x\\H_x\end{matrix}\right\}=0. \quad (3)$$

Eqs. (3), after separating the variables ζ and η, are known as the Mathieu equations,[8, 9] and their solutions as the Mathieu functions. The solutions give the following expression for E_x and H_x:

$$\left\{\begin{matrix}E_x\\H_x\end{matrix}\right\}=[B_1Se_n(\eta)Re_n(\zeta)+B_2So_n(\eta)Ro_n(\zeta)]e^{i\omega t-hx}, \quad (4)$$

where B_1 and B_2 are complex constants; Se_n and So_n are the even and odd angular Mathieu functions of order n, and Re_n and Ro_n are the even and odd radial Mathieu functions of order n, where n is a positive integer. All the Mathieu functions in (4) contain $(k^2+h^2)q^2$ as a parameter.

Perfectly Conducting Pipes

First, the case will be considered in which the conductor has infinite conductivity, and the dielectric has zero conductivity. The field does not penetrate into the wall and there is no attenuation. In (2) and (4), $\sigma=0$ and $h=i\beta$. The longitudinal components of the fields, E_x and H_x inside the pipe may exist at the same time, but the present investigation will be limited to the two cases where only one of these components exists at a time. Waves of these kinds may be defined as follows:[7]

Any hollow pipe wave having both a longitudinal and a transverse component of magnetic field but only a transverse component of electric field will be called an H wave. Any hollow-pipe wave having both a longitudinal and a transverse component of electric field but only a transverse component of magnetic field will be called an E wave.

H wave

Under the condition that $E_x=0$, the remaining components of the field may be obtained from (2) and (4):

$$\left.\begin{aligned}
H_x&=B\left\{\begin{matrix}Se_n(\eta)Re_n(\zeta)\\So_n(\eta)Ro_n(\zeta)\end{matrix}\right\}e^{i(\omega t-\beta x)},\\
H_\zeta&=-\frac{\beta}{\omega\mu}E_\eta=-B\frac{i\beta}{q_1(k^2-\beta^2)}\times\left\{\begin{matrix}Se_n(\eta)Re_n'(\zeta)\\So_n(\eta)Ro_n'(\zeta)\end{matrix}\right\}e^{i(\omega t-\beta x)},\\
H_\eta&=\frac{\beta}{\omega\mu}E_\zeta=-B\frac{i\beta}{q_1(k^2-\beta^2)}\times\left\{\begin{matrix}Se_n'(\eta)Re_n(\zeta)\\So_n'(\eta)Re_n(\zeta)\end{matrix}\right\}e^{i(\omega t-\beta x)}.
\end{aligned}\right| \quad (5)$$

The prime denotes the derivative with respect to ζ or η, as the case may be. The boundary condition requires that the tangential component of the electric field, E_η, must vanish on the elliptic

† A practical system of units will be used, where: **E** = electric field intensity in volts per cm, **H** = magnetic field intensity in amperes per cm², σ = conductivity in mohs per cm, μ = permeability in henrys per cm (for air $\mu=4\pi 10^{-9}$), ϵ = dielectric constant in farads per cm (for air $\epsilon=10^{-11}/36\pi$). For convenience in analysis, the complex field intensities, E and H will be employed throughout, of which the real parts are **E** and **H**, respectively.

cylinder with boundary $\zeta=\zeta_0$, consequently,

$$\left.\begin{matrix} Re_n'(\zeta_0) \\ Ro_n'(\zeta_0) \end{matrix}\right\}=0. \tag{6}$$

Since Re_n' and Ro_n' are also functions of $q(k^2-\beta^2)^{\frac{1}{2}}$, (6) is an equation from which the phase constant β may be determined. The constant $(k^2-\beta^2)^{\frac{1}{2}}$ will be abbreviated as k_0; it depends only upon the types of waves, and the shape and size of the pipe. Other transmission properties of the waves may be derived from β.[2, 3]

H waves without the components E_ζ and H_η are generally impossible in pipes of elliptic cross section; because, their nonexistence demands the independence of H_x from η, as may be seen by putting $E_\zeta=0$ in (2c). But H_x cannot be independent of η, since the wave equation (3) for H_x contains a term in $\sin^2\eta$. An exception to this situation is a pipe of circular cross section, which can support waves of the H type having no components E_ζ and H_η; because, in this case, $\sin^2\eta$ is negligible compared to $\sinh^2\zeta$ in the wave equation (3).

E wave

By putting $H_x=0$ in (2), the remaining five components of field are obtained as,

$$\left.\begin{aligned} E_x&=B\left\{\begin{matrix} Se_n(\eta)Re_n(\zeta) \\ So_n(\eta)Ro_n(\zeta) \end{matrix}\right\}e^{i(\omega t-\beta x)}, \\ E_\zeta&=\frac{\beta}{\omega\epsilon}H_\eta=-B\frac{i\beta}{q_1(k^2-\beta^2)} \\ &\quad\times\left\{\begin{matrix} Se_\eta(\eta)Re_n'(\zeta) \\ So_n(\eta)Ro_n'(\zeta) \end{matrix}\right\}e^{i(\omega t-\beta x)}, \\ E_\eta&=-\frac{\beta}{\omega\epsilon}H_\zeta=-B\frac{i\beta}{q_1(k^2-\beta^2)} \\ &\quad\times\left\{\begin{matrix} Se_n'(\eta)Re_n(\zeta) \\ So_n'(\eta)Ro_n(\zeta) \end{matrix}\right\}e^{i(\omega t-\beta x)}. \end{aligned}\right\} \tag{7}$$

The boundary conditions require that E_x and E_η vanish on the boundary $\zeta=\zeta_0$, that is

$$\left.\begin{matrix} Re_n(\zeta_0) \\ Ro_n(\zeta_0) \end{matrix}\right\}=0. \tag{8}$$

The phase constant β may be determined according to (8) from the zeros of the radial Mathieu functions. The other transmission properties are then obtained from β. None of the five components may vanish in an E wave, unless the ellipse degenerates into a circle, for a reason similar to that given for the H waves.

Behavior of Waves with Changing Eccentricity

An H or an E wave in an elliptic pipe will be designated by a prescript e or o, indicating that the wave is described by the *even* or the *odd* Mathieu Functions. Thus, the waves will be referred as even or odd waves. A double subscript n, m will also be employed; n denotes the order of the Mathieu functions, and m denotes the particular root of (6) or (8) used to obtain the value of k_0.

The present investigation will be limited to the first root, $m=1$, and the distinguishing subscript m will be omitted. The six lowest order waves will be studied quantitatively, namely, the ${}_eH_0$, ${}_eH_1$, ${}_oH_1$, ${}_eE_0$, ${}_eE_1$, and ${}_oE_1$ waves.

The waves in elliptic pipes are closely related to the waves in circular pipes. The elliptic cylinder degenerates into a circular one when the distance between the foci approaches zero, and consequently the Mathieu functions degenerate into circular functions in the following way:

$$\begin{aligned} &\lim Se_n(\eta)=\cos(n\theta), \\ &\lim So_n(\eta)=\sin(n\theta), \\ &\lim Re_n(\zeta)=\lim Ro_n(\zeta)=(\pi/2)^{\frac{1}{2}}J_n(k_0r) \end{aligned} \tag{9}$$

where θ and r are of the cylindrical coordinate system (x, r, θ) with the $\theta=0$ axis coinciding with the $\eta=0$ axis. By substituting these limiting values into (5) and (7), Table I is obtained,

Table I.

Waves in elliptic pipe	${}_eE_0$	${}_eE_n$, ${}_oE_n$	${}_eH_0$	${}_eH_n$, ${}_oH_n$
Corresponding waves in circular pipe	E_0	E_n	H_0	H_n

showing the degenerate forms of the waves for cylindrical pipes. In a circular pipe, the solution

for E_z or H_z is of the general form:

$$\left.\begin{matrix} E_z \\ H_z \end{matrix}\right\} = [B_1 \cos(n\theta) + B_2 \sin(n\theta)] \times J_n(k_0 r) e^{i(\omega t - \beta z)}. \quad (10)$$

Now assume that the cross section of the circular pipe is deformed into an ellipse whose foci lie on the $\theta = 0$ axis. A wave in which E_z or H_z is proportional to $\cos(n\theta)$ only ($B_2 = 0$) becomes an even wave in the deformed pipe. Similarly, a wave with E_z or H_z proportional to $\sin(n\theta)$ only ($B_1 = 0$) becomes an odd wave.

When the phase constant β is zero, waves cannot travel through the pipe. The value of wave-length for which the phase constant equals zero is called the critical wave-length λ_0. It is determined from the relation $k = k_0 = 2\pi/\lambda_0$. For calculating k_0 and λ_0, a Bessel-Fourier series expansion for the Mathieu functions* and a table of numerical values for the coefficients of these series as functions of $k_0 q$ were available. The series or its derivative with a given value of $k_0 q$ was put equal to zero, and the root ζ_0, that is, the value of ζ of the boundary ellipse, was calculated by successive approximation. For a given value of λ_0, q and ζ_0 are then fixed. The size and shape of the elliptic pipe are determined by q and ζ_0. In Fig. 2, the ratio λ_0/s for the six

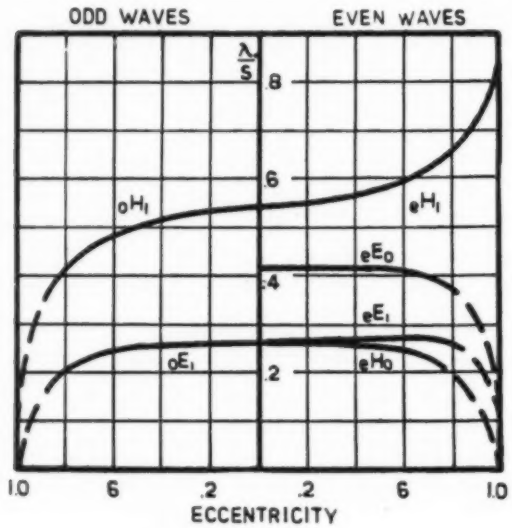

FIG. 2. Critical wave-length of waves in elliptic pipes.

* The Mathieu functions in series form and the numerical tables, from which calculations are based, were kindly supplied by Professor P. M. Morse of M.I.T. These tables have not been published.

waves are plotted as functions of the eccentricity; s is the periphery of the pipe, given by,

$$s = q \cosh \zeta_0 \int_0^{2\pi} (1 - (\cos \eta / \cosh \zeta_0)^2)^{\frac{1}{2}} d\eta. \quad (11)$$

Curves for the even waves are plotted on the right-hand side and those for the odd waves on the left-hand side. At zero eccentricity, corresponding to a circle, the even and odd curves are continuous. These curves show the change of the critical wave-lengths as the elliptic cross section is deformed along its major axis into a circle, and again elongated into an ellipse along an axis making an angle $\pi/2n$ radians from the original major axis. Since there are only even waves of the zero order, the curves for the ${}_eH_0$ and the ${}_eE_0$ waves turn back on themselves, having zero slopes at $e = 0$. For higher order waves ($n > 0$), the even and odd curves are not symmetrical about the line $e = 0$.

The field configurations of the six types of waves in the elliptic cross section for $e = 0.75$ are given in Fig. 3. A similar set of diagrams for waves for the degenerate case of a circular pipe has been given by Southworth.[1] A comparison of the two sets of diagrams will reveal the transformation accompanying a deformation of an elliptic pipe into a circular one. In these figures, the lines which apparently converge toward certain points within the ellipse, actually bend in the longitudinal direction. Such figures for cross sections along the axis are not shown.

Stability of Waves in Deformed Circular Pipe

The general solution of the longitudinal field E_z or H_z in cylindrical coordinates (x, r, θ) is given in (10). It may be considered that the two terms represent two distinct components of the wave having identical phase constants, and therefore traveling with the same phase velocity in the circular pipe. Now assume that the pipe is deformed by shortening the diameter along $\theta = \pm\pi/2$, so that the circle becomes an ellipse, keeping the periphery constant. As discussed in a previous section, the first component wave with the cosine factor becomes an even wave and the second component wave with the sine factor becomes an odd wave. The even and the odd

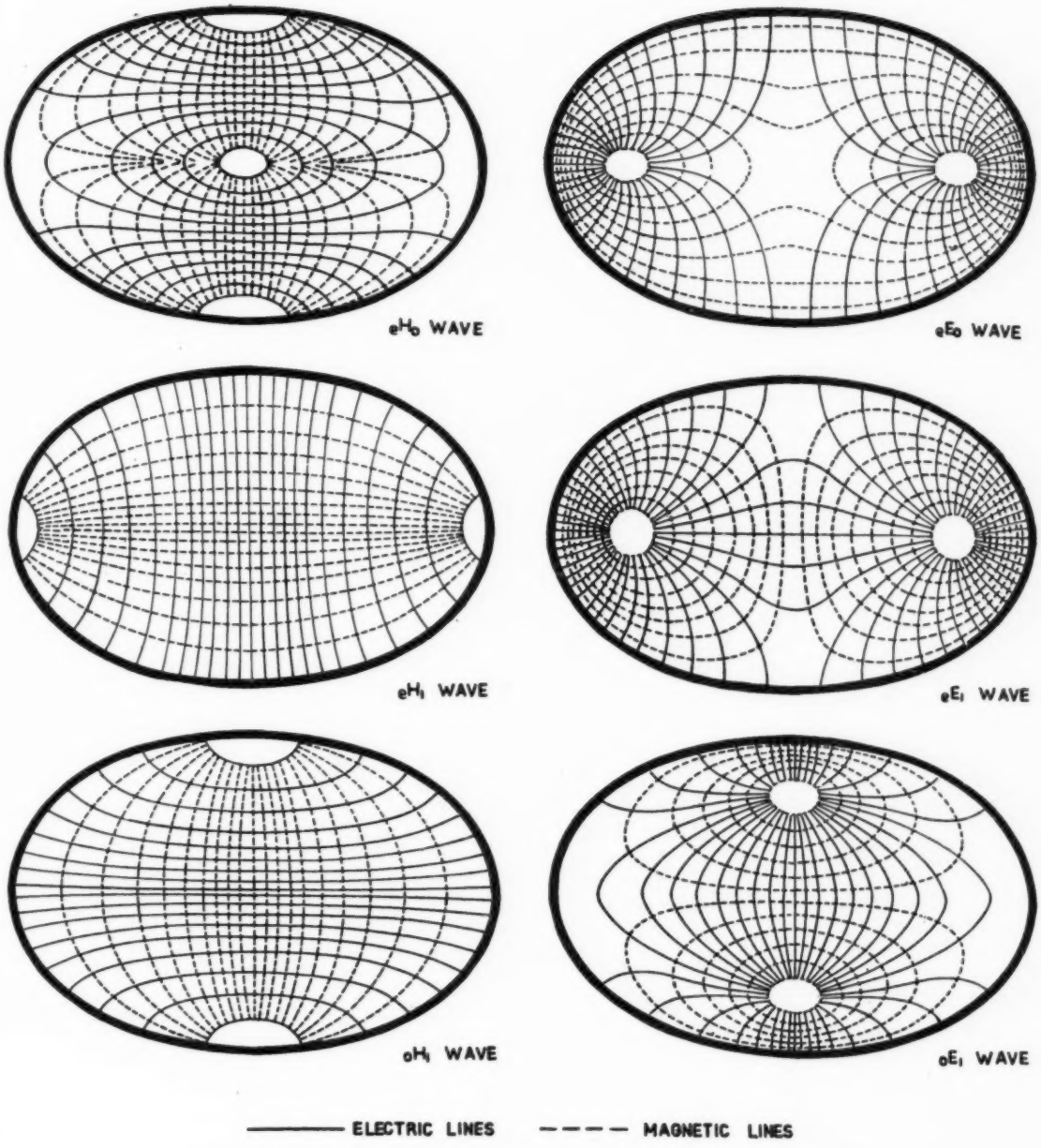

FIG. 3. Field configurations of waves in elliptic pipe of eccentricity of 0.75.

waves do not have the same critical wavelengths; therefore, one wave travels with a higher phase velocity than the other, and the two cannot remain together. Consequently, with the two important exceptions discussed below, all waves in a circular pipe tend to be unstable under slight deformation of the cross section.

The two exceptions are as follows: First, if one of the constants B_1 or B_2 in (10) is zero, that is, if the deformation takes place along one of the axes of symmetry, the deformed wave will either be an even or an odd wave alone, and no splitting will occur. Secondly, if n is zero, that is, if the wave in a circular pipe has circular symmetry, there is only one type of elliptic pipe wave into which it can be deformed, and again, no splitting can occur. In both of these cases, the waves are stable for small deformations.

The conclusion is that under a slight deformation of the geometrical shape of the circular pipe:

(1) the H_0 and the E_0 waves are stable, and
(2) all other waves are unstable unless the deformation occurs along one of the axes of symmetry.

Imperfectly Conducting Pipes

If the conductivity of the metal becomes finite, the field inside the pipe is evidently distorted from the shape assumed above. Consequently, it is sometimes misleading to consider that one of the longitudinal fields may be arbitrarily set equal to zero, since the finiteness of the conductivity requires different boundary conditions. However, if the conductivity of the wall is finite but very large ($\sigma' \gg \omega\epsilon'$),* it may be considered that the waves in the dielectric of such a pipe have the same forms as if the metal were infinitely conducting, with only slight modifications to take into consideration the finiteness of the conductivity.

The calculation of the attenuation constants will be illustrated by giving the details for the ${}_eE_n$ waves. In the perfectly conducting pipes, all components except E_ξ and H_η vanish at the boundary. In the imperfectly conducting pipe, the magnitudes of E_ξ and H_η will not be distorted appreciably with good conducting metals. From (7), the value of H_η in the dielectric at the boundary is

$$H_\eta|_{\xi=\xi_0} \cong -(i\omega\epsilon/q_1k_0^2)Se_n(\eta) \times Re_n'(\zeta_0)e^{i(\omega t-\beta x)}. \quad (12)$$

The wave in the metal must travel with the same speed in the x direction as that of the wave in the dielectric, hence $h=i\beta$ for both dielectric and conductor. For metals of high conductivity,

$$k'^2 = -i\omega\mu'(i\omega\epsilon'+\sigma') \cong -i\omega\mu'\sigma', \quad (13)$$

$$k'^2+h^2 \cong k'^2. \quad (14)$$

The solution of the longitudinal field E_x' in the metal, obtained from (2) and (3), is as follows:

$$E_x' = \sum_{p=0}^{\infty} A_p Re_p^4(\zeta)Se_p(\eta)e^{i(\omega t-\beta x)}, \quad (15)$$

* The constants σ, ϵ, μ and k and the fields E and H in the metal will be primed to differentiate them from the corresponding values in the dielectric.

where Re_p^4 is the even radial Mathieu function of the fourth kind. For a single ${}_eE_n$ wave in the dielectric, the field in the metal cannot be represented by a single term of the above series because the boundary conditions cannot even approximately be satisfied. In order to simplify the above series, the asymptotic expansion of Re_p^4 for large values of ζ and $k'q$ given by Stratton[10] is used:

$$Re_p^4(\zeta) \cong (k'q\cosh\zeta)^{-\frac{1}{2}}e^{-i[k'q\cosh\zeta-(2p+1)\pi/4]}. \quad (16)$$

Employing (16), E_x' for the even E wave becomes:

$$E_x' = B'Te_n(\eta)(k'q\cosh\zeta)^{-\frac{1}{2}}e^{i(\omega t-\beta x-k'q\cosh\zeta)} \quad (17)$$

where $B'Te_n(\eta) = \sum_{p=0}^{\infty} A_p e^{i(2p+1)\pi/4}Se_p(\eta)$,

and B' is a new constant. The longitudinal magnetic field H_x', if present, has a relative magnitude of infinitesimal order. H_η' is found from E_x' using (2f):

$$H_\eta' = B'Te(\eta)\frac{\sigma'}{q_1k'^2}\frac{ik'q\sinh\zeta}{(k'q\cosh\zeta)^{\frac{1}{2}}} \times e^{i(\omega t-\beta x-k'q\cosh\zeta)}. \quad (18)$$

The boundary condition requires that the two tangential fields H_η and H_η' shall be equal. In the expressions for H_η and H_η', only Se_n/q_1 and Te_n/q_1 are functions of η, hence the ratio Te_n/Se_n must be independent of η. This ratio may be set equal to unity, since the absolute magnitude of Te_n has not yet been fixed. The constant B' may then be determined in terms of B and ζ_0. In this way, the two tangential fields E_x' and H_η' at the boundary are obtained:

$$\left.\begin{aligned} E_x' &= -B\frac{\omega\epsilon}{k_0^2}\left[\frac{i\omega\mu'}{\sigma'}\right]^{\frac{1}{2}}\frac{1}{q\sinh\zeta_0} \times Re_n'(\zeta_0)Se_n(\eta)e^{i(\omega t-\beta x)}, \\ H_\eta' &= -B\frac{i\omega\epsilon}{q_1k_0^2}Re_n'(\zeta_0)Se_n(\eta)e^{i(\omega t-\beta x)}. \end{aligned}\right\} \quad (19)$$

The power loss, L, into the metal per centimeter length of the pipe is obtained by integrating the real part of the Poynting vector over the boundary for this unit length of the pipe:

$$L=\frac{|B|^2}{2\sqrt{2}}\left[\frac{\omega\mu'}{\sigma'}\right]^{\frac{1}{2}}\left[\frac{\omega\epsilon}{k_0^2}Re_n'(\zeta_0)\right]^2\frac{N_n}{q\sinh\zeta_0}. \quad (20)$$

The total power, S, transmitted through the pipe, is obtained by using the field expressions for a perfectly conducting pipe:

$$S=|B|^2\frac{\beta\omega\epsilon}{2k_0^4}\int_0^{\zeta_0}[M_n\{Re_n(\zeta)\}^2+N_n\{Re_n'(\zeta)\}^2]d\zeta. \quad (21)$$

In both L and S,

$$\left.\begin{aligned}N_n&=\int_0^{2\pi}[Se_n(\eta)]^2d\eta,\\ M_n&=\int_0^{2\pi}[Se_n'(\eta)]^2d\eta.\end{aligned}\right\} \quad (22)$$

The attentuation constant of the ${}_eE_n$ wave is therefore as follows:

$$\alpha=\frac{L}{2S}=\left[\frac{\pi\mu'\epsilon}{\sigma'\mu}\right]^{\frac{1}{2}}\frac{(f_0)^{\frac{1}{2}}}{2q\sinh\zeta_0}\frac{[Re_n'(\zeta_0)]^2}{(M_n/N_n)\int_0^{\zeta_0}[Re_n(\zeta)]^2d\zeta+\int_0^{\zeta_0}[Re_n'(\zeta)]^2d\zeta}\frac{(f/f_0)^{\frac{1}{2}}}{(1-(f_0/f)^2)^{\frac{1}{2}}}. \quad (23)$$

nepers per cm.

By a similar process, it can be proven that the attenuation constant of the ${}_eH_n$ wave is as follows:

$$\alpha=\left[\frac{\pi\mu'\epsilon}{\sigma'\mu}\right]^{\frac{1}{2}}\frac{(f_0)^{\frac{1}{2}}}{2q\sinh\zeta_0}\frac{[(f/f_0)^{\frac{1}{2}}+\{(N_n/M_n)k_0^2q^2\sinh\zeta_0-1\}(f_0/f)^{\frac{3}{2}}][Re_n(\zeta_0)]^2}{\int_0^{\zeta_0}[Re_n(\zeta)]^2d\zeta+(N_n/M_n)\int_0^{\zeta_0}[Re_n'(\zeta)]^2d\zeta}\frac{1}{(1-(f_0/f)^2)^{\frac{1}{2}}}. \quad (24)$$

nepers per cm.

The attenuation constant of the odd waves can be obtained by replacing the even Mathieu functions in (23) and (24) by the odd ones. There is no odd Mathieu function of the zero order.

The remaining task is to evaluate the integrals in these expressions. For a circular pipe, $e=0$, the expressions involve sinusoidal and Bessel functions in a form which is integrable.[2] For other eccentricities, N_n and M_n are the integrals of the square of Fourier series. The integrals of the square of the radial Mathieu functions were evaluated by graphical means.

In both expressions for the attenuation constants, there is a term proportional to $(f)^{\frac{1}{2}}$ which increases with the frequency. For the H waves, there is another term proportional to $f^{-\frac{3}{2}}$, which decreases with increasing frequency. The coefficient of $(f/f_0)^{\frac{1}{2}}$ does not vanish, except for the single case of the ${}_eH_0$ wave at zero eccentricity, that is, for the H_0 wave in a circular pipe.[2] In the latter case, $Se_0=1$ and its derivative becomes zero, consequently $M_0=0$. The attenuation of all waves in elliptic pipes, with this single exception, increases with increasing frequency.

Figure 4 shows curves of the attenuation constants as functions of frequency, for air filled copper pipes of equal peripheries ($s=40$ cm) but several eccentricities. All the curves, except the one representing the ${}_eH_0$ wave with $e=0$, rise with increasing frequency (the curve for ${}_eH_0$ with $e=0.256$ will rise for frequencies beyond the range shown in the figure). The attenuations of the two waves, ${}_eE_0$ and ${}_eH_0$, for a fixed operating frequency, are always increased, if the eccentricity is increased. As may be seen from the curves, the attenuations of the ${}_oH_1$ and the ${}_eE_1$ waves are not appreciably affected by changes of eccentricity. The attenuations of the ${}_eH_1$ and the ${}_oE_1$ waves are increased with increasing eccentricity.

The conclusions as to the stability are not altered by these facts concerning attenuations. In a slightly deformed circular pipe, the E_0 and the H_0 waves are stable, although they have higher attenuations than the ones in an undeformed circular pipe. The H_0 wave in a circular

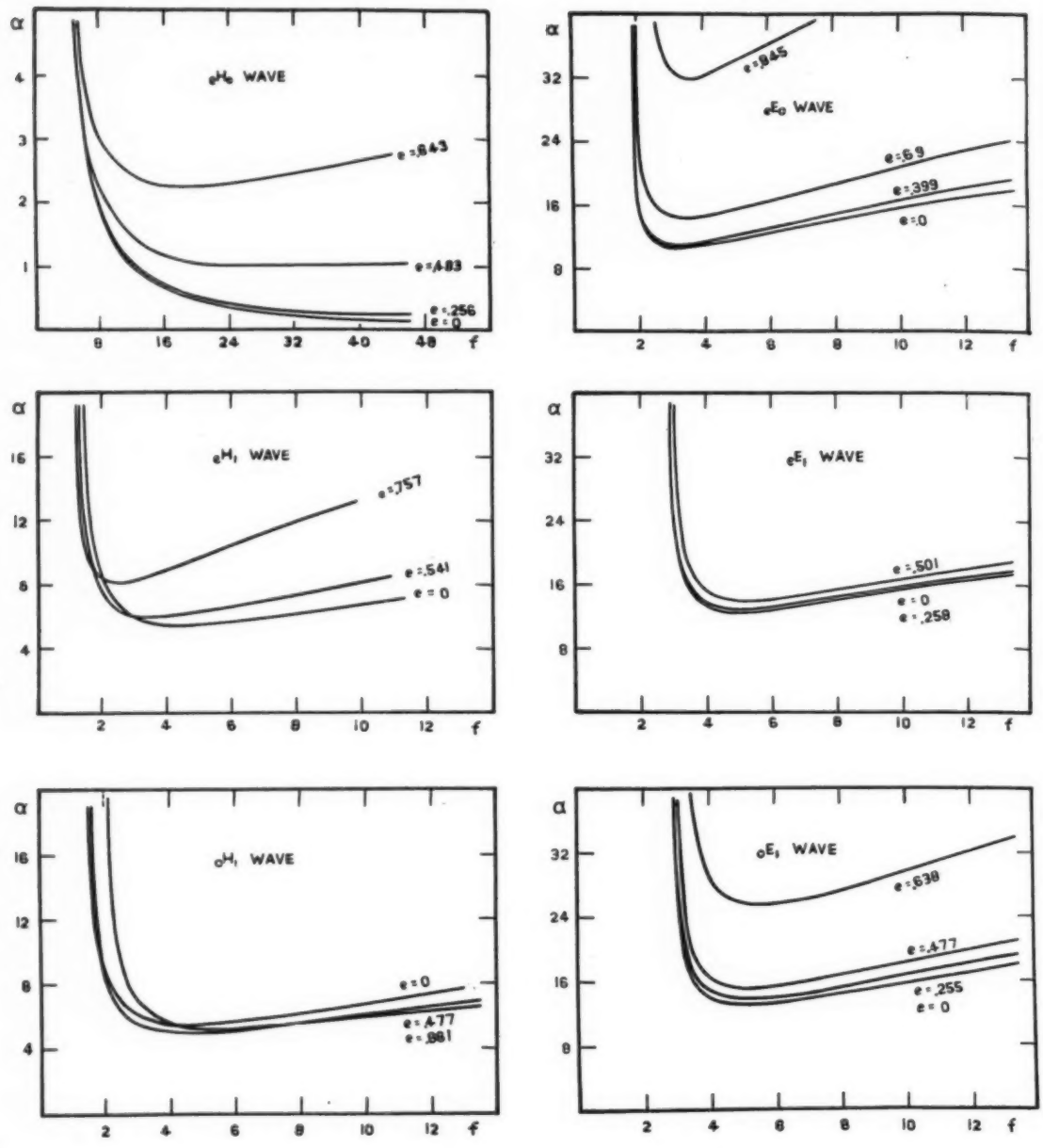

FIG. 4. Attenuation of waves in air-filled copper pipes of periphery of 40 cm. Abscissae—frequency in 10^9 cycles per sec. Ordinates—attenuation in decibels per mile.

pipe has a peculiar property that its attenuation always decreases with the increasing frequency. This property is lost when the cross section of the pipe is deformed into an ellipse. For the E_1 and H_1 waves, after the splitting caused by the deformation, one component wave has higher attenuation than the other. After traveling a considerable distance, it may therefore disappear, or become negligibly small compared to the other component.

In Fig. 5, the minimum attenuation constants obtainable with different waves regardless of the frequencies at which such attenuations occur, are plotted as functions of eccentricity, for elliptic pipes of equal peripheries ($s=40$ cm). The curves for the ${}_eH_0$ and the ${}_eE_0$ waves have

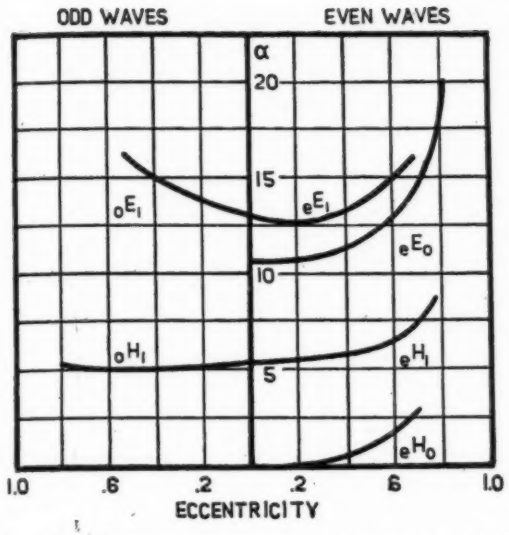

FIG. 5. Minimum attenuation of waves in air-filled copper pipes of periphery of 40 cm. Ordinates—minimum attenuation in decibels per mile.

zero slope at $e=0$ and rise as the eccentricity increases. The lowest attenuation of the H_1 wave occurs for the odd wave in pipes of $e=0.5$; while that of the E_1 wave occurs for the even wave in pipes of $e=0.2$.

CONCLUSIONS

The results obtained in this research lead to the following definite conclusions:

Stability: 1. Under a slight deformation of the cross section of a circular pipe along one of the axes of symmetry all waves are stable.

2. Under *any* slight deformation of the cross section of a circular pipe the H_0 and the E_0 waves are stable.

3. Except for the cases 1 and 2, all waves are unstable under cross-sectional deformations.

Critical wave-length: 1. For a given periphery, the $_eH_1$ wave possesses the longest critical wave-length, which becomes longer with increasing eccentricity, approaching the value $\lambda_0=0.83s$ for the limiting case of unity eccentricity.

2. The critical wave-lengths of the other five types of waves remain substantially unchanged or become shorter with increasing eccentricity.

Attenuation: 1. The H_0 wave in a circular pipe loses its anomalous attenuation characteristics under small deformation, and its attenuation is always increased by such a deformation.

2. The $_oH_1$ wave is next lowest to the H_0 wave in attenuation. With a fixed periphery, the minimum attenuation occurs, not in a circular pipe, but in an elliptic pipe of eccentricity of about 0.5.

ACKNOWLEDGMENT

The author acknowledges his gratitude to Professor W. L. Barrow, under whose supervision this research was carried on, and to Professor J. A. Stratton for numerous helpful discussions.

BIBLIOGRAPHY

1. C. Southworth, Bell Sys. Tech. J. **15**, 284–309 (1936).
2. J. R. Carson, S. P. Mead and S. A. Schelkunoff, Bell Sys. Tech. J. **15**, 310–333 (1936).
3. W. L. Barrow, Proc. I.R.E. **24**, 1298–1328 (1936).
4. L. Brillouin, Rev. Générale de l'Électricité **40**, 227–239 (1936).
5. L. Page and N. I. Adams, Jr., Phys. Rev. **52**, 647–651 (1937).
6. S. A. Schelkunoff, Proc. I.R.E. **25**, 1457–1493 (1937).
7. L. J. Chu and W. L. Barrow, to be published in the Proc. I.R.E.
8. E. T. Whittaker and G. N. Watson, *A Course of Modern Analysis* (1927).
9. S. Goldstein, Trans. Camb. Phil. Soc. **23**, No. 11 (1927).
10. J. A. Stratton, Proc. Nat. Acad. Sci. **21**, 51–56 and 316–321 (1935).
11. P. M. Morse, Proc. Nat. Acad. Sci. **21**, 56–62 (1935).

Method of Measuring Luminescent Screen Potential

HERBERT NELSON
Research and Engineering Department, RCA Manufacturing Co. Inc., Harrison N. J.
(Received April 29, 1938)

A method has been devised for the determination of potentials of areas on the interior surface of the glass envelopes of vacuum tubes. Measurements by this method may be made on almost any type of finished tubes. Results obtained have been checked by a second method. Determinations of luminescent-screen potential as a function of second-anode voltage have been made for kinescope tubes under different conditions as to type of screen material, manner of bombarding the screen, beam-current density and previous electron bombardment. It was found as a general feature that as the second anode is made increasingly positive, the screen follows and remains a few volts negative with respect to the second anode until it starts to approach an upper limit of potential with respect to the cathode. When this occurs, the screen rapidly becomes more negative with respect to the second anode. Calcium-tungstate screens and clean Nonex glass surfaces have been found to reach upper limits of potentials between 2500 and 5000 volts, while willemite screens have been carried to potentials as high as 20,000 volts. The upper limit of potential for a particular type of screen varies from tube to tube. Values as different as 4000 and 20,000 volts have been obtained for willemite. In general, the upper limit of potential is found to be lowered as an effect of increased current density in the bombarding beam. Aging of a screen has been found to lower permanently its upper limit of potential. Accumulation of negative charges on the glass base of a screen and on depressed surfaces in the screen layer appears to be important in determining the upper limit of screen potential.

IT is generally recognized in tube engineering practice that the bulb wall and other surfaces of insulating material in a tube often play important parts in determining the operating characteristics of the tube. Little is known, however, about the exact potentials that these surfaces assume due to electron bombardment, secondary emission, and electrical leakage. As a result, tube characteristics which are affected by these surface potentials are not entirely predictable. In the case of kinescope tubes, it is particularly important to know what potential the screen assumes at different second-anode potentials. It is known that, in general, the fluorescent screen floats at a potential very near that of the second anode, but in many cases, especially at high voltages, it floats at a potential several thousand volts lower.[1,2] Little exact knowledge exists, however, concerning the variation of the screen potential with the second-anode potential and concerning the manner in which the variation is affected by such factors as type of screen material, current density, and tube life.

As a partial remedy for this situation, a method has been developed in this laboratory which makes possible the measurement of the potentials of areas on the interior surface of the glass envelope of vacuum tubes. A particular advantage of the method is that it lends itself to the making of measurements on finished tubes of almost any type. From these measurements, secondary-emission characteristics of various areas on the glass wall may be determined as well as the potentials of these areas. This paper describes the method, which may be referred to as the glass-conduction or the GC method, and illustrates its particular application to kinescope screen potential measurements.

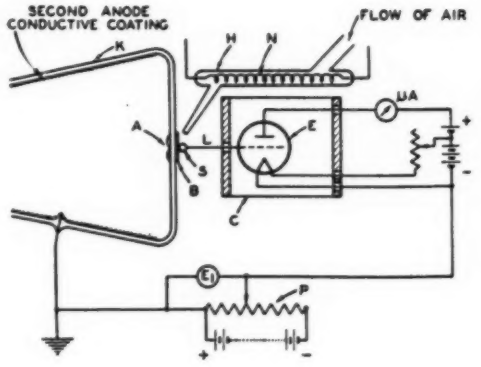

FIG. 1. Diagram of experimental arrangement for measuring the potentials of areas on the interior surface of the glass envelope of vacuum tubes.

[1] T. B. Brown, J. Opt. Soc. Am. **27**, 186 (1937).
[2] W. B. Nottingham, J. App. Phys. **8**, 762 (1937).

1. Experimental Method

A diagram of the experimental arrangement is shown in Fig. 1. K is a kinescope and A is an area of the screen, the potential of which is to be determined. The grid lead L of a special type electrometer tube[3] E makes direct contact with a

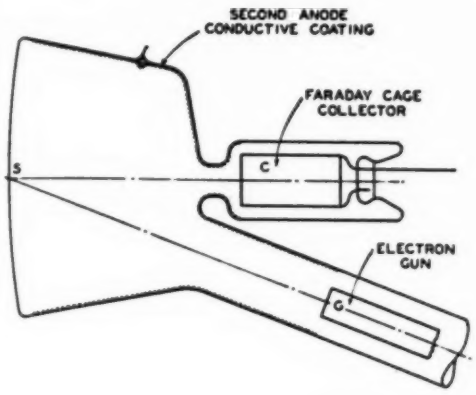

Fig. 2. Design of tube for check of experimental method.

graphite-coated area B on the external glass surface directly opposite A. The electrical contact between L and B is made by means of a fine metal spring S which presses against the graphite coating. The electrometer tube is enclosed in a metal can C which serves as an electrostatic shield. Some $CaCl_2$ is introduced into C to keep the electrometer tube dry and prevent electrical leakage over its external surface. The grid lead L is brought out from C through a sulphur bushing. A flow of air is established through the heater tube H. The air is heated by means of the hot Nichrome coil N and directed in a fine jet against the graphite spot B. In the electrical circuit, the microammeter μA is used to measure the anode current I_b of the electrometer tube. The potential E_1 of the negative terminal of the electrometer-tube filament with respect to the second anode of the kinescope may be varied by means of the potentiometer system P.

If, in the set-up as described above, the electrical resistance R_g through the glass wall between A and B is very small compared to the input impedance R_i of the electrometer tube, it follows that

$$E_s = E_1 + E_c, \tag{1}$$

where E_s is the potential of the area A of the kinescope screen with respect to the second anode and E_c is the potential of the control element of the electrometer tube with respect to the negative terminal of the filament. Since the potential E_1 may be obtained directly from a voltmeter reading, and since a determination of E_c from the value of I_b may be made on the basis of a previous calibration of the electrometer tube, it follows that the value of E_s may be determined. In the course of measurements, the value of E_1 may be adjusted so that the value of E_c to be determined is always in the order of -2 volt.

As stated above, Eq. (1) is valid only when $R_g \ll R_i$. An electrometer tube of high $R_i (>10^{13}$ ohms) is, therefore, chosen for the experiment. By heating the glass at B, R_g is reduced to a value of about 10^{10} ohms. Under these conditions, Eq. (1) is valid since practically the entire voltage drop from A to the negative terminal of electrometer-tube filament occurs across the electrometer tube. In order that a sufficiently low value of R_g may be obtained, the glass must be heated at B to some temperature between 50°C and 200°C, depending on the nature of the glass. In case of Nonex, a temperature of about 125°C is found satisfactory. Since only a small area of the glass is heated to this maximum temperature,

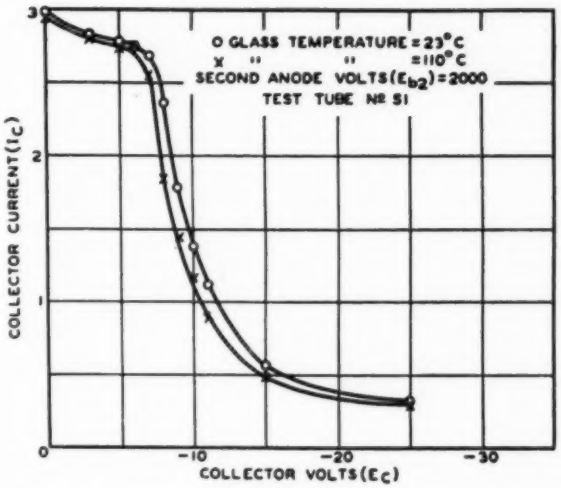

Fig. 3. Secondary emission from a phosphor No. 1 (green willemite) screen. The break in the curves occurs when collector and screen are at approximately equal potentials.

[3] H. Nelson, Rev. Sci. Inst. 1, 281 (1930).

the surrounding glass at increasingly lower temperatures forms an insulating ring around the "conducting" section at B.

2. Check of the Experimental Method

In order to check the reliability of the experimental method, a test kinescope No. S1 was constructed so that its screen potential could be determined by the VD method (the velocity-distribution method as used by Brown[1]) as well as by the author's glass-conduction method. In the VD method, the secondary electron current from the bombarded target to a collector is determined as a function of the collector potential with respect to the second anode. The potential of the screen may be determined from the data obtained, since a sharp break in the collector voltage-collector current curve occurs at the point where the collector potential is just equal to that of the screen. At more positive potentials of the collector, there is little change in current with voltage while at less positive potentials, the secondary electrons are retarded and a rapid decrease in the collector current results as the low velocity secondaries are repelled.

Characteristic I_c–E_c curves are shown in Fig. 3. The electron current I_c to the collector is plotted as a function of the potential E_c of the collector with respect to the second anode. The break in one curve occurs at $E_c = -7$ volt approximately.

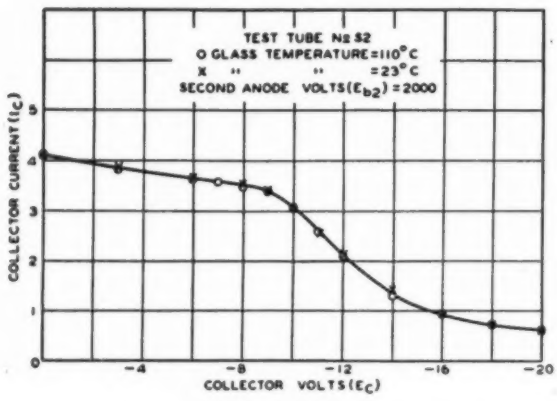

FIG. 4. Secondary emission from a Nonex glass surface (test tube No. S2).

This indicates that the screen in this particular case floats at a potential E_s of -7 volt with respect to the second anode.

A diagrammatic sketch of the experimental tube is shown in Fig. 2. The screen S consists of a standard green willemite coating (phosphor No. 1) on Nonex glass. The graphite coating on the inside bulb surface constitutes the second anode of the tube. G is a standard kinescope electron gun.[4] The screen is bombarded by an electron beam at point S and a fraction of the emitted secondary electrons are collected by the Faraday cage collector C.

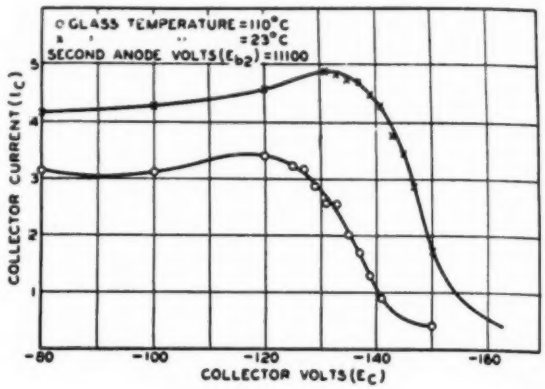

FIG. 5. Secondary emission from a phosphor No. 1 (green willemite) screen with second anode at a high voltage.

In order to make possible measurements on clean Nonex glass as well as on a willemite-coated glass, a tube No. S2 was constructed identical with tube No. S1 except that no willemite was applied on the screen. The Nonex bulbs used for the tubes were thoroughly washed internally with a chromic-acid solution and rinsed with distilled water before being worked.

Characteristic results obtained are illustrated by the curves in Figs. 3 to 7 inclusive. The data were obtained during bombardment of a $\frac{1}{2}$ inch diameter area on the screen by a defocused stationary electron beam. The beam current was maintained equal to 10×10^{-6} ampere. The curves in Fig. 3 are plots of data from tube No. S1 taken at a second-anode potential $E_{b2} = 2000$ volts. These curves show screen potentials E_s of -7 and -6.5 volt (with respect to the second anode) at glass temperatures of 23° and 110°C, respectively. The screen potential determined by the GC method at 110°C was found to be -10.4

[4] Orth, Richards and Headrick, Proc. I.R.E. **23**, 1308 (1935).

volt. The results for clean Nonex glass (tube No. S2) at the same second-anode potential are shown in Fig. 4. The screen potential is −9 volt at a glass temperature of either 23° or 110°C. The GC method also gives approximately the same value, −9 volt.

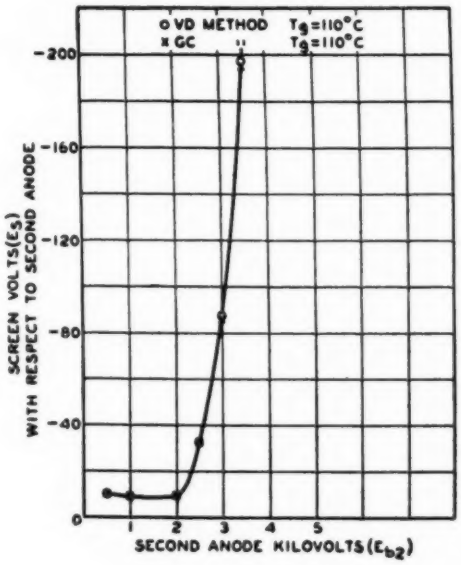

FIG. 6. Check of experimental method for an uncoated Nonex glass target.

Since the GC and VD methods give identical results in case of a clean glass surface and different results in case of a willemite-coated surface, it appears that the electrical resistance through the willemite coating is sufficiently high to allow the glass base and the top surface of the willemite layer to "float" at different potentials. This condition and the effect produced by increasing the temperature of the screen will be discussed below.

The curves in Fig. 5 representing data obtained from tube No. S1 at $E_{b2}=9000$ volts, show screen potentials of −137 and −127 volt at 23° and 110°C, respectively. The screen potential determined by the GC method is −148 volt. The values obtained for the screen potential by means of the VD and the GC methods are shown as functions of the second-anode voltage in Figs. 6 and 7. The curves in Figs. 6 and 7 represent the data for clean glass and willemite, respectively. For clean glass, the two methods give identical results. For willemite as previously noted, the two methods give slightly different results. The difference, however, is so small that for practical purposes the potential of the glass base of the willemite coating may be regarded as the potential of the screen.

The fact that the glass base of the willemite layer tends to float at a lower negative potential than the willemite surface indicates that electrons from the primary beam strike the glass base and that the loss of electrons from it becomes equal to the number absorbed only after it has become charged to some negative equilibrium potential with respect to the outer willemite surface. A consideration of the nature of the willemite layer indicates that a condition as suggested above is to be expected. The willemite coating as applied in standard kinescope tubes is a layer composed of aggregates of fine willemite particles. The layer which is rough and microscopically nonuniform has a large number of pin-hole pits where the glass base is uncoated. It is to be expected that when primary electrons strike the glass base at the bottom of these pits, the number of secondary electrons escaping is less than the number of primary electrons impinging. This is particularly true at electron velocities above 2500–3000 volts where the true secondary-to-primary ratio for Nonex glass is less than unity. (In this paper, the ratio of the number of

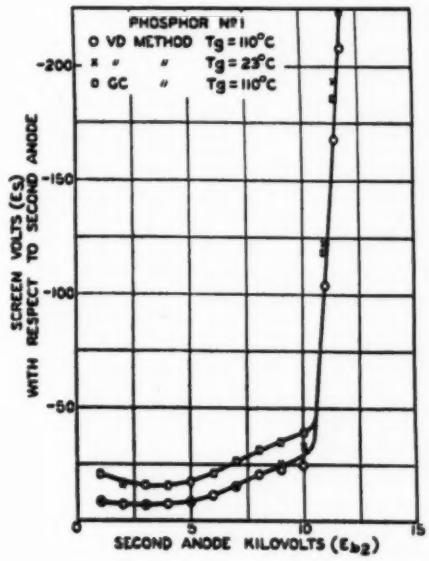

FIG. 7. Comparison of data obtained by VD method and GC method on test tube No. S1.

secondary electrons emitted to the number of primary electrons impinging is referred to as the "true secondary-to-primary ratio" while that of the number of secondaries actually escaping from the screen to the number of primaries impinging is referred to as the "effective secondary-to-primary ratio.") Electrical leakage through the willemite aggregates will have a tendency to prevent large potential differences from being established. In addition to the negative charging of the glass base which may occur at relatively low primary-electron velocities, it is to be expected that at higher velocities a similar charging of the depressions in the willemite will also occur. As the primary-electron velocity is increased and the true secondary-to-primary ratio of the willemite decreases, the effective ratio of the willemite in a depression will become less than unity before that of the willemite comprising the elevated areas of the surface. Where this occurs, the willemite in the depression will accumulate a negative charge until it reaches an equilibrium potential with respect to the adjacent elevated areas at which as many electrons are lost by secondary emission and leakage as are absorbed from the primary beam.

The accumulation of charges will tend to depress the potential of the screen as a whole. The negatively charged points in the screen will exert a grid action on the adjacent areas of the surface and tend to prevent the escape of low velocity secondaries from these areas. Also the effective secondary-to-primary ratio of the elevated areas needs to be higher to counteract the charging effect of the leakage electrons from the negative depressions. As a result, an increased second-anode-to-screen potential is required for the maintenance of an equilibrium condition where the effective secondary-to-primary ratio of the screen as a whole is equal to unity.

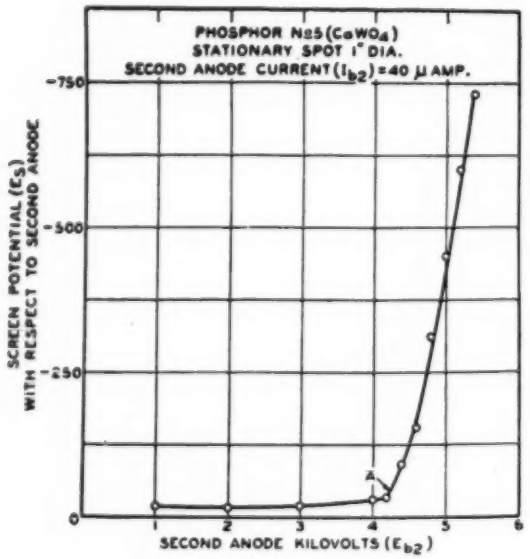

FIG. 8. Screen potential determined by the GC method. The low voltage break has been observed as characteristic of calcium-tungstate screens (test tube No. 1254B).

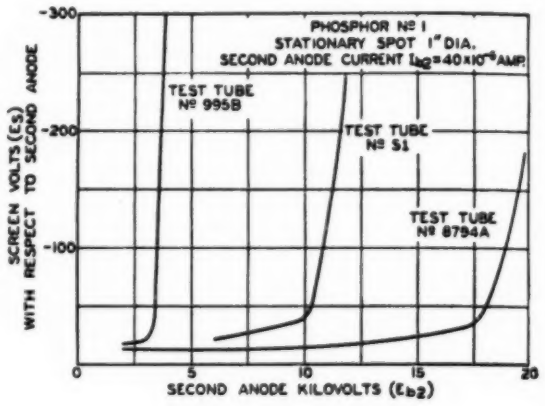

FIG. 9. Screen potential curves showing large variations from tube to tube for the same screen material (green willemite).

It is beyond the scope of the present paper to attempt a quantitative analysis of the effects discussed above especially in view of our present knowledge concerning the exact physical structure and the electrical resistance properties of the willemite layer. A consideration of effects such as these, however, is necessary for a better understanding of the manner in which the screen potential varies with that of the second anode. It affords, for instance, an explanation of the results represented by the curves in Fig. 5. The high value of E_s may be ascribed to grid and leakage effects, while the decrease in E_s caused by an increased temperature of the screen may be thought of as due to a decrease in the grid effects. The leakage resistance of the willemite decreases as its temperature is increased and consequently the depressions become less negative and exert less grid action on the adjacent elevated areas. This temperature effect has been directly observed in case of the glass base. With the second-

anode at high potential, the glass base of the screen as measured by the GC method is found to become less negative as the temperature is increased.

3. Application of the GC Method to the Measurement of Screen Potentials of Kinescope Tubes

Measurements of the screen potential E_s as a function of the second-anode voltage E_{b2} were made for several standard kinescope tubes. In general, the measurements were made while a one-inch diameter area of the screen was bombarded by a defocused stationary electron beam at a second-anode current $I_{b2}=40\times10^{-6}$ ampere. In some cases, however, a large area of the screen was scanned by a focused electron beam. Characteristic results obtained are shown by the curves in Figs. 8 to 10, inclusive. In general, it

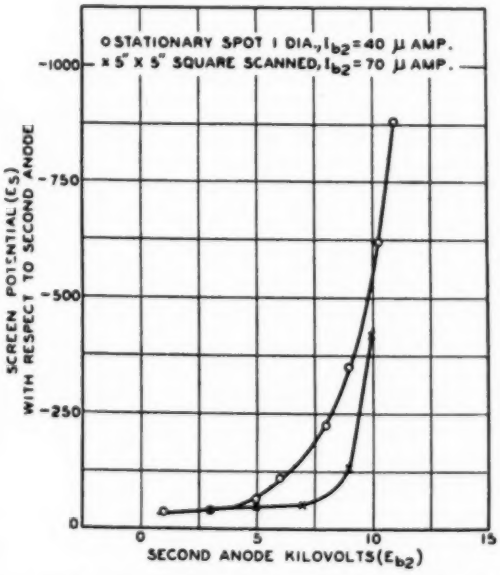

Fig. 10. Screen potential curves for test tube (No. 6167B) with blue zinc-sulphide screen.

may be noted that the curves exhibit two distinct regions. In the "low voltage" region, i.e. from the second-anode potential at which the curves start to some value as represented by point A on the curve of Fig. 8, it is found that E_s is low and varies only slightly with the second-anode potential. Above A, E_s increases rapidly with E_{b2} and in case of certain tubes, becomes as large as several thousand volts at $E_{b2}=10{,}000$ volts. In the "low voltage" region, the ratio of true secondary-electron emission from the screen to the number of primary electrons striking it is greater than unity and the screen becomes charged positively with respect to the cathode potential until it reaches a potential near that of the second anode at which only one of the secondary electrons per primary electron can be collected by the second anode (the remainder of the secondary electrons return to the screen). In general, this condition is reached when the screen is slightly negative with respect to the second anode. The exact value of E_s for this condition depends chiefly on the geometry of the tube and to a less extent on the type and state of the screen phosphor. The tests show that for Kinescope tubes with graphite-coated bulbs, E_s in the "low voltage" region is usually less than -50 volt, while for tubes with uncoated bulbs, it is greater, though usually less than -150 volt. (See paper by Nottingham[2] for discussion of similar curves.)

The high voltage region above the break A corresponds to a condition at which the true secondary-to-primary ratio of the screen material has decreased to a value not much greater than unity and at which the effective secondary-to-primary ratio of the screen as a whole becomes as large as unity only at higher values of E_s. In this voltage region, the field intensity required at the surface to give an effective secondary-to-primary ratio equal to unity increases rapidly with the screen potential. The dependence of the number of secondaries leaving the screen surface on the electrical field intensity is likely to be largely affected by negative charging effects of the type discussed in the preceding section of this paper. As shown by the curve in Fig. 8, for one particular tube, a value of E_s of -730 volts is required to maintain a secondary-to-primary ratio of unity at a screen potential of 5400 volts. Considering the rate at which E_s increases with E_{b2}, we may deduce that at $E_{b2}=10{,}000$ volts, the screen will float at a potential several thousand volts lower.

From practical considerations, the most important characteristic of the screen surface in regard to its secondary-emission properties is the potential at which the break A occurs. Obviously, if this break occurs at a low screen potential, this potential will remain low no

matter how high the second-anode potential is made, especially when the increase in effective secondary emission with field strength becomes small or zero. When the change in secondary emission with field strength is zero, the screen will remain at a fixed potential as the second-anode potential is raised.

Some experimental results were obtained to show the effect of aging on the secondary-electron emission characteristics of the screen. Fig. 11 shows how the break A in the E_s–E_{b2} curve shifts toward lower values of E_{b2} as the aging progresses. These data[5] were obtained for a kinescope tube with a manganese-activated zinc-beryllium-silicate screen (posphhor No. 3), the aging of which consisted in a continuous scanning of a $5\frac{1}{2}''\times7\frac{1}{4}''$ area of the screen at a second-anode potential of 6000 volts, a beam current of 150×10^{-6} ampere, and a spot diameter of 0.07 cm.

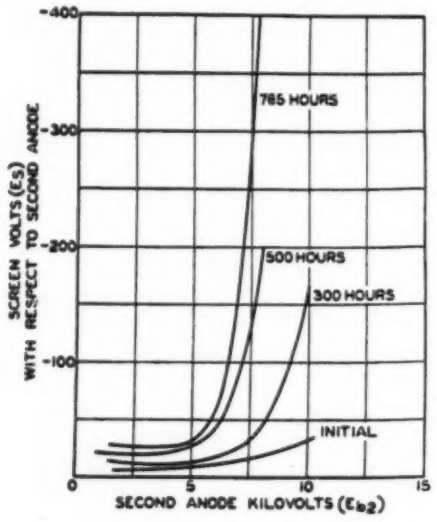

FIG. 11. Screen potential curves showing decrease in the secondary emission from a manganese-activated zinc-beryllium-silicate screen at "high" potentials as a result of continued electron bombardment of the surface.

Some results were also obtained to show the effect on the screen potential of the current density in the bombarding beam. The curves A and B in Fig. 12 show respectively how the screen potential varies with the current density at second-anode potentials below and above the break A in the E_{b2}–E_s curve. The variation in screen potential with current density is greater at the high than at the low potential. This is to be expected since the previously mentioned grid effects which occur at screen potentials above that of the break A depend upon the current density. As the current density increases the number of electrons which at equilibrium must be carried away from the depressions in the willemite layer by electrical leakage becomes larger. As a result, the negative potential of the depressions with respect to the surrounding elevated willemite areas increases and consequently a higher second-anode-to-screen potential is required to counteract the increased "grid" potential.

Nottingham[2] has reported data which he interprets as showing a large variation in screen potential with current density. He considers but dismisses nonuniformity in the secondary-emission properties of the surface as a cause of the variation. A consideration of the conditions under which these results were obtained, however, leads to the conclusion that the increase in screen potential observed is chiefly an effect of permanent changes in the secondary-emission characteristics of the spot in the willemite screen bombarded. As maximum current density or minimum spot size (I_{b2} is kept constant) is approached, the large energy input per unit area causes chemical and physical changes in the willemite at the point under bombardment. This

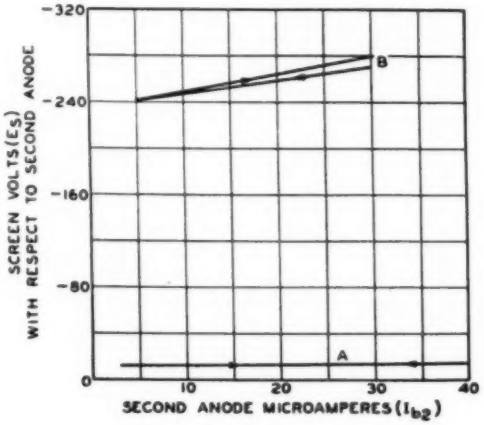

FIG. 12. Curves showing the variation of screen potential with beam current density at "low" and "high" screen potentials.

[5] From unpublished material by S. T. Martin on light output and screen potential of kinescope tubes. This material is scheduled for later publication.

permanent change is not noticeable as the current density is again decreased by increasing the spot size, since at lower current density the larger area under bombardment has been permanently affected only at a small point. The permanency of the decrease in secondary emission occurring at high energy input has been observed in an experiment where the current density was varied at constant spot size. The secondary emission was found to decrease permanently at energy inputs per unit area comparable to those reached near the minimum spot size in the data by Nottingham.

Conclusion

The purpose of this paper has been mainly to describe a method whereby the potential of an insulator surface may be determined and to point out how the method may be used for measurements on regular production tubes. The data on kinescope tubes are intended chiefly to be an illustration of the reliability, usefulness, and applicability of the method. The results obtained, however, may serve as a basis for future investigations. The fact that the secondary-emission characteristics of supposedly identical screens vary from tube to tube is not surprising in view of the difficulty of avoiding variations in the structure of the applied phosphor layers and in the degree of contaminations on the surface of these layers. It is interesting to note that in spite of variations from tube to tube, uncoated Nonex glass surfaces and calcium-tungstate screens have been found to attain their maximum potentials below 5000 volts while some willemite screens have been carried to 20,000 volts without showing evidence of a definite break. The experimental results showing that the screen potential varies with the beam-current density and life of the tube are also of practical importance. In general, the results also lead to the implication that the accumulation of negative charges on the glass base of the phosphor layer and on depressed surfaces in the layer affects the manner in which the screen potential varies with that of the second anode.

It is a pleasure to express my indebtedness to Dr. G. R. Shaw and to Dr. L. B. Headrick for valuable suggestions made during the course of the investigation.

Characteristics of the Glow to Arc Transition in Mercury Vapor

FREDERICK A. MAXFIELD AND GORDON L. FREDENDALL*
Department of Electrical Engineering, University of Wisconsin, Madison, Wisconsin
(Received March 2, 1938)

The probability of the transition from glow discharge to arc discharge at graphite electrodes has been investigated under carefully controlled cathode conditions. The transition probability was found to increase in an approximately linear fashion with an increase in cathode current density and glow voltage. The curve of transition probability as a function of cathode temperature was found to have a distinct maximum at a temperature of about 400° or 450°C. The probability of the transition occurring at temperatures 50° lower or higher was not more than about one-fourth the maximum. It was also found that the frequency with which the glow to arc transitions occurred depended greatly on the previous history of the discharge and the amount of high voltage positive ion bombardment experienced by the cathode under test. A possible explanation of these results has been based on the hypothesis that it is never possible to de-gas completely the cathode electrode even after prolonged operation in a high voltage discharge. It has been shown that the nonuniform emission of this gas from the cathode in the form of bursts from minute patches can lead to a greatly increased probability for transition from glow to arc.

INTRODUCTION

WITH a glow discharge at low pressure it is often impossible to increase the current and pass continuously from the glow form to the arc form of discharge. A continuous transition is possible only when the cathode is a refractory material such as tungsten and then only under special conditions. In all other cases the transition is sudden and discontinuous. The continuous transitions observed with increasing current when high melting point cathodes are used can be ascribed to an increasing amount of thermionic emission present as the cathode temperature is raised.[1, 2] Up to the present, a simple explanation such as that applied to the continuous transitions has not been available to explain the sudden transitions from glow to arc that occur when low melting point materials are used for the cathode and even in many cases when carbon or graphite is used for the cathode. Since conditions at the cathode of a stable arc are quite different when high and low melting point materials are used, it is not surprising that the thermionic emission theory cannot explain conditions in the two different kinds of transitions.

Any glow is a stable self-maintaining discharge characterized by a definite cathode current density and cathode voltage drop at any given pressure and electrode separation. There is no reason, according to present theories of the glow and arc, why the stable glow should change suddenly to an arc without some external initiating circumstance. There have been many explanations[3] offered for the cause of the sudden transitions which occur even under carefully controlled conditions but no explanation seems to cover all situations. For example, the transitions have been ascribed to (1) particles breaking off from the cathode, (2) particles hitting the cathode, (3) local high temperature spots on the cathode, (4) patches of impurity in poor thermal contact, (5) insulated patches of impurity on the cathode which become charged and periodically allow the charge to leak off at high current density, (6) surface irregularities producing enough distortion in the electric field to cause high field emission, and (7) spontaneous variations in current density at the cathode. Any one of these causes would be sufficient to initiate the glow-arc transition, yet even when the experimental conditions apparently rule them out, the transitions continue to appear.

Because of the importance of the glow-arc transition in many engineering applications, such as the mercury arc rectifier where unwanted transitions can produce a great deal of inconvenience and actual damage, it was felt that

* Now with RCA Mfg. Co., Camden, N. J.
[1] Wehrli, Zeits. f. Physik **44**, 301 (1927).
[2] Seeliger, Physik. Zeits. **27**, 28 (1926).
[3] Slepian and Ludwig, Trans. A. I. E. E. **51**, 99 (1932).

more study of the glow to arc transition was desirable. Accordingly apparatus was prepared and experiments were performed to determine the factors influencing the glow to arc transition when all conditions in the discharge were carefully controlled. Because of the fact that in a self-maintaining glow discharge the cathode fall of potential depends on the cathode current density and that it is not possible to vary one without changing the other, a self-maintaining glow discharge was not used for these experiments. An arc discharge between auxiliary electrodes was used as the source of ionization for the glow. This is not an unjustified procedure because by an increase in vapor pressure the discharge can be made to pass continuously from the non-self-maintaining to the self-maintaining form without any noticeable change in the characteristics or properties of the discharge. With this type of a discharge, it was possible, by changing the current density in the auxiliary arc, to change the ion concentration near the test electrode and consequently the glow current density without altering the cathode fall of potential in the glow. This permitted the study of the influence of one more independent variable on the transition from glow to arc.

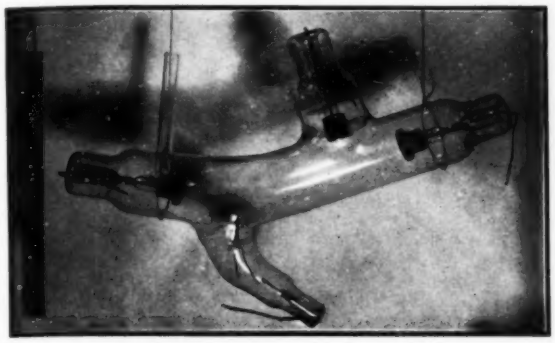

FIG. 1. The experimental tube.

APPARATUS

Figure 1 shows the experimental tube first constructed. The figure shows the essential parts of the tube and their dimensions. The tube was, however, modified after the preliminary experiments and the test electrode (cathode) mounted on a ground glass seal, so that it could be removed easily for replacement or repairs. An arc with a mercury pool cathode was used as the source of ionization for the glow, but in order to make the discharge more stable and vapor flow conditions more constant a tungsten rod was mounted on the mercury surface. With this arrangement the cathode spot fixes itself at the junction of the tungsten and the mercury instead of wandering about over the mercury surface.[4] The test electrode (designated by A_T in Fig. 3) was so situated with respect to the mercury pool that no mercury drops could fly up and hit it and thereby initiate a transition. The test electrode was constructed of graphite, because with a graphite cathode the amount of sputtering observed under high voltage conditions is reduced to a minimum. Other materials may perhaps sputter less, aluminum for example, but they are usually attacked by mercury vapor. Graphite is not affected by mercury vapor and it can be heated to a high temperature for degassing purposes without damage. It is true that graphite can support a thermionic cathode spot but in the low pressure glow discharge the current densities observed are so small that random fluctuations in current density cannot account for enough local heating to produce a cathode spot. A graphite electrode, then, should and does behave just as any low melting point material when used as the cathode in the unstable glow discharge.

The test electrode A_T was mounted so that it projected into the positive column of the arc between A_L and the mercury pool. A large density of positive ions was then always present and the current density at the electrode A_T could be varied by changing the current in the auxiliary arc to A_L. The discharge between A_R (see Fig. 3 for the electrode markings) and the mercury pool was maintained simply to keep a cathode spot on the mercury pool all the time. Great care was taken in the assembly of the apparatus to see that no impurities were introduced, and the whole tube was baked at 350°C while being evacuated to remove as much of the gas as possible.

[4] L. Tonks, Physics **6**, 294 (1935).

A diagram of the test cathode assembly is shown in Fig. 2. The electrode was mounted so that only the face of the electrode was exposed to the ionized gas. Since the electrode was 2.38 cm in diameter, the area available for current collection was 4.46 square centimeters. Quartz

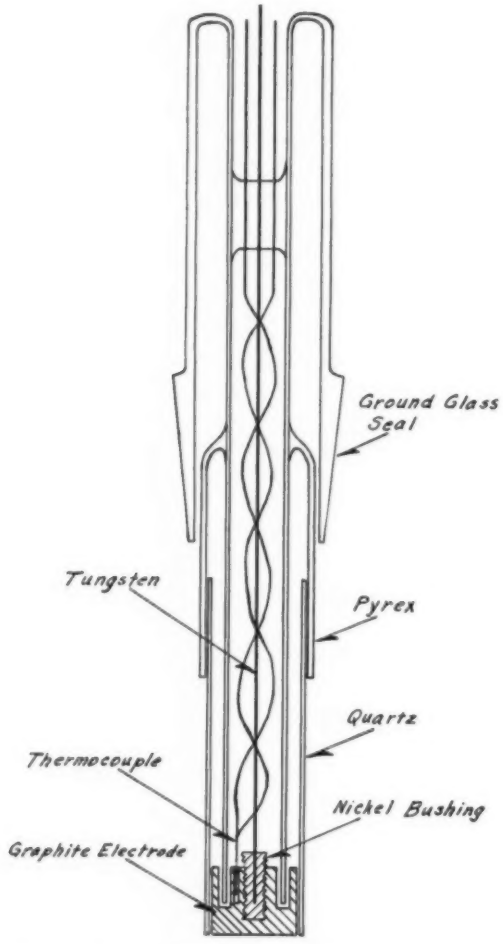

FIG. 2. Schematic diagram of the test electrode.

shielding was used for the sides of the electrode. The quartz was spaced from the graphite by a No. 28 nickel wire at the top of the electrode so that the quartz could not touch the graphite. Preliminary tests had shown that whenever the quartz and graphite came into contact in a region of high ion density a transition to an arc occurred and a cathode spot formed at the point of contact. A thermocouple was included in the cathode assembly to measure the cathode temperature. The cold junction of this thermocouple was mounted as far as possible from the cathode but the cold junction had to be inside the tube. The temperature of the cold junction was estimated from measurements made outside the tube but because of the temperature gradient along the seal this reading only gives a minimum value for the temperature. Probably all temperatures should be slightly higher than those recorded.

The circuit used for the tests is shown in Fig. 3. A continuous current arc was run to A_R simply to maintain a cathode spot on the mercury surface. The current to A_L could be varied to change the ion density in the region adjacent to the test electrode A_T and consequently the positive ion current collected by the electrode or what will be called the glow current density. A high voltage half-wave rectifier and filter circuit was arranged to supply a steady negative voltage for the glow cathode and a commutator was arranged to switch on alternately the high negative voltage and a low positive voltage for heating the electrode by using it as an anode in an ordinary arc circuit. The rotating switch was adjusted to give the following switching cycle: 15 sec. for heating the electrode, 12

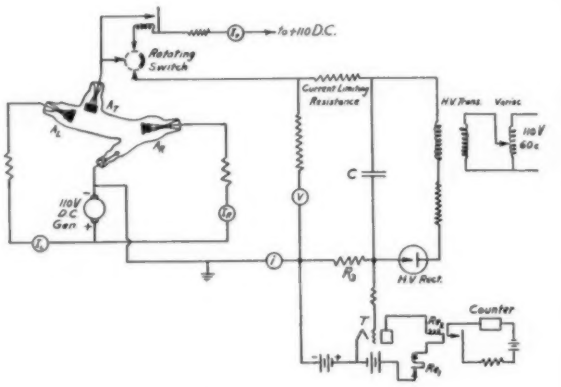

FIG. 3. Circuit diagram.

sec. without heating or high voltage during which time conditions could become stabilized, 5.3 sec. with high voltage applied, and 1.2 sec. without heating or high voltage before the cycle was repeated. A thyratron counter T was used to count the number of times the condenser C discharged. Normally the current collected by A_T was small (about 10 milliamperes) but every once in a while something would happen on the surface of A_T and the form of the discharge would

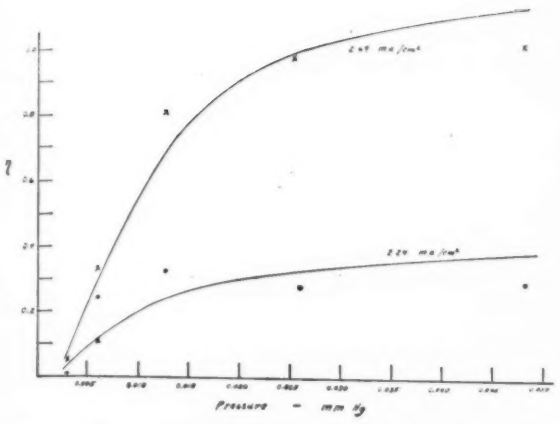

FIG. 4. Effect of vapor pressure on transition frequency.

change suddenly to an arc—a cathode spot appearing on A_T. When this occurred, the condenser C was discharged, the counter operated, and since the current that could flow continuously from the charging circuit was limited to a value smaller than necessary to maintain a stable arc, the cathode spot would be lost after the condenser discharge and the voltage would build up to its original value and maintain that value until the next transition occurred. With this arrangement it was possible to determine the dependence of the glow-arc transition on gas pressure, glow current, glow voltage (cathode fall), electrode temperature, and time. The dependence on all these variables was expressed by the frequency with which the glow to arc transition occurred. This frequency, designated by η in all curves, was obtained by taking the total number of transitions occurring in any one test or series of test intervals and dividing that number by the number of seconds over which the test extended. The frequency thus obtained is an average over a finite time. This method of obtaining the frequency is allowable, since it has been well established[5–7] that the transitions occur in a perfectly random manner. Because the frequency, as plotted on the curves, is obtained by averaging over a relatively short time and depends on so many variables, it is not unexpected that the experimental points do not fall exactly along a smooth curve.

[5] Slepian and Ludwig, reference 3, p. 92.
[6] G. L. Fredendall, Thesis, Univ. of Wis. (1936).
[7] Leblanc and Demontvignier, Rev. Générale de l'Electricite **29**, 948 (1931).

The glow current density was always obtained by dividing the total current collected by A_T by the exposed area of the electrode, 4.46 cm².

RESULTS

Figure 4 shows the variation observed in the glow to arc transition frequency as the mercury vapor pressure was varied in the tube by raising the temperature of the oil bath in which the tube was immersed. The two curves correspond to two different glow current densities, i.e., 2.24 ma/cm² in the case of the lower curve and 2.69 ma/cm² in the case of the upper curve. The voltage for these curves was maintained constant at 6000 and the electrode temperature at 500°C. There are two important facts to be gained from this figure. First the influence of vapor pressure is not very pronounced if the pressure exceeds about 0.025 mm of mercury, but below this pressure the probability of a transition drops off very rapidly and tends to approach zero at low values of pressure. Second, the dependence on glow current is very pronounced especially at high vapor pressures; an 11 percent increase in current density producing about a 200 percent increase in transition frequency.

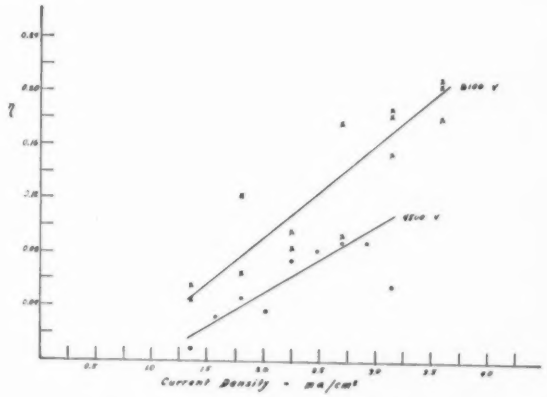

FIG. 5. Effect of cathode current density on transition frequency.

At low vapor pressures, the dependence of transition frequency on glow current is not quite so pronounced as at high vapor pressures. Fig. 5 illustrates the dependence on glow current observed when the pressure is maintained constant at 0.0028 mm of mercury. Only two curves,

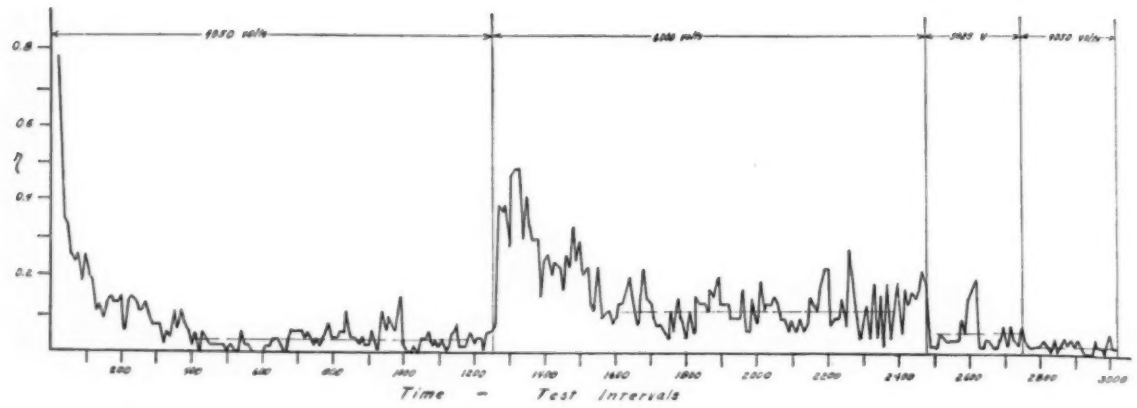

FIG. 6. Effect of glow voltage and time of test on transition frequency.

corresponding to 4500 and 8100 volts are shown. Curves at other voltages are similar. It is noticeable that the increase in transition frequency is of the same order of magnitude as the increase in voltage (80 percent) but that, even at this low vapor pressure, a corresponding increase in glow current density produces about a 200 percent increase in transition frequency. In these tests the electrode temperature was again maintained at 500°C as it was in all cases except that illustrated by Fig. 8. The scattering of the points is due, as mentioned previously, to the fact that each point represents an average over only 40 or 50 test intervals or about 6 minutes of actual high voltage operation.

The fluctuations that can occur in the transition frequency even when all conditions are held constant are exhibited clearly in Fig. 6. The data for this curve were taken over a continuous period of 27 hours, the equivalent time that high voltage was applied was, however, less than four and one-half hours. The electrode temperature was maintained at 500°C and the glow current was maintained at 2.69 ma/cm². The ordinates were obtained by plotting the average number of glow to arc transitions occurring in successive 10-cycle periods. The wide variations with time are clearly indicated. Over periods of 50 or 100 intervals the average transition frequency can be seen to be considerably above or below the long time average indicated by the dotted line—the period of averaging being equal to the length of the line. This shows that it is only by such long time tests as this that any definite trend can be determined. Individual tests extending over 40 or 50 intervals may give values quite different from the "true" average. The fact that the data do not give perfectly smooth curves is not unexpected and is another evidence of the random occurrence of the transitions. This figure also shows that the transition frequency decreases continually with time until the test has been extended over an appreciable length of time—a time of several hundred intervals. This may introduce another source of error in the interpretation of results unless sufficient time is allowed to elapse for the transition rate to assume a nearly constant value. This decrease with time is observed whenever the glow voltage is raised but is not observed as the voltage is lowered. This effect is evident from Fig. 6 in which the glow voltages are indicated for the various parts of the curve. This same decrease in transition rate with time is also observed whenever a test is started after the tube has been cold for some time, for example, after standing over night.

The dependence of transition frequency on glow voltage is shown in Fig. 7. The two curves correspond to the same constant glow current of 2.69 ma/cm² and the same electrode temperature of 500°C. There is this difference between the two, the data for the upper curve were obtained from Fig. 6, while the data for the lower curve were obtained in a much earlier test. The two curves have the same general shape but the data for the lower curve were obtained as the glow voltage was *reduced* from 8100 volts while

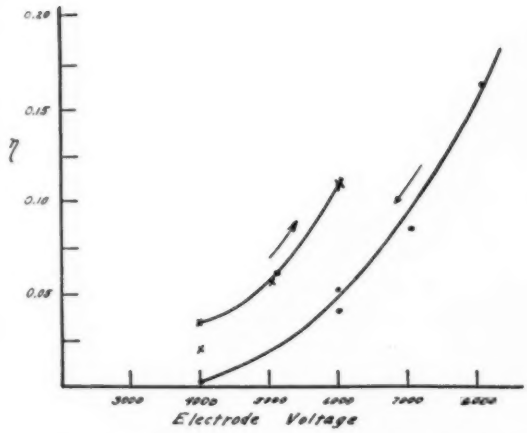

FIG. 7. Effect of glow voltage on transition frequency.

the other curve was obtained as the voltage was being *raised*. The previous history of the electrode is important and the difference between the two curves can be explained on that basis. It has always been found that the transition rate obtained as the glow voltage is decreased is less than that obtained as the voltage is increased. Even the data of Fig. 6 show this. The average obtained at 4000 volts was lower after the glow had been operated for a time at 6000 volts. It is reasonable to suppose that the two curves might have been much closer together if the voltage had been raised to 8100 volts before being reduced.

The effect of electrode temperature on the probability of transition from glow to arc is very interesting. Fig. 8 shows the results obtained. The two curves were obtained under quite different conditions and at quite different times in the experiment yet they exhibit the same shape. Curves of this same shape were obtained whenever the test was repeated. Two curves are shown to indicate the consistency of the results. The upper curve was obtained very early in the experiment before the electrode was considered to be de-gassed—the glow voltage in this case was 3600 volts and the current density was 1.34 ma/cm². The lower curve was obtained in one of the last tests—the glow voltage being 6000 volts and the current density 3.14 ma/cm². The indications from both curves are the same. There is a critical range in cathode temperature within which the probability of a transition occurring increases greatly. This critical range is relatively narrow covering only about 75°C from 375°C to 450°C. Except for this hump the probability of a transition occurring seems to increase uniformly but not rapidly with electrode temperature.

CONCLUSIONS

If we try to find an explanation for the results obtained in this experiment we can very easily discard the seven suggestions made in the introduction.

1. Particles breaking off from the cathode: Other experimenters[8] have found that the sputtered particles leaving the cathode in a glow discharge are of molecular size. Examination of the experimental tube in the case of this particular experiment, showed the glass to be covered with a uniform layer of sputtered graphite. The thickness of this layer gradually increased with high voltage operation and there was no evidence from the sputtered material on the glass or mercury that the particles leaving the graphite cathode were of a sufficient size[9, 10] to produce transitions. In addition to this, the observed increase and subsequent decrease in the transition rate whenever the glow voltage is changed is inconsistent with any mechanism which would imply that the transitions are due to sputtering.

2. Particles hitting the cathode: These could only be mercury drops from the mercury pool

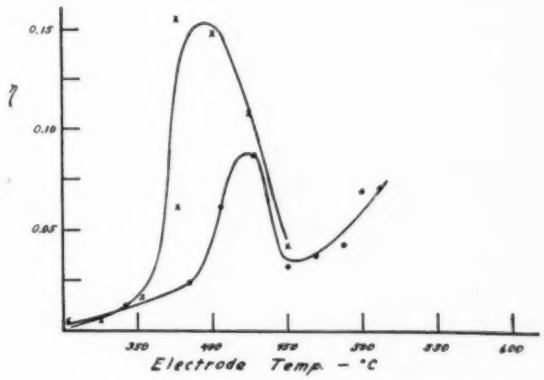

FIG. 8. Effect of cathode temperature on transition frequency.

[8] Compton and Langmuir, Rev. Mod. Phys. **2**, 186 (1930).
[9] Slepian and Ludwig, reference 3, p. 99.
[10] Jurriaanse and Druyvesteyn, Physica **3**, 825 (1936).

acting as cathode for the auxiliary arcs. The probability of mercury drops hitting the glow cathode was reduced almost to zero by bending the arm carrying the mercury pool back so that there was a glass shield between the mercury and the glow cathode. Furthermore a tungsten rod was placed on the mercury surface so that at all times the cathode spot was fixed on the tungsten. (See Figs. 1 and 3.) In this way no mercury drops which might be thrown up from the cathode spot could hit the test electrode. It was quite clear that this means was effective in keeping mercury drops from hitting the glow cathode, for whenever the cathode spot moved off the fixer the probability of a transition occurring increased greatly. Data obtained when the cathode spot was not fixed were not used.

3. Local high temperature spots on the glow cathode: The possibility of local high temperature spots appearing on the cathode can be discounted since, aside from the possibilities listed and discussed here, there is no apparent mechanism which could cause them to appear.

4 and 5. Patches of impurities in poor thermal contact and insulated patches of impurity on the cathode which become charged and periodically allow the charge to leak off at high current density: Either one of these could cause local high temperature spots on the cathode but neither one is probable since great care was taken in the assembly of the tube to eliminate all impurities. The graphite used for the cathode was a high grade graphite (PL AGX graphite rods from National Carbon Co., Cleveland) with less than 1.5 percent of impurities. The mercury used in the tube was triple distilled mercury which was distilled into the experimental tube. It is true that even with these precautions impurities may be introduced, but if this is the case, it is impossible to explain the dependence of transition probability on such things as voltage, pressure, and electrode temperature. Only the dependence on glow current can be explained on this basis.

6. Surface irregularities producing enough distortion in the electric field to cause high field emission: The possibility of this has been considered by others[11] and discarded because the results of a calculation of transition probability on this basis show that fluctuations in the electric intensity of a sufficient magnitude to produce a transition can occur only once in many years. Actually the transitions occur at relatively short intervals.

7. Spontaneous variations in current density at the cathode: This also may be discarded, for if we try to explain even the observed variation of transition probability with glow current we arrive at contradictory conclusions. (See Appendix.)

If none of these hypotheses is sufficient to explain the experimental conclusions, to what can we ascribe the fact that these transitions do occur and occur in a completely random manner? It seems that there is one other explanation that, up to now, has been neglected. Initially all the graphite electrodes contained a large amount of gas. Some of this gas is removed by baking the tube and some is removed by heating the electrodes, but a quite definite amount can only be removed by high voltage treatment. This is a well-known fact and it is common practice in the construction of tubes in which a very high vacuum is desired to use the electrode to be de-gassed as the cathode of a high voltage glow discharge in order to clean up a large part of the residual gas after the usual baking and heating has removed most of the gas from the electrodes and the tube walls. It is also well known that the probability of a glow to arc transition is very high with a poorly treated cathode but decreases after a considerable period of operation in a glow discharge or after the cathode is thoroughly outgassed. Fig. 9 illustrates the importance of high voltage treatment on the glow to arc transition probability. The glow voltage in this case was 3600 volts and the cathode current density was 1.34 ma/cm^2. Treatment with high voltage caused the transition frequency to decrease very rapidly during the first 100 test intervals, but removal of the high voltage for about four hours during which time the electrode was maintained at 500°C, all other conditions being constant, and subsequent reapplication of the high voltage showed that during the time the high voltage was removed nothing had been done to the cathode to cause

[11] Slepian and Ludwig, reference 3, p. 102.

the transition frequency to change. On the reapplication of the high voltage, however, the transition rate again decreased regularly. If the whole period during which high voltage was applied is treated as a single test extending over 200 test intervals, we see that all the experimental points lie on a smooth curve. (Left-hand solid and dotted curve.) The decreasing transition rate clearly indicates that conditions at the cathode were changing during and only during the time the high voltage was applied.

It is very easy to see that if the gas were not emitted continuously over the whole cathode surface, just this sort of a characteristic could be

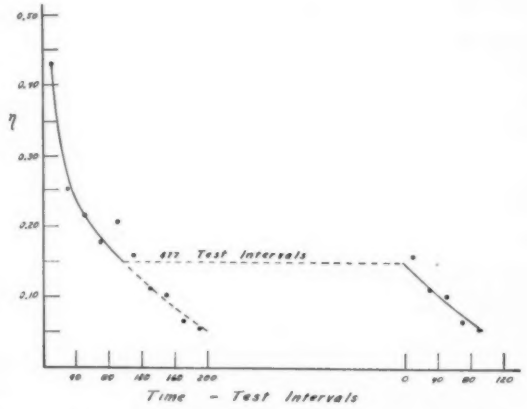

FIG. 9. Effect of high voltage treatment on gas removal from the cathode.

obtained. It is possible to explain all the results of this experiment if we assume that the gas is emitted from the glow cathode in small bursts. That is, we can assume that the gas diffuses toward the surface of the electrode but the molecules of the gas do not possess enough energy to escape from the surface after reaching it. In this event the gas will collect in small pockets and when the gas pressure increases to a sufficiently high value in this pocket or when the molecules gain sufficient energy by positive ion bombardment, they leave in a rush or in a small burst of gas. It is quite common in the use of glow discharges to observe gas leaving an electrode at a single point rather than uniformly over the electrode surface. In many glow discharges between electrodes which are not too well de-gassed one observes the glow on one electrode concentrated at a single point or in a ball, indicating that at that point the vapor density is higher than at other points on the electrode surface. These concentrated glows move about over the electrode surface indicating that the local high vapor density is not always confined to one point. It is not unreasonable to suppose then that the same sort of local gas emission occurs on the glow cathode even after extensive treating but on a much smaller scale. The fact that the transition rate only decreases when the high voltage is applied means that the gas molecules must gain energy from the incoming positive ions in order to escape. Whenever a burst of this kind occurs the positive ion density increases greatly over a small area of the cathode and it is possible for the glow to change suddenly to an arc. It may seem peculiar that the cathode can continue to give out gas over long periods of time but it is not necessary for all the gas to be initially contained in the graphite of the cathode although a very large quantity is absorbed by the graphite when it is exposed to air at atmospheric pressure. Some of the gas emitted by the electrodes is undoubtedly mercury vapor absorbed by the electrode during the time it is cold and a large part is undoubtedly gas absorbed in the mercury pool and emitted gradually as the mercury is vaporized and revaporized by the arc. Because evaporation only occurs from the surface of the mercury pool and because the condensed mercury flows back directly into the pool it is not possible to remove the gas contained in more than the surface layer of mercury. A very long time may then be necessary to remove completely foreign gas from the tube and electrodes and, of course, it is never possible to remove the mercury vapor as long as a mercury electrode is used.

If we adopt the view that gas is emitted from the cathode in small bursts during the time of application of high voltage, then the effect of the cathode temperature can be explained as follows: At low temperatures the gas diffuses slowly toward the surface and a great amount does not accumulate in gas pockets on the electrode surface. The number of bursts that occur is thus relatively small and the probability of a glow-arc transition occurring is small. As the electrode temperature is raised the rate of gas diffusion to

the surface increases and the number of bursts increases resulting in a rapid increase in transition probability with temperature. However, as the cathode temperature is raised further the amount of gas given off in each burst must decrease since the number of bursts of gas is increasing rapidly and at any given temperature there is a maximum rate at which the gas can diffuse to the electrode surface depending upon the total amount of gas present in the electrode. The transition probability will decrease with the size of the bursts and we would expect the curve of transition probability to pass through a maximum. At low temperatures nearly every burst may result in a glow to arc transition and with an increase in cathode temperature and an increase in the number of bursts we would expect an increased number of transitions to occur in a unit time. As the temperature is raised still higher we would expect less gas to be given off in each burst and consequently a decreased probability of any one burst resulting in a transition. If this probability decreased rapidly enough, we would expect a decreased number of transitions to occur although the number of bursts might be increasing. Except for the hump in the neighborhood of 400°C we would expect the general trend of the curve to be upward since with increased electrode temperature the rate of gas diffusion to the surface of the electrode is increased. The experiment seems to indicate that at a temperature of about 500°C the cathode is emitting gas more or less uniformly over the whole surface, i.e., the amount of gas in each burst is very small and the number of bursts occurring is very large. It may be that in addition to the effect of bursts of gas there is a definite effect of temperature on gas emission and that at about 400°C the total rate of gas emission is much higher than at any other temperature. Lowry[12] has observed an effect of this kind in the degassing and preparation of oxide coated cathodes.

Not every burst of gas from the cathode should result in a glow to arc transition because the initiation of a transition depends on the ease with which the current can be amplified in the neighborhood of a small spot on the cathode surface, and this in turn depends on the total number of positive ions present or the current density at the point where the burst occurs. If a burst appears the current density at a small spot on the cathode surface increases due to the high gas density in that region. It is then possible for an electron leaving the cathode to generate more positive ions per centimeter of travel and these ions can in turn produce more electrons. A glow to arc transition results. Over any small area of the cathode surface the current density fluctuates continuously, thus if a burst occurred when the current density is low a transition may not occur whereas if the same burst had occurred when the current density was high a transition might surely have occurred. From this we might guess that there is a certain probability of a transition occurring under practically any condition. This is found to be so experimentally as is shown by the curves above.

The effect of changing the *average* current density will be to change the average number of ions coming up to a small area of the cathode and consequently the magnitude of the current fluctuations. A change in transition frequency would then be expected. The results in Fig. 5 bear out this conclusion.

The effect of increasing the vapor pressure is to increase the gas density in the neighborhood of the cathode and consequently the probability that any current fluctuation will produce a transition. (See Fig. 4.)

Changing the glow voltage will change the energy of the incoming positive ions at the cathode and increased positive ion energy means that more electrons can be emitted per incident positive ion. Moreover it is probable that increased positive ion energy would mean that bursts of gas could occur more easily from the cathode surface. Either one of these events would be sufficient to explain the observed increase in transition probability with glow voltage as shown in Fig. 7.

Summary

The results of this experiment show quite conclusively that increases in current density, vapor pressure, and glow voltage result in an

[12] E. F. Lowry, Rev. Sci. Inst. **4**, 606 (1933).

increased probability of a glow-arc transition taking place in a glow discharge. The results show that the probability of a transition does not increase much faster than the first power of variables mentioned. The results of this experiment show quite conclusively also that there is a definite dependence of the glow-arc transition probability on the cathode temperature. In a narrow temperature range around 425° C the probability of a transition occurring is four to six times as great as the probability at temperatures 50° C lower or higher. Finally an explanation of the results obtained has been offered which is based on the continual nonuniform emission of gas from the cathode in the form of bursts from minute patches.

The next step in this investigation, is obviously to try to remove more of the gas from the tube and electrodes and determine the effect of the gas removal on the transition frequency. Since most of the gas is probably trapped in the mercury, one way to facilitate its removal would be to pass the mercury over a heater and raise its temperature to 1000 or 1200 degrees centigrade. This could be done as the mercury is distilled into the tube. Another way would be to provide a means for the mercury to circulate in the cathode pool so that as mercury is evaporated from the surface it flows back into the bottom of the pool instead of the top as at present.

The authors wish to express their indebtedness to Professor Edward Bennett for his encouragement and counsel, to Mr. Joseph Zamsky for his assistance in setting up the apparatus, and to Mr. Zamsky and Mrs. Maxfield for their help in the accumulation of data. The authors also wish to acknowledge the receipt of a Wisconsin Alumni Research Foundation grant-in-aid which is making possible the continuation of this research.

Appendix

Probability of random fluctuations in current accounting for transitions from glow to arc

If we were to attempt to attribute all glow-arc transitions to fluctuations in the number of ions which strike a small area ΔA of the cathode, we could attack the problem in the following way. With a given glow current we expect a certain average number of positive ions to strike the cathode per unit area per second. We can consider a small element of surface area ΔA and say that the number striking this area per second is $N\Delta A$. If the glow is to change to an arc, the number of ions striking the area ΔA in time Δt must increase by a factor β. It is not necessary for the average number of ions coming up to ΔA to increase to a value corresponding to the current density in the cathode spot of a stable arc, for it is conceivable that if the positive ion current density increases by a factor β less than necessary to give the positive ion current density in an arc that a chain of events will be initiated which will lead to the formation of an arc. That is, the increased positive ion current may cause a sufficient current of secondary electrons so that these can produce more positive ions which distort the field and initiate a series of events leading to the formation of a cathode spot.

The probability of n ions striking an area ΔA in a time Δt when the expected number of ions is $N\Delta A\Delta t$ is given by the ordinary Poisson probability formula since the incidence of any one particle or group of particles is entirely random. We can say then that

$$P(n)=\frac{(N\Delta A\Delta t)^n}{n!}e^{-N\Delta A\Delta t}. \tag{1}$$

We are, however, interested in the probability that *more than* n ions will strike ΔA in time Δt when the expected number is $N\Delta A\Delta t$. This probability is given by

$$Q(n)=\sum_n^\infty P(n)=\sum_n^\infty\frac{(N\Delta A\Delta t)^n}{n!}e^{-N\Delta A\Delta t}. \tag{2}$$

This can be rewritten as follows:

$$Q(n)=\frac{(N\Delta A\Delta t)^n}{n!}e^{-N\Delta A\Delta t}\times\left[1+\frac{(N\Delta A\Delta t)}{n+1}+\frac{(N\Delta A\Delta t)^2}{(n+2)(n+1)}+\cdots\right] \tag{3}$$

or

$$Q(n)=\frac{(N\Delta A\Delta t)^n}{n!}e^{-N\Delta A\Delta t}f(n) \tag{4}$$

where

$$f(n)=1+\frac{N\Delta A\Delta t}{n+1}+\frac{(N\Delta A\Delta t)^2}{(n+2)(n+1)}+\frac{(N\Delta A\Delta t)^3}{(n+3)(n+2)(n+1)}+\cdots \tag{5}$$

but

$$f(n)<1+\frac{(N\Delta A\Delta t)}{n}+\frac{(N\Delta A\Delta t)^2}{n^2}+\frac{(N\Delta A\Delta t)^3}{n^3}+\cdots. \tag{6}$$

Therefore we can say

$$1<f(n)<\frac{1}{1-N\Delta A\Delta t/n}. \tag{7}$$

We can thus establish an upper and lower limit for the

probability $Q(n)$. That is,

$$\frac{(N\Delta A\Delta t)^n}{n!}e^{-N\Delta A\Delta t} < Q(n) < \frac{(N\Delta A\Delta t)^n}{n!}e^{-N\Delta A\Delta t}\frac{1}{1-N\Delta A\Delta t/n} \quad (8)$$

or

$$P(n) < Q(n) < P(n)\frac{1}{1-N\Delta A\Delta t/n}. \quad (9)$$

But β was defined by the relation

$$n = \beta N\Delta A\Delta t \quad (10)$$

to be the ratio of the number of ions necessary to initiate a transition to the expected number striking ΔA in a time Δt. $Q(n)$ then lies between the limits

$$P(n) < Q(n) < P(n)\frac{1}{1-1/\beta}. \quad (11)$$

$Q(n)$ gives the probability that during any interval of time Δt, the actual number of ions coming up to the small element of surface ΔA will exceed n when n is equal to β times the expected number. The number of transitions expected per second on this hypothesis would be given by

$$\eta = \frac{A}{\Delta A}Q(n)\frac{1}{\Delta t} \quad (12)$$

where A is the area of the cathode. Thus

$$\eta < \frac{A}{\Delta A\Delta t}\frac{(N\Delta A\Delta t)^n}{n!}e^{-N\Delta A\Delta t}\frac{1}{1-1/\beta}. \quad (13)$$

An examination of this inequality shows that there are possibly four variables present, namely, n, β, N, and $(\Delta A\Delta t)$. It is interesting to note that ΔA and Δt do not occur separately but always occur as the product $(\Delta A\Delta t)$. Since N is the average number of positive ions striking a unit surface area per second and since in the glow discharge most of the current is carried by positive ions at the cathode, we will not be far wrong in assuming that all the current at the cathode consists of positive ions. N is then directly proportional to the glow current density. n is the number of ions, coming up to ΔA in time Δt, that is necessary to initiate the glow-arc transition. Under constant conditions of glow voltage, cathode temperature, and vapor pressure, this should be a constant. β is not an independent variable, but is related to N, n, and $\Delta A\Delta t$ by Eq. (10).

A convenient way to test the validity of this equation is to try to adjust the variables n and $\Delta A\Delta t$ so that the equation fits the experimental data obtained. Since the experiment shows that the cathode current can be varied over a wide range without making the probability of a glow-arc transition a certainty, it is evident that β must be greater than two even at the largest current used. Thus the term $1/(1-1/\beta)$ can, at the most, increase η by a factor of two. It will simplify the calculations to neglect this term since we are only interested in orders of magnitude. If we take the data of Fig. 5, we see that an increase of the glow current by a factor of about 2.5 produces about a four- or sixfold increase in the transition probability. If we use this fact we can get a relation connecting $\Delta A\Delta t$ and n, as follows

$$\frac{\eta_2}{\eta_1} = \left(\frac{N_2}{N_1}\right)^n e^{-(N_2-N_1)\Delta A\Delta t} \quad (14)$$

or

$$\Delta A\Delta t = \frac{n\log(N_2/N_1) - \log(\eta_2/\eta_1)}{N_2 - N_1}. \quad (15)$$

Using the following data from Fig. 5

$\eta_1 = 0.045$ transitions/sec., $\eta_2 = 0.190$ transitions/sec.,
$J_1 = 1.35$ amp./cm², $J_2 = 3.375$ amp./cm²,
$N_1 = 0.844\times10^{16}$ positive ions/sec., $N_2 = 2.11\times10^{16}$ positive ions/sec.,
$\eta_2/\eta_1 = 4.2$, $N_2/N_1 = 2.5$,

Eq. (15) becomes

$$\Delta A\Delta t = 0.722\times10^{-16}n - 1.13\times10^{-16}. \quad (16)$$

This shows that the relation between n and $\Delta A\Delta t$ is a linear one and n cannot be smaller than 1.56 for then $\Delta A\Delta t$ would be negative.

If now we say that Eq. (13) can be rewritten as

$$\eta = \frac{A}{\Delta A\Delta t}\frac{(N\Delta A\Delta t)^n}{n!}e^{-N\Delta A\Delta t}, \quad (17)$$

in which we have neglected the term involving β, it is possible to find a value for n by cut and try methods that will make Eq. (17) fit the experimental data of Fig. 5. Substituting for $\Delta A\Delta t$ its value in terms of n as determined by Eq. (16) and setting $\eta = \eta_1 = 0.045$ and $N = N_1 = 8.44\times10^{15}$, n comes out to be approximately 300. Using this value of n we find that $\Delta A\Delta t$ has the value 2.155×10^{-14} and $N_1\Delta A\Delta t$ is 181.9. This calculation would say then that if the number of positive ions coming up to ΔA in time Δt exceeds 300 when the expected number is 181.9 we would be sure to get a transition from a glow to an arc. However, when $\Delta A\Delta t$ has the value 2.155×10^{-14} and N_2 is equal to 2.11×10^{16} (as it must be at the larger current density used in calculating the relation between n and $\Delta A\Delta t$) the value of $N_2\Delta A\Delta t$ comes out to be 455. This number is larger than the number which presumably produces a transition.

The calculations show that if we expect on the average 182 ions on ΔA in time Δt, the incidence of 300 ions might produce a transition, but if this is to be true, then, in order to explain the observed increase in transition frequency with current we would have to say that when the expected number is 450 ions again the incidence of 300 ions will produce a transition. Actually, however, if we expect that the incidence of any number of particles, n, will initiate a glow-arc transition, certainly the incidence of more than n particles during Δt will also initiate a transition. If this is so, then, in order to fit the experimental data, we find that the expected number of particles is greater than the number of particles necessary to initiate a transition. The probability of a transition in this latter case is then actually almost unity.

These calculations clearly indicate that we cannot explain the observed transitions from glow to arc as simply due to random fluctuations in the number of ions incident on a small portion of the cathode surface.